SÃO PAULO STATE UNIVERSITY – UNESP

JABOTICABAL CAMPUS

QUANTIFICATION OF LITHOPEDOGENIC IRON OXIDES BY DIFFUSE REFLECTANCE SPECTROSCOPY AND MAGNETIC SUSCEPTIBILITY FOR MAPPING PURPOSES

Laércio Santos Silva

Agronomic Engineer

2020

SÃO PAULO STATE UNIVERSITY – UNESP

JABOTICABAL CAMPUS

QUANTIFICATION OF LITHOPEDOGENIC IRON OXIDES BY DIFFUSE REFLECTANCE SPECTROSCOPY AND MAGNETIC SUSCEPTIBILITY FOR MAPPING PURPOSES

Laércio Santos Silva

Advisor: Prof. Dr. José Marques Júnior

Co-advisor: Prof. Dr. Vidal Barrón Lopés de Torre

Thesis presented to the College of Agricultural and Veterinarian Sciences – UNESP, Jaboticabal Campus, as partial fulfillment of the requirements for obtaining the title of Doctor in Agronomy (Soil Science).

2020

S586q

Silva, Laércio Santos

Quantification of lithopedogenic iron oxides by diffuse reflectance spectroscopy and magnetic susceptibility for mapping purposes / Laércio Santos Silva. -- Jaboticabal, 2020

110 p. : il., tabs., fotos, mapas

Tese (doutorado) - Universidade Estadual Paulista (Unesp), Faculdade de Ciências Agrárias e Veterinárias, Jaboticabal

Orientador: José Marques Júnior

Coorientador: Vidal Barrón Lopés de Torre

1. Mineralogy (oxide minerals). 2. Magnetic properties. 3. Pedology (Soil science). 4. Geomorphology. 5. Environmental mapping. I. Título.

Sistema de geração automática de fichas catalográficas da Unesp. Biblioteca da Faculdade de Ciências Agrárias e Veterinárias, Jaboticabal. Dados fornecidos pelo autor(a).

Essa ficha não pode ser modificada.

unesp

UNIVERSIDADE ESTADUAL PAULISTA

Câmpus de Jaboticabal

CERTIFICADO DE APROVAÇÃO

TÍTULO DA TESE: QUANTIFICATION OF LITOPEDOGENIC IRON OXIDES BY DIFFUSE REFLECTANCE SPECTROSCOPY AND MAGNETIC SUSCEPTIBILITY FOR MAPPING PURPOSES

AUTOR: LAÉRCIO SANTOS SILVA
ORIENTADOR: JOSÉ MARQUES JUNIOR
COORIENTADOR: VIDAL BARRÓN LÓPEZ DE TORRE

Aprovado como parte das exigências para obtenção do Título de Doutor em AGRONOMIA (CIÊNCIA DO SOLO), pela Comissão Examinadora:

Prof. Dr. JOSÉ MARQUES JUNIOR
Departamento de Solos e Adubos / FCAV / UNESP - Jaboticabal

Prof. Dr. ZIGOMAR MENEZES DE SOUZA
Departamento de Água e Solo / Universidade Estadual de Campinas - Campinas/SP
(VIDEOCONFERÊNCIA)

Prof. Dr. GENER TADEU PEREIRA
Departamento de Ciências Exatas / FCAV / UNESP - Jaboticabal
(VIDEOCONFERÊNCIA)

Prof. Dr. ANTONIO CARLOS SARAIVA DA COSTA
Universidade Estadual de Maringá-UEM / Maringá/PR
(VIDEOCONFERÊNCIA)

Prof. Dr. ROGÉRIO TEIXEIRA DE FARIA
Departamento de Engenharia Rural / FCAV / UNESP - Jaboticabal
(VIDEOCONFERÊNCIA)

Jaboticabal, 30 de junho de 2020

AUTHOR DETAILS

LAÉRCIO SANTOS SILVA (soil scientist)- born in Barreiros - Pernambuco, studied Agronomic Engineering at the Federal Rural University of Pernambuco - Recife - UFRPE, from 2009 to 2014. During that time, Dr. Laércio Santos Silva developed scientific studies at the Department of Soil Science and at the Empresa Brasileira de Pesquisa Agropecuária (Embrapa - UEP Recife), in the areas of soil and water management and conservation, soil physics, fertility and mineralogy, geoprocessing of soil data, and plant improvement. He also attended a master's degree in the Graduate Programs in Agronomy (Soil Science) of University Estadual Paulista (Unesp Jaboticabal – São Paulo). His PhD was taken on soil mineralogy in the Universidade Estadual Paulista, with studies **Fundação de Amparo à Pesquisa do Estado de São Paulo — FAPESP** (process: 2017 / 01704-2) in the period from 2018 to 2020. He attended part of his PhD at the University of Córdoba-ES under the guidance of the renowned Doctor and Scientist Professor Vidal Barrón Lopés de Torre. Scientist Laércio Santos Silva develops studies in the following alignments: applied mineralogy, mapping, pedometry and photochemistry of NO*x* gases in soils.

Silva, L.S

“Nordestino sim, sim senhô”.

"The difference between the traditional and the quantitative approach ceases to exist when technology and formal knowledge come together to produce relevant information for society".

unknown author

Dedicated

To God in the first place, for having given me the gift of life, in addition to allowing the completion of another stage of my life and for many other achievements.

ACKNOWLEDGMENTS

To my parents Amauri Bernardo da Silva and Laudicéia dos Santos Silva, the reason for my life, who have tirelessly accompanied me, always providing support in difficult times and celebrating in each small and big achievement.

To the Faculdade de Ciências Agrárias e Veterinárias, Universidade Estadual Paulista “Júlio de Mesquita Filho”, Campus de Jaboticabal (FCVA – Unesp), and to the post-graduation program “Ciência do Solo”, by reception and learning opportunities.

To advisor and mentor Prof. Dr. *José Marques Júnior* by his years of interaction, advice, exchange of experiences and opportunities for personal and scientific evolution. My scientific father.

To my co-advisor Prof. *Vidal Barrón Lopés de Torre* from whom I learnt a lot. It was an honor to work with you and an unspeakable opportunity for my personal, scientific, and professional life.

To Department of Agronomy (Soil Science) of the University of Córdoba (UCO), Spain, especially to Prof. Dr. *José Torrent* for the moments of conversations about Fe oxides, which contributed to the innovation and improvement of this study. To scientist *José María Méndez* for his contribution to laboratory analysis.

I thank all the members of the Soil Characterization for Specific Management Purposes group (CSME), faithful friends who accompanied me during the research and the realization of this work: *Romário Pimenta Gomes, Vinicius Augusto Filla, Luiz Gustavo Rosa Campos, Renato Nery Malmegrim Junior, Luis Fernando Vieira da Silva, Luigi Cicilini Benedini Moura, Angelina Pedro Chitlhango, Daniel De Bortoli Teixeira, Ludmila de Freitas, Ivanildo Amorim, Renato Eliotério de Aquino.*

To the examination panel members of the thesis defense: Prof. Dr. Antônio Carlos Saraiva da Costa, Prof. Dr. Rogério Teixeira de Faria, Prof. Dr. Gener Tadeu Pereira, and Zigomar Menezes de Souza, who dedicated the evaluation of the thesis, timely and constructive criticisms that contributed to the improvement of this thesis. My sincere gratitude to all.

I thank the São Paulo Research Foundation (FAPESP), Brazil for funding this study (Doctorate fellowship no. 2017/01704-2 and BEPE, Spain, no. 2018/15694-1).

SUMMARY

Page

QUANTIFICATION OF LITOPEDOGENIC IRON OXIDES BY DIFFUSE REFLECTANCE SPECTROSCOPY AND MAGNETIC SUSCEPTIBILITY FOR MAPPING PURPOSES

ABSTRACT - The Western Paulista Plateau (WPP) corresponds to approximately 13 million hectares (~ 50% of the state of São Paulo) and stands out in the production of citrus in the country (80% of the national production) and significant participation in the production of sugar and alcohol. The geological and geomorphological diversity of the region are the main cause for the spatial variability of Fe oxides, mainly goethite (Gt), hematite (Hm), maghemite (Mh) and Magnetite (Mt). Thus, recognizing the spatial variability of these oxides makes possible to identify the potential of agricultural areas, allowing the establishment of minimum management areas and the strategic planning of agricultural activities, minimizing environmental risks and optimizing operating costs. An alternative for developing the agricultural practices in these areas is the identification of the variability of soil attributes. Therefore, this study aimed to characterize the spatial variability of Fe oxides in WPP soils, using X-rays diffraction (XRD), diffuse reflectance spectroscopy (DRS) and magnetic susceptibility (χ). Sustained by sandstone (Vale do Rio do Peixe Formation — VRP) and basaltic (Serra Geral Formation — SG) rocks, WPP soils are distributed in three stages of landscape evolution: slightly, moderately and highly dissected. A total of 300 samples, collected at a depth of 0.0–0.2 m and representative of the geological and geomorphological compartments, were characterized by XRD, DRS and χ. The results were evaluated through spatial variability, relating the mineralogical data with the geomorphometric map, through statistical and geostatistical analysis. The lithological contrast between sandstone and basalt and the degree of dissection of the landscape control the spatial variability of Hm, Gt, Mh and Mt, in environments with low and high levels of Fe oxides. The similarity between maps obtained by conventional technique (XRD) and indirect methods (DRS and χ) highlights the efficiency and reliability of DRS and χ in the spatial characterization of soil Fe oxides in large areas, under complex soil-landscape relationships, in less time and investment cost.

Keywords: goethite, hematite, maghemite, magnetite, pedometry, spatial variability

QUANTIFICAÇÃO DE ÓXIDOS DE FERRO LITO-PEDOGÊNICOS POR ESPECTROSCOPIA DE REFLETÂNCIA DIFUSA E SUSCETIBILIDADE MAGNÉTICA PARA FINS DE MAPEAMENTO

RESUMO - O Planalto Ocidental Paulista (POP) corresponde a aproximadamente 13 milhões de hectares (~ 50% do estado de São Paulo) que se destaca na produção do cultivo de citros do país (80% da produção nacional) e significativa participação na produção de açúcar e álcool. A diversidade geológica e geomorfológica da região é responsável pela variabilidade espacial dos óxidos de Fe, principalmente, goethita (Gt), hematita (Hm), maghemita (Mh) e magnetita (Mt). Assim, o reconhecimento da variabilidade espacial desses óxidos torna possível a identificação de áreas com diferentes potenciais agrícolas, permitindo estabelecimento de áreas mínimas de manejo e o planejamento estratégico das atividades agrícolas, minimizando riscos ambientais e otimizando os custos operacionais. Uma alternativa para o avanço agrícola nessas áreas é a identificação da variabilidade dos atributos do solo. Este estudo objetivou caracterizar a variabilidade espacial dos óxidos de Fe nos solos do POP, utilizando Difratometria de raios-X, Espectroscopia de Reflectância Difusa (ERD) e Suscetibilidade Magnética (χ). Sustentados por rochas areníticas e basálticas, os solos do POP estão distribuídos em três estágios de evolução da paisagem: pouco, intermediariamente e altamente dissecada. Um total de 300 amostras, coletadas na profundidade de 0,0 - 0,2 m e representativas dos compartimentos geológicos e geomorfológicos, foram caracterizadas por DRX, ERD e χ. Os resultados foram avaliados no estudo da variabilidade espacial, relacionando os dados mineralógicos com o mapa geomorfométrico, por meio de análise estatística e geoestatística. O contraste litológico arenito-basalto e o grau de disseção da paisagem controlam a variabilidade espacial de Hm, Gt, Mh e Mt, em ambientes com baixos e altos teores de óxidos de Fe. A semelhança entre os mapas obtidos por técnica convencional (DRX) e métodos indiretos (ERD e χ) enaltece a eficiência e confiabilidade da ERD e χ na caracterização espacial de óxidos de Fe do solo em grandes áreas, sob complexas relações solo-paisagem, em menor tempo e custo de investimento.

Palavras-chave: goethita, hematita, maghemita, magnetita, pedometria, variabilidade espacial

ABBREVIATIONS LIST

a	Range
Hd	Highly dissected
Ana	Anatase
C_0	Nugget effect
$C_0 + C_1$	Sill
DCB	Dithionite–citrate–bicarbonate
DRS	Diffuse reflectance spectroscopy
Fed	Free-crystallinity iron
Feo	Low-crystallinity iron
DSD	Degree of spatial dependence
H_2SO_4	Sulfuric acid
Hm	Hematite
Gb	Gibbsite
Gt	Goethite
Kt	Kaolinite
LVef	Rhodic Eutrudox
PVA	Typic Kandiudalf
ME	Mean error
Mh	Maghemite
Mt	Magnetite
Qz	Quartz
Pd	Slightly dissected
POP	Planalto Ocidental Paulista
Md	Moderately dissected
R^2	Coefficient of determination
RT	Rietveld
RMSE	Root mean square error
SDE	Sandard deviation of the error
WPP	Western Paulista Plateau
χ	Magnetic susceptibility
χ_{lf}	Magnetic susceptibility in low frequency
χ_{hf}	Magnetic susceptibility in high frequency
$\chi_{fd\%}$	Frequency-dependent magnetic susceptibility
XDR	*X*-ray diffraction

TABLES LIST

CHAPTER 2 **Page**

CHAPTER 3

FIGURES LIST

CHAPTER 1 **Page**

CHAPTER 2

CHAPTER 3

CHAPTER 1 - General considerations

1.1 Introduction

Brazilian agribusiness boosts the Brazilian economy, with an emphasis on the global production of soybean, sugar cane, coffee and beef. Modern and globalized agriculture has been marked by digital technology and Big Data connected by software linked to agricultural equipment that optimize production during the entire production stage. Among the sectors that most advanced in technology can be mentioned the improvement of plant genetics (Carrer et al., 2010) and the agricultural machinery industry, with sensors and the development of “intelligent” machines. Paradoxically, or in a situation of constant inertia, soil mappings are found. Analogous to this, contemporary agriculture resembles a “*Ferrari” car (technological evolution) on a “pothole” road (gaps left by current soil mapping)*.

Brazil pays a high price because it don't know better his soils (Polidoro et al., 2016), making difficult to prevent natural problems such as floods and landslides that plague urban areas and agricultural areas during the rainy season, bringing irreparable disruption to society Brazilian. With a focus on agricultural environments, the lack of information on soil attributes prevents the development of suitable agricultural practices. The result of this is the increase in desertified areas, compaction and intense erosion processes, making the soil unsuitable for food production.

The history of the first mapping of Brazilian soils dates back to the 1940s, so that Brazilian pedology was imminent (Santos et al., 2011). In 1981, the first exploratory soil maps were produced on a scale of 1: 5,000,000. Over the years, public agencies under the Ministry of Agriculture and state institutes such as Campinas (IAC) and the National Land Survey and Conservation Service (SNLCS) have been tasked with updating existing ones and drawing up new maps. A major project was active in this process of diagnosing the potential of natural resources in the Brazilian territory: RADAMBRASIL. Operated between 1970 and 1985, RADAMBRASIL was a challenging and audacious project, responsible for mapping 2.5 million km^2 of Brazilian territory by aerial radar images, captured by plane. About 70% of the efforts were

concentrated in the Amazon region and the remaining 30% in the northeastern and pre-Amazon regions.

In 2001, IBGE in partnership with Embrapa launched a new approach to Brazilian soils, with updated information from the one developed in 1981. The improvements were only taxonomic in nature, with no change in scale (Embrapa, 2011). Therefore, depending on the user's interest and with a focus on agriculture, the current soil mappings are outdated, without accuracy, full of technical terminologies that, sometimes, the information contained is difficult to interpret. For modern agriculture, the level of detail of the maps on the scale of 1: 5,000,000 is inefficient for the development of precision agriculture, in which the lowest cost with agricultural inputs and the increase in production is sought.

Due to the need to know the soil better, in 2016, a new soil survey proposal was launched coordinated by Embrapa, called the National Soil Program of Brazil (Pronasolos). The goal is to build more detailed maps on a scale of 1:25,000, 1:50,000, 1:100,000, that meets government needs. For Planasolos, the information from the 1:25,000 maps may assist decision making in the agricultural sector. This would be the first step in overcoming the impeding gaps inherited from the pioneering soil surveys carried out in 1981 and 2001.

The prediction for completion is 30 to 40 years and will cost to governmental budget a total of R$ 3 billion, with return of R$ 40 billion for the country in a decade. The high monetary cost and the long term of accomplishment are discouraging in the face of the current technological scenario that Brazilian agriculture is experiencing. Possibly, the methodologies used are the main reason for increasing costs and delivery time to users. It is in this panorama that alternative methods can be the key to assist conventional methods, generating accurate and reliable results, in a timely manner and with a lower investment cost (Carvalho et al., 2013; Silva et al., 2020).

The pioneering spirit of the state of São Paulo in mapping soil attributes by indirect methods inspires and attests to their potential in mapping soil attributes (Siqueira et al., 2010; Marques Jr et al., 2015; Peluco et al., 2015; Camargo et al., 2016; Silva et al., 2020; Demattê et al., 2020). The research group of Professor Dr. José Alexandre Melo Demattê from the University of São Paulo (USP) has been betting on the spectral library for characterization and design of soil surveys based on soil

color, using diffuse reflectance spectroscopy. In 2010, through magnetic susceptibility, Professor Antônio Carlos Saraiva da Costa's Mineralogy group prepared the magnetism map for soils in the state of Paraná.

The ***Soil Characterization for Specific Management Purposes group (CSME)***, under the coordination of Professor Dr. José Marques Júnior, has numerous works published in high impact scientific journals, demonstrating the efficiency and reliability of indirect methods - magnetic susceptibility and reflectance spectroscopy diffuse - in the spatial characterization of soil attributes. In addition, the CSME over 20 years of existence has formed and stimulated new soil scientists with affinities and mastery of mathematical models (Siqueira et al., 2010; Teixeira et al., 2017; 2018) that help to describe processes of soil, reducing the subjectivity of traditional models of mapping soil attributes. Scientific publications confirm the acceptance of indirect methods and mathematical modeling by the scientific community.

In fact, the main research funding agency in the state of São Paulo, FAPESP, has credited confidence in this new problem-solving horizon. For example, funding for research and training of masters and doctors with the purpose of generalizing the information on spatial variability of soil attributes can be mentioned: Lívia Arantes Camargo (nº: 17 / 01790-6), Diego Silva Siqueira (nº: 11 / 06053-3; 08 / 07693-3 and 04 / 09552-7), Angélica de Souza Bahia (nº: 13 / 17552-6), Kathleen Fernandes (nº: 17 / 05477-0 and 15 / 20692-0) and Laércio Santos Silva (nº: 17 / 01704-2 and 18 / 15694-1). The products of the aforementioned dissertations and theses were detailed maps of soil attributes, in the soil-landscape context and lithological complexity, providing detailed information on soil attributes for teaching, research and extension purposes, tactical and operational planning of agricultural activities, governance of soils and more effective public policy decisions.

Twenty years ago, the CSME group approached quantitative mathematical, statistical and geostatistical methods to Soil Science in an attempt to describe, analyze and interpret soil data. This quantitative character of interpreting the soil and the processes involved was called pedometry (Webster, 1994). There are reports that pedometry emerged in the face of criticism of conventional soil surveying methods, as they are very qualitative and subjective (McBratney et al., 2000). Thus, studying the soils by metrics has made it possible to recognize, for example, the spatial pattern in

a more objective way, as shown by some studies developed in Brazil (Camargo et al., 2008ab; Siqueira et al., 2010; Oliveira Jr et al. , 2011; Camargo et al., 2013; Barbieri et al., 2013; Marques et al., 2014; 2015; Peluco et al., 2015; Camargo et al., 2016; Teixeira et al., 2017; Teixeira et al., 2018; Silva et al., 2020).

It is evident that the adoption of pedometry and indirect methods of soil mapping yield faster returns and reduce costs when compared to conventional methods (Bahia et al., 2015; Camargo et al., 2016; Demattê et al., 2020). However, in addition to the promising methods of soil mapping, it is still necessary to select “key attributes”. These are attributes that coordinate, and that the behavior of others can be gauged from them - basic principle of pedotransfer function modeling (PTFs). The PTFs allows predicting more complex attributes from another strongly correlated, easily measured and obtained at lower costs (Budiman et al., 2003; Lagacherie and McBratney, 2007).

The mineralogy of the soil, specifically, of the clay fraction, has gained prestige as a key attribute for the prediction and characterization of the spatial pattern of covariate attributes (Barbieri et al., 2013; Peluco et al., 2015; Camargo et al., 2016). Among the minerals of the clay fraction, Fe oxides are preferred candidates in prediction studies, as they control the physical and chemical properties of the soil (Camargo et al., 2013). Other factors confirm Fe oxides as strategic minerals, such as: *(I)* they persist in the soil and record environmental changes in color and crystallographic properties (Fernandes et al., 2004; Silva et al., 2020); *(II)* markers of environmental processes and source material (Long et al., 2015; Silva et al., 2020); paleoclimatic (Maher et al. 2003) and palioenvironment (Torrent et al., 2010; Wang et al., 2016); *(III)* some exhibit magnetic properties, *(IV)* reflect the pedoenvironmental conditions that were formed, reasons that praise its function as a natural pedoindicator (Cornell and Schwertmann, 2003).

In order to confirm the potential of applying diffuse reflectance spectroscopy (DRS) and magnetic susceptibility (χ) in the quantification and mapping of iron oxides - goethite, hematite, maghemite and magnetite - as well as the accuracy of these techniques in the prediction of the respective minerals in large areas, some hypotheses have become relevant in the present study:

(I) The spectral signature and magnetic susceptibility of soil samples can be used to estimate the content of antiferromagnetic (hematite and goethite) and ferrimagnetic

(magnetite and maghemite) minerals with good precision and accuracy for WPP soils when compared with the traditional X-rays diffractometry technique.
(II) The spatial variability of the hematite, goethite, maghemite and magnetite contents are influenced by the geomorphological compartments at different stages of evolution.
(III) The geomorphological environments identified by the geomorphometric signature technique coincide with different environments for the formation of hematite, goethite and maghemite pedogenetic minerals.
(IV) Maps of soil minerals obtained by DRS and χ and information on geomorphological compartments at different stages of evolution can assist in the identification of areas with different agricultural potentials; (V) DRS and χ techniques can be applied reliably in large and complex areas.

In view of the statement of the problem addressed, the study had the general purpose of: ***Characterizing (identifying and quantifying) the spatial variability of litho-pedogenic Fe oxides in the soils of the Western São Paulo Plateau, using X-rays diffraction, diffuse reflectance spectroscopy and magnetic susceptibility***. This purpose was developed into two specific objectives: **Chapter 2.** We assessed the efficiency of DRS for estimating the spatial variability in Gt and Hm in the framework of soil–landscape relationships in the Western Paulista Plateau (Brazil) to facilitate the development of ancillary methods for mapping large areas. **Chapter 3.** We assessed the potential of magnetic susceptibility (χ) for predicting spatial variability in the magnetic minerals maghemite (Mh) and magnetite (Mt) in soils developed on sandstones and basalts in relation to alternative determination methods.

1.2 Literature review

1.2.1 Fe oxides in tropical soils

Fe oxides, a generic nomenclature to define Fe oxides and oxidroxides (Melo and Aleonni, 2009), are important components of the mineralogical assembly of soils, especially those in the last stage of evolution (Ker, 1997; Santos, 2018). Among the oxides of Fe occurring in the soil, such as ferrihydrite, lepdocrocyte, schwertmannite, specifically hematite (Hm = α-Fe_2O_3) and goethite (Gt = α-FeOOH) are the most

abundant (Schwertmann and Taylor, 1989), being present in soils with low and high levels of total Fe (Campos et al., 2007; Metri et al., 2008; Camargo et al., 2013; Bahia et al., 2015; Carvalho Filho et al., 2015 ; Camêlo et al., 2017; Poggere et al., 2018; Silva et al., 2020).

In the soil, Fe oxides are products of the dissolution of primary (lithogenic) and secondary (pedogenic) minerals that contain iron (Fe^{+2}) in their crystalline structure (Cornell and Schwertmann, 1996). Free in solution, the Fe^{+2} and / or Fe^{+3} ions can combine with other species in the soil (O^{-}, OH^{-}, H^{+}) and form Fe oxyhydroxides, like goethite and hematite (Schulze, 1989; Sposito, 1989). Although they are formed from Fe ions and normally coexist in the soil, the occurrence of one is to the detriment of the other (Schwertmann and Taylor, 1989; Kämpf and Curi, 2000). In addition, the concentration of these oxides greatly depends on the factors and processes of soil formation, especially rock.

Unlike goethite, hematite has its preferential formation in soils derived from material rich in Fe, such as basalt rocks (Schwertmann, 1985; Bigham et al., 2002). Inda Junior and Kämpf (2005) reported that, in addition to the source material, the formation and stability of these minerals are conditioned by the pedoenvironmental characteristics (temperature, humidity, organic matter content, pH, Eh, among others), characteristics that provide great variation in color, in the form and in the very constitution of Fe oxides (Schwertmann and Carlson, 1994). Reasons that give Fe oxides the function of environmental pedoindicators, as they reflect the conditions of pedogenesis under which they would have been formed (Fitzpatrick and Schwertmann, 1982).

Some soils, especially those derived from basic rocks, may have magnetic properties, due to the presence of magnetite (Mt = $FeO.Fe_2O_3$) and maghemite (Mh = γ-Fe_2O_3) (Costa et al., 1999; Cornell and Schwertmann, 2003; Schaefer et al., 2008). When these minerals occur simultaneously in the soil, maghemite can be formed from the direct oxidation of magnetite (Barrón and Torrent, 2002). The transformation of goethite, hematite and ferrihydrite into maghemite is common in soils that have suffered from burning, in the presence of organic compounds (Mullins, 1977; Schwertmann and Cornell, 1991). According to Costa et al. (1999), although Mh occurs in lower concentrations in the soil, it can constitute up to 40% of the total iron oxide

content. However, there is no evidence in the maghemite literature as the only existing Fe oxide, always occurring associated with hematite (Costa and Bigham, 2009).

The content of total Fe oxides (in the form of Fe_2O_3) is a diagnostic attribute of the Brazilian Soil Classification System (SiBCS) in the differentiation of soil classes and, consequently, in the evaluation of the degree of weathering (Santos et al., 2018). This Fe is obtained in air-dried fine earth after sulfuric digestion (H_2SO_4) (Donagema et al., 2011). Although it is common to call it "total Fe_2O_3", it would be better to call it "pseudototal", since sulfuric digestion little attacks minerals in the coarse fractions (sand and silt) that may contain Fe in its structure, being effective in the clay fraction. However, as the tropical soils are well evolved, it can be said that the totality of Fe in these is found in the clay fraction.

Considering the Fe_2O_3 content, it is possible to classify the soil in low levels of Fe (hypoferric; Fe_2O_3 < 8%), medium (mesoferric; 8% < Fe_2O_3 ≤ 18%), high (ferric; 18% < Fe_2O_3 ≤ 36%) and very high (ferric; Fe_2O_3 > 36%). This classification is commonly used for the Latosol and Nitosol classes. High levels of Fe_2O_3 are usually associated with soils from volcanic eruptive rocks. The studies by Carvalho Filho et al. (2015) recorded levels above 70% in Ferruginous dolomite soil, that is, in 1 kg of soil, 700 g are Fe_2O_3 - such high values were unknown in Brazilian literature. Another importance of Fe_2O_3 is as an indication of the degree of weathering of the soil [Ki = 1.7 ×% SiO_2 /% Al_2O_3, Kr = 1.7 ×% SiO_2 / (% Al_2O_3 + 0.6325 ×% Fe_2O_3)], whose values separate oxidic soils (very weathered) ; Ki and Kr <0.7) of those kaolinitic (slightly weathered; Ki and Kr > 0.7).

Another important aspect of the soil is the color, indispensable in SiBCS, considered the basis for surveying Brazilian soils (Santos et al., 2018). In general, color is a safe pedoindicator morphological property of the presence and type of Fe oxides, even in low concentration (Fernandes et al., 2004), of covariate attributes (Camargo et al., 2016) and of organic matter. For example, more yellowish soils (2.5Y and 7.5RY) indicate goethite as the main Fe oxide, while hematite gives the soil a more reddish color (5R and 2.5YR) (Ker, 1997; Bigham et al., 2002; Santos et al., 2013). In turn, maghemite has a hue ranging from 2.5YR to 5YR, commonly associated with hematite with a brighter hue (2.5YR - 5YR) (Schwertmann, 1993; Costa and Bigham, 2009).

Easy to identify, color expresses the interaction of soil formation factors and processes (Torrent and Barrón, 1993; Santos et al., 2018), providing valuable information on the environment in which the soil would have been formed. Among some examples, the color helps to differentiate the horizons of the soil profile and may indicate a pedoenvironment with poor internal drainage, whose absence of oxygen promotes the reduction of Fe^{3+} — Fe^{2+}, a formation process marked by the expression of mottled (plinthite) to the gray color from soil. Easily determined, based on a letter from Munsell (Munsell, 1994), color is used for order differentiation. As a legacy of the rock, the variation in the color of the soil may indicate a difference from the source material (Silva et al., 2020). This would be one of the reasons why color is a diagnostic attribute in other soil classification systems, such as Chinese (Chinese Soil Taxonomy, 2001) and American (Soil Survey Staff, 2003).

1.2.2 Spatial variability of Fe oxides

Studies of soil-landscape relationship show that the formation and spatial variability of iron oxides are conditioned by landscape shapes (geomorphology), by interfering in the distribution of water in the soil, in promoting chemical reactions and in the transport of solids or materials in solution (Marques Jr and Lepsch, 2000; Schoorl et al., 2000; Ghidin et al., 2006). The studies by Camargo et al. (2008a) and Montanari et al. (2010) found a predominance of goethite in the concave forms of the landscape, while hematite had its formation favored in linear and convex. This is because in linear and convex pedoenvironments, water infiltration is facilitated, conditioning a drier environment and higher temperatures, that is, oxidizing conditions that favor the formation of hematite. In concave pedoforms, the soils remain moist for a longer time and tend to accumulate organic matter, providing reducing conditions that provide the formation of goethite (Schwertmann, 1985).

Geomorphology, mentioned here as the degree of dissection of the landscape (Figure 1), also determines the formation of iron oxides, as reported by Coventry et al. (1983) and Williams and Coventry (1979) on North Carolina (USA) soils. In a cause-effect relationship, these authors reported that in the poorly dissected pedoenvironments of the landscape, that is, where weathering was more active

(pedogenesis prevailed over morphogenesis), the soils were deeper with good drainage conditions, that is, in environments oxidants predominated the hematite with better crystallinity in the clay fraction. In turn, goethite was the main iron oxide in highly dissected pedoenvironments, where the soils were shallower (lithic contact), with the presence of water stagnation for a certain period of time, configuring reducing conditions. In this regard, Curi and Franzmeier (1984) state that this occurs because goethite is formed in the first stages of weathering of primary minerals, therefore it accumulates in young soils or in the horizons near the rocks.

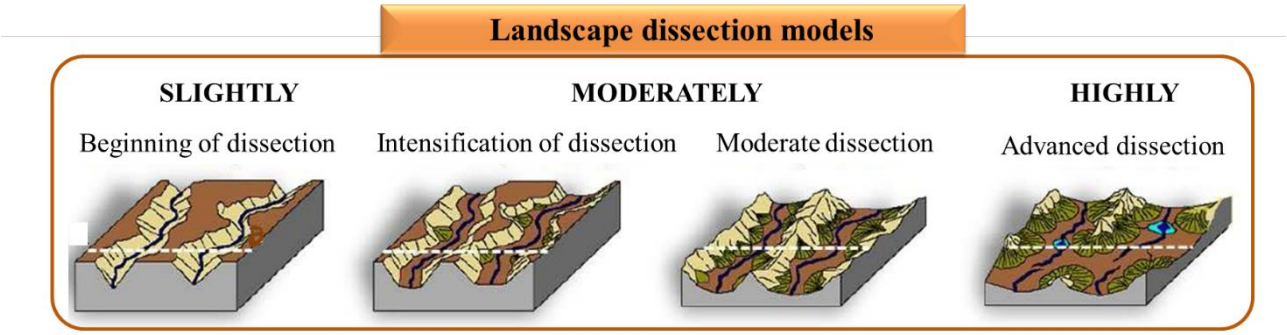

Figure 1. Landscape evolution model (geomorphogenesis) in Western Paulista Plateau (WPP).

Studies on spatial variability of mineralogical attributes, their relationship with chemical and physical soil attributes and the productivity of different crops were carried out in areas of varying dimensions from 1 to 500 ha in soils originating from Basalt and Sandstone (Montanari et al., 2010; Marques Jr et al., 2012; Camargo et al., 2013, 2014; Dantas et al., 2014; Peluco et al., 2015; Bahia et al., 2015; Camargo et al. , 2016). However, in large territorial areas, detailed knowledge of the soil is difficult. Among the causes are the natural variability of the conditioning factors of the spatial variability of the soil (geology, landscape shapes, among others) (Legros, 2006), lack of experienced professionals (Demattê et al., 2007), lack of government incentives (Bazaglia Filho, 2012) and deficit in the formation of staff in the geostatistics area.

The delimitation of homogeneous areas may correspond to future soil series, however the use of conventional methods of mapping soil attributes would make the establishment of specific management areas unfeasible. Soil properties are generally

described in detail by a pedologist and then validated and elaborated by chemical analysis (Ben-Dor et al., 2008). In the field, diagnostic descriptions, mainly associated with soil color, are subject to problems such as subjectivity. Laboratory chemical analyzes are time-consuming, costly and require complex sample treatment procedures, which are common problems for both the Brazilian soil system and other countries, such as China (Chinese Soil Taxonomy, 2001) and the United States (Soil Survey Staff, 2003).

For the reasons presented, pedometry has been well accepted among modern soil researchers, who recognize the obstacles and the high cost of traditional mapping methods. Although pedometric methods have a strong scientific basis, with a statistical and mathematical basis, the presence of an experienced pedologist is indisputable, in order to interpret the important qualitative parameters in pedometric models, minimizing inferences of modeling, erroneous conclusions, or emotive of metric models (Mendonças-Santos, 2007).

1.2.3 Methods of quantification of Fe oxides

1.2.3.1 X-ray diffraction (XRD)

Traditionally, X-ray diffraction (XRD) is considered the standard method for characterizing the mineral phases of the soil (Whitting and Alardice, 1986). However, considering the soil as a mixture of inorganic and organic particles, the concentrations and degree of crystallinity of minerals are sometimes impediments in the evaluation of the crystalline phases, and can generate misinterpretations (Silva et al., 2020). For this reason, soil analysis by XRD is accompanied by a series of procedures, including the separation of the sand, silt and clay fractions, the removal of minerals such as kaolinite and gibssite, and the concentration of oxides (Kämpf and Schwertmann, 1982; Balsam et al., 2014). These procedures are essential for the safe assessment of the mineral phases of the soil, avoiding misinterpretations. However, the laboratory processing time (Bahia et al., 2015; Silva et al., 2020) and the interpretation and cost of the analyzes make the characterization of iron oxides in large areas unfeasible, due to the need for a large number of samples.

Other limitations can be mentioned: (I) overlapping diffraction peaks; (II) low sensitivity to low Fe levels in soils inherited from the source material itself; (III) high isomorphic substitution of Fe for Al (Scheinost et al., 1998); (IV) imperfect crystalline and reduced size of the mineral (Jenkins and Snyder, 1996; Kämpf and Curi, 2000; Fabris et al., 2009). In general, XRD equipment is found in major research centers, due to the high cost of acquiring the equipment and the need for a professional to operate and interpret the data. In view of these obstacles, alternative techniques have been gaining ground in the mapping of soil minerals at a detailed level, allowing for precise inferences, with low cost of characterizing the minerals for the purpose of soil mapping and in relatively faster time compared to conventional methods, such as the XRD.

1.2.3.2 Diffuse reflectance spectroscopy (DRS)

1.2.3.2.1 Theoretical basis of DRS in soil

Diffuse reflectance spectroscopy (DRS) is an indirect method of analysis for quantitative applications (Minasny and McBratney, 2008; O'Rourke et al., 2016;). The basic theoretical principle of the technique is based on radiation (incident light) and its interaction with soil constituents (Stenberg et al., 2010). Depending on the constituents of the soil, radiation promotes vibrations of the individual molecular bonds, allowing the absorption of light to varying degrees, due to the difference between the two energy levels. The soil sample submitted to the light source produces a characteristic spectrum, which, for Salvaggio and Miller (2001), allows it to be used for analytical purposes. The resultant of absorption at a given wavelength (λ), that is, the frequencies at which light is absorbed on the ground, is given in percentage reflectance [(R%): A = log (1 / R)].

R can be understood as the ratio between the radiant flow reflected by incident radiant flow (Wyszecki and Stiles, 1982). In turn, maximum reflectance is obtained when a body lets practically all the light falling on it, and on the ground it never occurs (Torrent and Barrón, 2007). The light, when striking the surface of a body, follows different paths, depending on the size of particles, angle of reflection, free space

between the particles and degree of compaction in the preparation of the soil sample. The way the reflected light acts or interacts with soil particles occurs at any wavelength, discriminating the ***regular*** (specular or mirrored) and / or ***diffuse*** reflectance.

When the surface affected by the light has flat (smooth) faces, or when the size of the particles is relatively uniform (the angles of incidence and reflection are the same), the impacted light follows a unidirectional path, receiving the name of ***regular*** reflectance, situation in that the size of the surface particles is less than the wavelength of the incident radiation. There is the opposite behavior for ***diffuse*** reflectance, which predominates on a rough surface, due to the distinct and random size of the particles, in such a way that the incident light disperses in different angular directions. In a situation of diffuse reflectance, the wavelength of the incident radiation is less than the size of the surface particles. The radiation reflected in all directions provides more information about the soil in relation to the regular, being more affective in the characterization of soil attributes and processes (Torrent and Barrón, 2007).

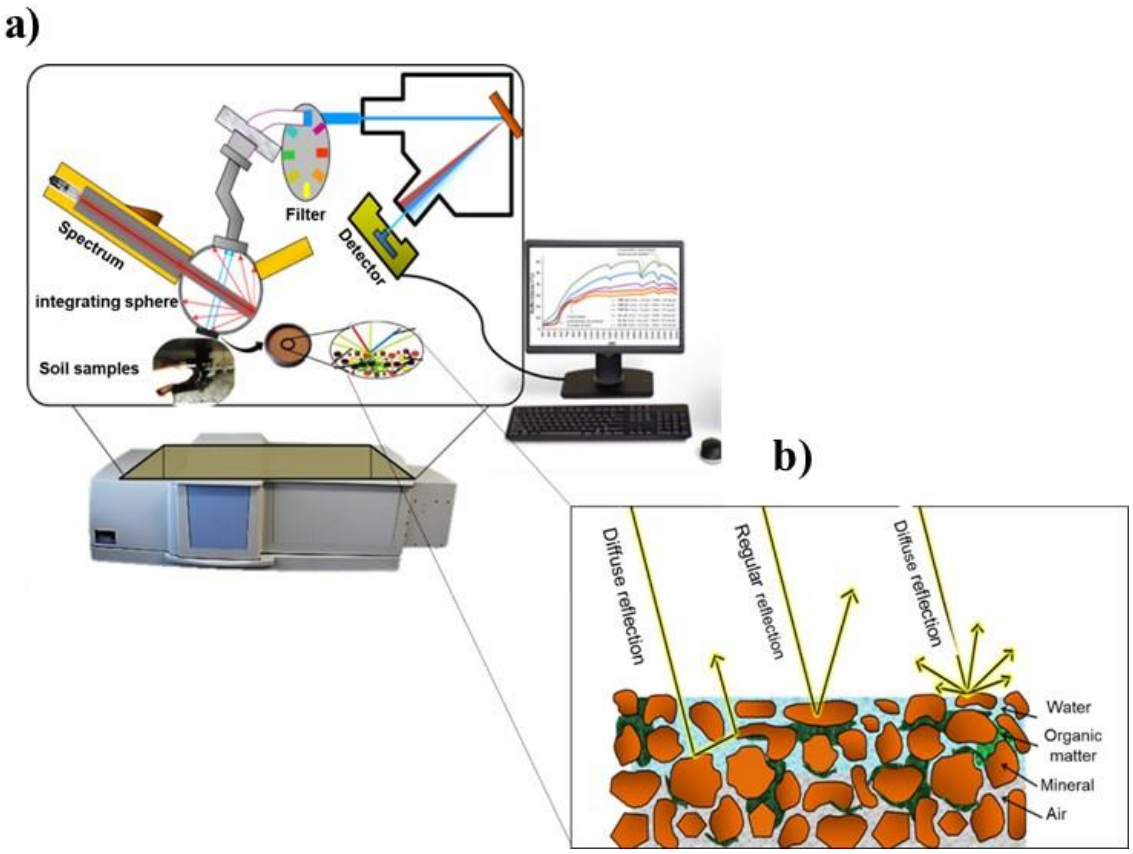

Figure 2. (*a*) Scheme of diffuse reflectance spectroscopy equipment and (*b*) type of reflectance when interacting with soil particles. Adapted from Gomes (2017).

The ability of matter color to absorb more or less light at different wavelengths (Barrón et al., 2000), applies very well to soil, since it is a mixture of mineral and organic particles that absorb and scatter the incident light (Barrón and Torrent, 1986; Fernandes et al., 2004). The interaction of light with soil properties, resulting in a spectral curve, aroused scientific interest in applying the applications of DRS in the characterization and estimation of soil attributes, in order to be used in laboratory analysis and even in the field.

In the soil, some properties control the reflectance of the spectral curve (Hunt et al., 1971; Janik and Keeling, 1996): organic matter, humidity, concentration and type of Fe oxides and relative proportions of sand, silt and clay (Demattê et al., 2012; Dotto et al., 2014; Coblinski et al., 2020).

1.2.3.2.2 Vis-NIR-MIR and applications in pedology

The attributes of the soil can be identified in three sensitive regions, defined as: ***Visible*** (Vis) - characterized by electronic excitations due to the high radiation energy in the wavelength of 400 to 780 nm (Figures 3a and 3b). Information about soil color, Fe content and composition, water molecules and organic matter (Sherman and Waite, 1985; Mortimore et al., 2004) are recognized in this region.

According to Hunt et al. (1971) the visible region is typical of opaque minerals typical of basic rocks such as goethite, hematite, magnetite and ilmenite (Figure 3a). Goethite is characterized in the 425 to 450 nm ranges and, for hematite, in the 545 to 590 nm ranges. The presence of these oxides in the soil reduces reflectance, due to the charge transfer between Fe ions and oxygen (Sellitto et al., 2009). Another indication of Fe oxides in the soil is the more pronounced concavity (Bahia et al., 2015). Demattê et al. (2012) reported the increase in reflectance in soil samples after removal of organic matter, validating the energy absorption capacity of organic matter (Gmur et al., 2012).

When the proportions of hematite and goethite are greater than that of maghemite, this has not been considered because it does not influence the spectral curve. This is because the reflectance pattern of maghemite occurs in an intermediate

range to hematite and goethite, as illustrated by Torrent and Barrón (2008) in Figure 4. Considering the coexistence of these oxides, it can be said that the behavior of the

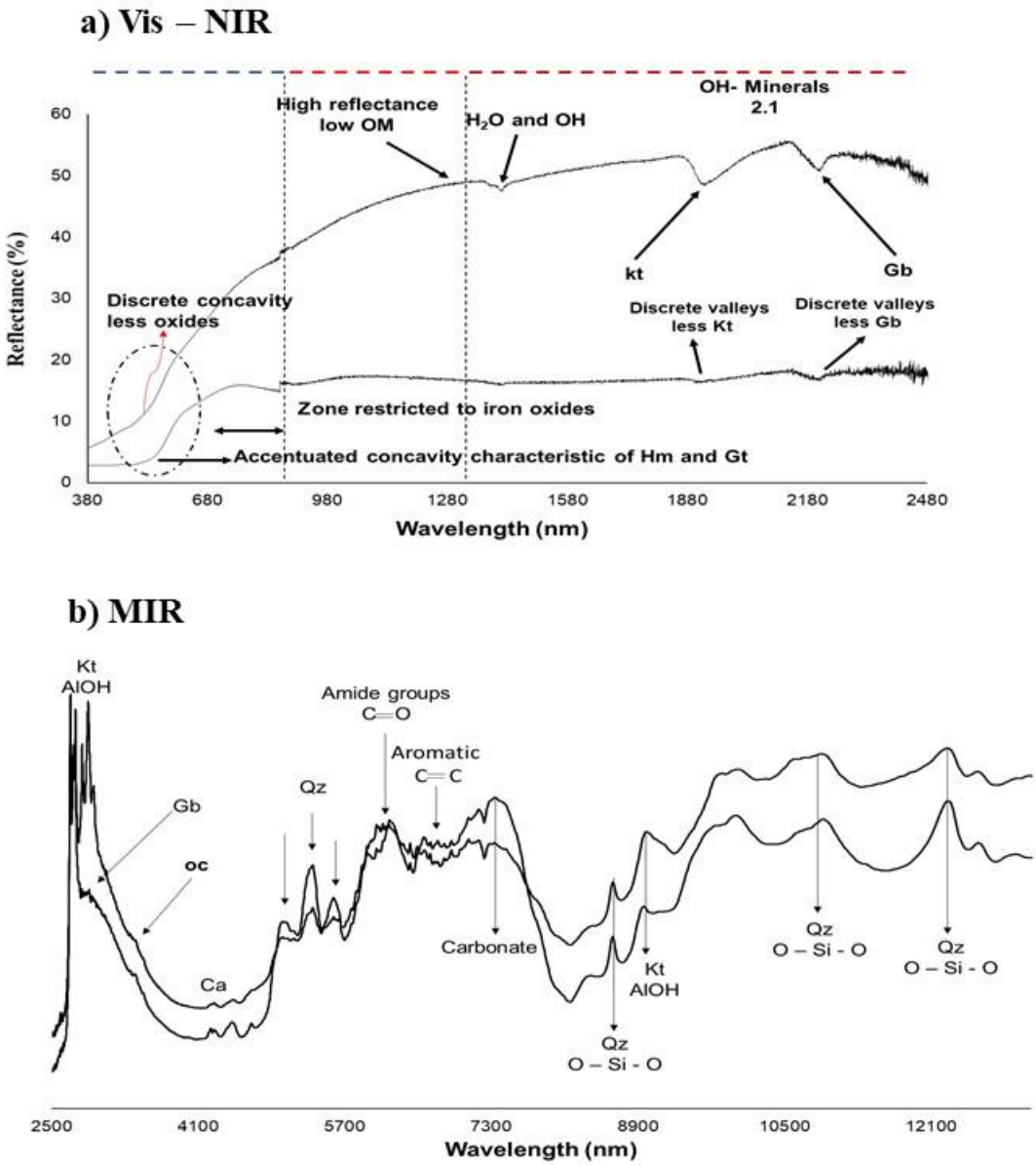

Figure 3. Hypothetical schematic analysis of diffuse reflectance spectroscopy of soil sample and respective attributes in the regions of the visible (Vis - 400 to 780 nm) and near infrared (VIR - 800 to 2500 nm) (*a*) and mid infrared (MIR - 2500 to 25000 nm) (*b*). OM – organic matter, Qz - quartz as sand, OC - organic compounds, Ca - calcite, Kt - Kaolinite, Gb - Gibbsite, Hm - hematite, Gt - goethite, OH - characteristics of mineral water.

spectral curve is governed by minerals hematite and goethite, main soil color conditioners. Inda et al. (2013) report that maghemite has expression in the 410 - 445 nm band, the same as that of goethite. Thus, for low levels of maghemite, its influence on reflectance patterns is usually disregarded.

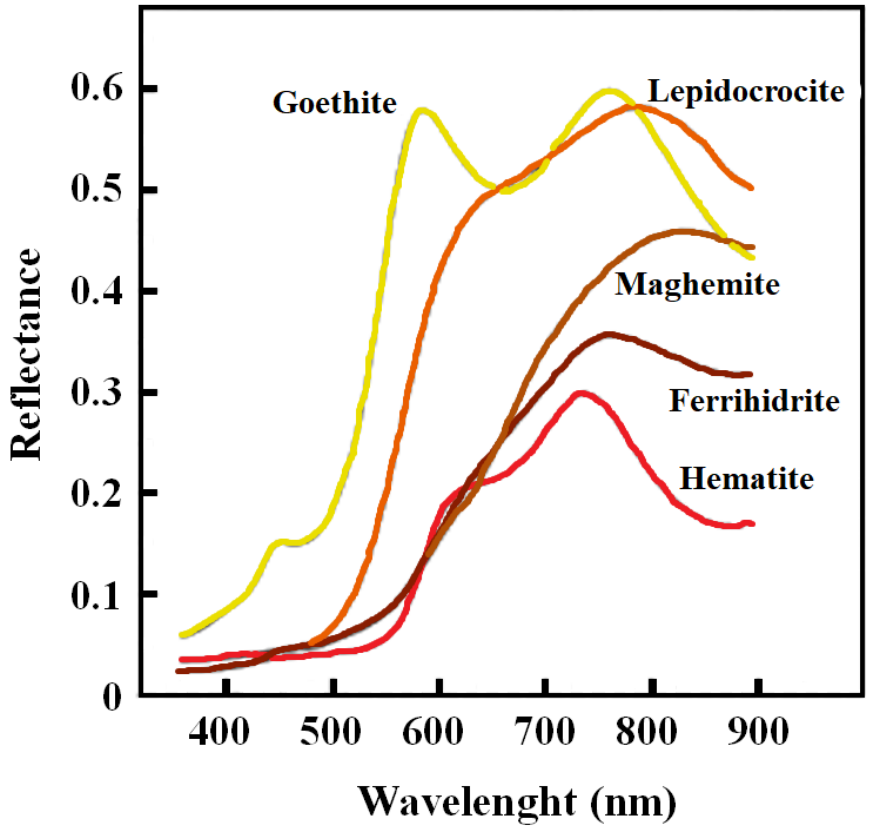

Figure 4. Diffuse reflectance spectroscopy for the main pedogenic Fe oxides. Model presented by Torrent and Barrón (2008).

The region from 780 to 2500 nm is called ***near infrared (NIR) or short – wave infrared (SWIR)*** (Figure 3a). Typical range of OH molecular vibrations, phyllosilicates, sorosilicates, hydroxides, sulfates, amphiboles, carbonates, soil water molecules and organic matter (Clark, 1999; Viscarra Rossel et al., 2006a). Water molecules have a strong influence on Vis-NIR, being found in several regions, but their presence is defined around 1400 to 1900 nm (Liu et al. 2002). Important minerals in the soil such as kaolinite and gibbsite are also characterized in Vis-NIR, however, unlike Fe oxides, they do not have a strong influence on the reflectance intensity, the presence of which is characterized by features in the form of valleys around 1880 at 2300 nm.

The ***mid – infrared*** (MIR - 2500 at 25000 nm) has as its fundamental principle the electronic transition of atoms, longer vibrations of molecules and crystals, depends on a frequency (Figure 3b). Electronic excitation sets up the formation of peaks characteristic of soil constituents (Stenberg et al., 2010). For example, strong Si-O, Al-O, Fe-O peaks, HO, HC and HN bonds in the MIR region are related to the presence of silicates, Fe and Al quartz oxides, calcium carbonate and organic compounds (Nguyen et al., 1991; Cañasveras et al., 2010).

In quantitative pedology, DRS has gained more and more applications. The fact that it is a non-destructive technique and does not require prior preparation of the sample under study, draws the attention of soil scientists, especially when working with a large database (large number of samples). Another reason is its use in pedotransfer function studies, combined with chemometric programs, such as ParLeS (Viscarra-Rossel, 2008) making it possible to correlate spectral information with the mineral composition of the soil. ParLeS has principal component analysis (PCA), NIPALS algorithm (Martens and Naes, 1989) and regression analysis of partial least squares (PLSR) (Geladi and Kowaslski, 1986), making it possible to calibrate, validate and obtain the best model of prediction of atributes.

Because it is a fast, less expensive, non-destructive and simple operation technique (Bahia et al., 2015; Camargo et al., 2016; Silva et al., 2020), DRS is promising in pedology. In addition, this technique allows the simultaneous characterization of many soil attributes with agronomic and environmental relevance (McBratney et al., 2002, 2006; Viscarra Rossel et al., 2006, 2010; Cañasveras et al., 2010; Kodaira and Shibusawa, 2013), in addition to being adaptable for use in the field (Viscarra Rossel and Mcbratney, 1998). Several countries have adopted this technique for and quantification of soil minerals and ore areas, such as Spain (Torrent & Barrón, 2002), China (Chen et al., 2002; Hu et al., 2013), Australia (Viscarra Rossel et al., 2010) and Brazil (Fernandes et al., 2004; Carioca et al., 2011; Silva et al., 2020).

In 1993, Torrent and Barrón proposed the use of DRS to quantify hematite and goethite, based on the Kubelka-Munk function (1931). By this method, the spectra coming from the samples' DRS are transformed into absorbance spectra, and with certain treatment the optical band-gap values are calculated. The application of the Kubelka-Munk function in the quanfication of goethite and hematite was applied by

Bahia et al. (2015), Camargo et al. (2016) and by Silva et al. (2020) in soils, compared with the results obtained by XRD. These authors found very close values for hematite and goethite between DRS and XRD, with R^2 values above 60% for Gt and 80% for Hm. In all of these cases, DRS color saturation was observed in soils with high concentrations of Fe_2O_3 and Hm, but not enough to compromise the quality of the results compared to those of the XRD.

The need to meet the growing demand for detailed information on tropical soils, especially mineralogical attributes, has increasingly used the use of indirect techniques, such as Australia, the country where the spectral signature for orbital sensors was obtained to build the hematite and goethite map of the entire federation (769,902,400 hectares) (Viscarra Rossel et al., 2010). In Brazil, incipient studies in small areas have already been developed using the spectral signature by DRS (Almeida et al., 2003; Bahia et al., 2015; Peluco et al., 2015; Camargo et al., 2016).

1.2.3.4 Magnetic susceptibility (χ)

The χ identifies Fe-bearing minerals. It turns out that Fe is an external transition element, in which its most energetic electrons in the 3d sublevel are incomplete, giving it a magnetic moment with orbital motion (Thompson and Oldfield, 1986). The χ intensity is a result of how the molecular and atomic structure of a substance is organized (Thompson and Oldfield, 1986). Therefore, the magnetic moment depends on the arrangement of the electrons (e^-) inside, and each electron has a magnetic moment associated with its spin. This occurs when a subatomic particle is subjected to a magnetic field it assumes a unilateral and, or varied direction, with a direct effect on the magnetic expression, which depending can be null or positive (Thompson and Oldfield, 1986; Cornell and Schwertmann, 2003).

In a more simplistic way, magnetism can be understood, as the property that some substances and or minerals have to be attracted by a magnet (Resende et al., 1988; Ferreira et al., 1994). In the soil, Fe oxides such as magnetite, maghemite and ferrimagnetic ferrihydrite are the main holders of magnetism and, based on this property, it is possible to recognize five magnetic groups (Thompson and Oldfield,

1986): ***Ferromagnetic, Diamagnetic, paramagnetic, ferrimagnetic and antiferromagnetic*** (Figures 5a-5e). The ferromagnetic group is a particular case, since there is no representative in the mineral form, only for pure substances: Fe, Co and Ni (Melo and Aleonni, 2009). These substances have the electron spins always aligned even when in the absence of an external magnetic field and have extreme χ values around 27,600,000 × 10^{-8} m^3 kg^{-1}.

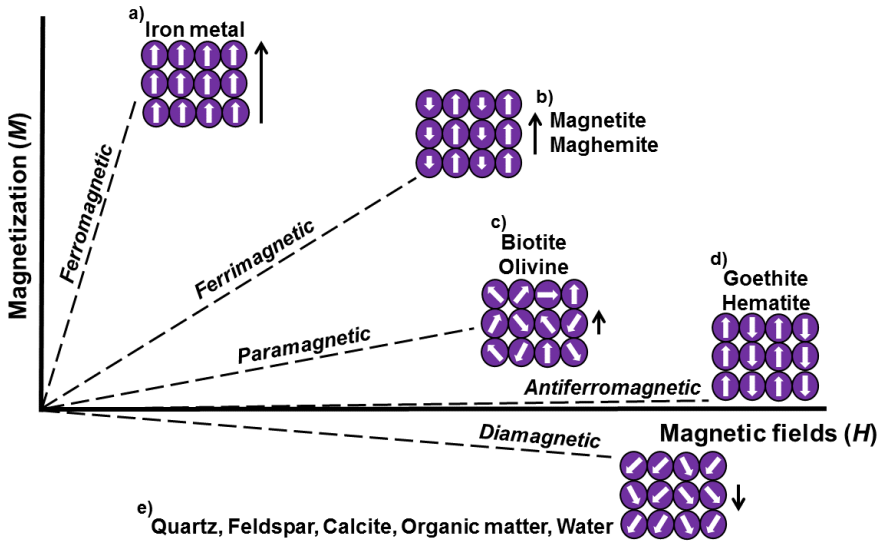

Figure 5. Magnetic behavior in the presence of an external magnetic field. Adapted from Barrón (2020), personal communication.

Classified as diamagnetic (Figure 5e) are those minerals that do not have χ (χ <0), that is, they are not attracted by a magnet, so they assume negative χ values. As an example of some representatives of this group, kaolinite, gibssite [$Al_2Si_2O_5$ $(OH)_4$] and quartz (SiO_2), calcite ($CaCO_3$), albite ($NaAlSi_3O_8$) and apatite [Ca_5 $(PO_4)_3$] are mentioned. They are minerals made up of atoms and or molecules in which all the electrons are paired, causing an inversion of the electron orbital movement, which gives zero magnetic moment. Paramagnetics define minerals with positive χ (χ > 0), but weak. This occurs when the electron spins in the presence of an external magnetic field, however, as it is an imposed magnetization, it is not permanent. Representatives of paramagnetic minerals are ilmenite ($FeTiO_3$) and lepidocrocyte (γ - FeOOH).

Certain minerals have a strongly aligned magnetic moment, but with unequal opposing forces controlled by the crystalline structure (Figure 5b), called ferrimagnetic

minerals. This category includes the main magnetic minerals in the soil of lithogenic origin, such as magnetite and titanomagnetite (Fe_2TiO_4), and pedogenic, such as maghemite, (Dearing et al., 1994). Coexisting in the soil, the magnetic signal of maghemite is masked by magnetite, which prevents it from identifying its origin, that is, lithogenic, pedogenic or mixture origin. In general, they are common minerals in basic soils, for example, basaltic rocks and itabirite (Costa et al., 1999; Silva et al., 2010; Camêlo et al., 2017; Pogerre et al., 2018; Silva et al., 2020).

Common in tropical soils, especially in advanced weathering stages, goethite and hematite (Cornell and Schwertmann, 2003; Melo and Aleonni, 2009) are antiferromagnetic minerals (Figure 5d). The representatives of this group have the spins of identical magnetic moments aligned in opposite directions, giving positive or zero net magnetization. According to Peters and Dekkers (2003), the magnetic signal of these minerals varies from 0.13 to 3.83 × 10^{-6} m^3 kg^{-1} for goethite, and from 0.46 to 5.92 × 10^{-6} m^3 kg^{-1} for hematite, which may explain the χ in soils with low levels of Fe_3O_3, in which the formation of maghemite and magnetite is disadvantaged. Although the contribution of hematite and goethite in the magnetic signal of the soil is modest when compared to maghemite and magnetite, it should not be ruled out, especially in soils with low levels of Fe_2O_3 (*e.g*. sandstone soils), as goethite and hematite may be the only source magnetic field (Siqueira et al., 2010; Camargo et al., 2016).

In addition to the intrinsic characteristic of the mineral, the magnetic signal of the soil is controlled by the type of rock, climate, vegetation, relief and anthropic activity (Grimley et al., 2004; Hanesch and Scholger, 2005). Fontes et al. (2000) analyzed the χ of the sand, silt and clay fractions of ten Brazilian soils, and concluded that the magnetic behavior of the soils was coordinated by the nature of the source material. A similar result was found by Camêlo et al. (2017) in soils of different origins: basalt, tufite, itabirite, amphibolite and gabbro. Pedological studies indicate an increase in χ with the degree of weathering in well-drained soils (Camêlo et al., 2017; Poggere et al., 2018), but this is not always the case. The enrichment of magnetic minerals with the weathering of the soil seems to occur in soils formed from the same source material (Hanesch and Scholger, 2005).

In the soil, the particle size of the magnetic minerals and the phenomenon of isomorphic substitution also contribute to different and wide χ values (Batista et al.,

2010). The influence of particle size on soil χ can be inferred by the frequency dependent on magnetic susceptibility ($\chi_{fd\%}$), which, according to Dearing (1994), assumes values between 0 to 14%. Based on the size of particles, magnetic minerals can be classified into multidomains (MD: Ø between 100 - 1000 μm), pseudo-domain (PSD), single stable domain (SSD) and superparamagnetic (SP: Ø <1 μm). Very large particles have multiple magnetization zones, a typical case of magnetite, being characterized by magnetic multidomains. Small particles, less than 1 μm, characterize single-domain magnetic minerals, called superparamagnetic, such as maghemite. Thus, $\chi_{fd\%}$ suggests the origin of magnetic minerals in the soil.

Another common phenomenon in soil is the isomorphic substitution in Fe oxides (Cornell and Schwertmann, 2003). In general, in an advanced stage of pedogenesis it is common to exchange Fe in the crystalline structure of magnetic oxides by diamagnetic elements, such as Al (aluminum), providing a χ decay, a finding clarified by Batista et al. (2010). There is little information in the literature about maghemite, and the limit of Al and Fe isomorphic substitution is not yet known; such information would be of great value to elucidate the participation of maghemite in the mechanism of adsorption of ionic species from the soil and, consequently, for the definition of management zones.

Large variations in the isomorphic substitution capacity in maghemite, from 16 to 26 mol% of Fe by Al in highly weathered soils, were found by Fontes and Weed (1991). In synthetic samples, Gillot and Rousset (1990) reported up to 66 mol% of Al in maghemite prepared from organic precursors, while Wolska and Schwertmann (1989) proposed a limit of 10 mol% for samples prepared from inorganic precursors. However, the isomorphic substitution of Fe for Al in the structure of the magnetic oxides does not only occur with Al, with a cation exchange record for Cd and Zn (Barista et al., 2008). Therefore, the replacement of Fe by diamagnetic elements reduces the magnetic signal from the soil.

The magnetic signal from the soil can also be affected by agricultural activities (Barrios et al., 2017). It turns out that Fe oxides are sensitive to environmental changes (Cornell and Schwertmann, 2003). In fact, Camargo et al. (2016) found high $\chi_{fd\%}$ values, above 14% in sugarcane areas, which in the past were burned to facilitate

harvesting. Values of this magnitude, for Dearing (1994), are strong indications of a predominance of superparamagnetic minerals, such as maghemite. Oxidation of ferrihydrite from fire in the presence of organic matter, or antiferromagnetic minerals such as goethite and hematite, becomes maghemite (Schwertmann and Fechter, 1984; Anand and Gilkes, 1987). This would be the main thesis for the high values of χ in soils of Terra Preta de Indio da Amazônia, Brazil (Oliveira, 2017), with its genesis intertwined with the practice of fire by indigenous peoples.

χ has facilitated the recognition of specific management areas, assisting in the tactical and operational decisions of agricultural activities (Siqueira et al., 2010; Camargo et al., 2013; 2016; Marques Jr et al., 2015; Peluco et al., 2015; Barbosa et al., 2019) and as a digital marker of environmental quality (Hanesch et al. 2001; Jordanova et al. 2004). Barbosa et al. (2019) used χ to predict soil erodibility of a basalt-sandstone transect, aiming at a less expensive mapping. The results of Peluco et al. (2015) ratified the potential of χ in recognizing specific areas for application of phosphorus at a varied rate. Reasons such as *(I)* low equipment acquisition cost; *(II)* easy operation; *(III)* non-destructive technique (that is, it does not require chemical extractors); *(IV)* does not require prior preparation of the samples; *(V)* providing instant results; (VI) ease of measurements in the laboratory and in the field, *(VII)* and *(VIII)* are measures that complement many other types of environmental analysis. These advantages make χ promising in the management of agricultural activities.

The proposal of the spectral signature by DRS and χ is complementary to the results of conventional analyzes, such as XRD (Silva et al., 2020), dissolution of Fe (Mehra and Jackson, 1960; Schwertmann, 1964; McKeague and Day, 1966), spectroscopy de Mössbauer (Murad and Johnston, 1987), which are routinely used in the analysis of Fe oxide minerals in a smaller amount. DRS results are also complementary to magnetic signature results (Grimley and Vepraskas, 2000; Grimley et al., 2004; Siqueira et al., 2010; Marques Jr et al., 2014) and orbital sensor spectroradiometry (Viscarra Rossel et al., 2009, 2010, 2015) and proximal (Demattê et al., 2004; 2007; 2015).

Given the current scenario of modern and globalized agriculture, the technological advent of sensors makes it feasible to know the soil on a detailed scale,

responding to some gaps left by traditional soil mapping that limit the development of precision agriculture. Although, pioneering studies in Brazil (Camargo et al., 2008ab; Siqueira et al., 2010; Marques Jr et al., 2015; Peluco et al., 2015; Teixeira et al., 2018; Barbosa et al., 2019) have raised the potential of DRS and χ, so far they have only been implemented in smaller areas. Therefore, it is substantial to prove simpler techniques, of low cost and with known accuracy to provide opportunities for mapping soil attributes at a detailed level in large areas.

1.3 General material and methods

1.3.1 Site and geomorphological background

The study area was located in the Western Paulista Plateau, which spans about 13 million hectares (roughly 45% of the São Paulo state, Brazil). Also, their locations spanned the climatic spectrum of the area. Based on the classification of Thornthwaite (1948), the climate is tropical with dry winters ($C_2rA'a'$) in the north and northwest; humid temperate with hot summers ($B_4rB_4'a$) in the south; and temperate humid with dry winters and hot summers ($B_2rB_3'a$) in the east and southeast. The natural vegetation consists of Atlantic forest species in the west, and Savannahs in the east and southeast.

Geologically, the Plateau dates from the higher Cretaceous (88–65 million years) and was formed largely (57%) from sandstones in the Vale do Rio do Peixe formation (VRP), Bauru Group, over the basaltic spills (15%) of the Serra Geral formation (SG), and other sedimentary formations (27%) (Fernandes et al., 2007) (6a). The landform map was elaborated according to the method proposed by Vasconcelos et al. (2012), based on the geomorphometric signature. The method aims to classify subtle changes in landforms, reducing the subjectivity of identifying compartments by conceptual landscape models (Troeh, 1965; Daniels et al., 1971), applicable at several scales (Teixeira et al., 2018). Information from the Shuttle Radar Topography Mission (SRTM) was used for elaborating the geomorphometric signatures. The SRTM Digital Elevation Model (DEM) is a regular grid with a spatial resolution of 03 arcsec (~90 m) and a vertical accuracy of 15 m (Smith and Sandwell, 2003).

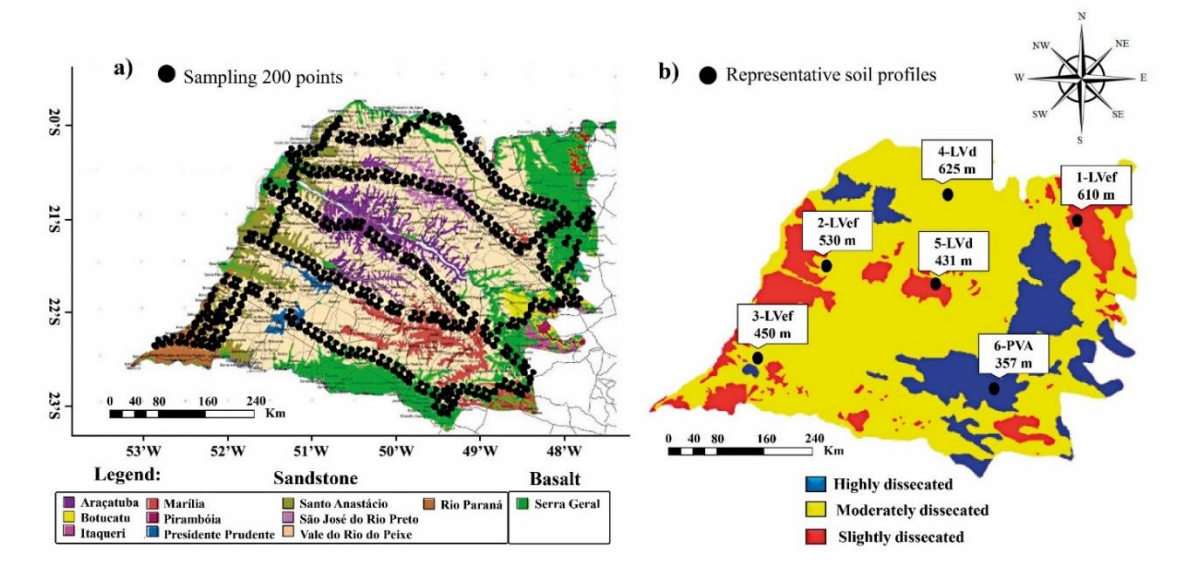

Figure 6. Geological maps (Fernandes et al., 2007) (*a*) and landscape dissection units (Vasconcelos et al., 2012) (*b*) representative soil profiles in the Western Paulista Plateau: 1, 2 and 3 - Rhodic Eutrudox (LVef), 4 and 5 - Rhodic Hapludox (LVd) and 6 - Typic Kandiudalf (PVA) (Soil Survey Staff, 2010).

By interpreting the landform intensity map of Fernandes et al. (2007) for the Western Paulista Plateau, Vasconcelos et al. (2012) succeeded in identifying three different levels of landscape dissection, namely: slightly dissected (Sd), moderately dissected (Md), and highly dissected (Hd) (Figure 6b). The identification of dissection levels was supplemented with field observations intended to confirm the mutual relationships between components of the physical environment. Sd units characterize the most stable landscapes, soft wavy and flat, convex and linear-convex relief, predominating at the top of the landscape, with an altitude of 450–610 m, and occupying an extension of 20,365 ha. Md units dominate the landscape, with an extension of 92,209 ha, found at altitudes of 431–529 m, and soils in evolution processes. Spanning approximately 21,629 ha, Hd units are depressed areas, where drainage networks are located, with the occurrence of less weathered soils and water table fluctuation. It has steep relief, of concave-convex type and V-shaped valleys, whose altitude varies from 250 to 550 m.

1.3.2 Soil sampling

Soil surveys were carried out and six profiles representing the geological diversity and landscape dissection units were selected (Figure 6) in order to examine the variation of the total iron oxide (Fe_2O_3) content with depth as an indicator of lithological contrast. The trenches were dug at altitude from 250 m to the greatest in the Plateau (610 m). The soils are mainly Latosols (Oxisols) or Argisols (Ultisols) (Soil Survey Staff, 2010; Santos et al., 2018).

The state highway map of the Brazilian roads and traffic department was used to construct a sampling plan with the aid of the ET GeoWizards tool in the software ArcView 9.3. A total of 300 samples were collected from the 0.0–0.2 m soil layer at representative points with minimal anthropic interference (Figure 6a). However, with routine laboratory analyzes, some samples were lost or contained an insufficient quantity for specific analyzes. Thus, 200 soil samples were used for the elaboration of the second chapter, and 291 for the third chapter. The shortest and longest distance between sampling points was 10 and 60 km, respectively. The points were well distributed in space to ensure that the samples would be representative of lithology and landscape dissection units (Figure 6). The number of sampling points used was based on the experience gathered in previous geostatistical studies on WPP (Marques Jr et al., 2015; Teixeira et al., 2018).

1.3.3 Laboratory analysis

1.3.3.1 Conventional soil analysis

Soil samples were passed through 2 mm sieves (air-dried fine earth, ADFE) from the studied profiles (B horizons) were analyzed for Si, Al, and Fe by total analysis with sulfuric acid (H_2SO_4, ratio 1:1). The total contents thus determined were used to calculate Ki and Kr (Santos et al., 2018). The $Ki = 1.7 \times \%SiO_2 / \%Al_2O_3$ and $Kr = 1.7 \times \%SiO_2 / (\%Al_2O_3 + 0.6325 \times \%Fe_2O_3)$ indices were used to indicate the development stage of soils: more weathered–leached soils show low indices (Donagema et al., 2011; Silva et al., 2020). Crystalline free iron (Fed) was extracted with sodium dithionite–citrate– bicarbonate (DCB) at 25 °C for 16 h and determined according to

Mehra and Jackson (1960). Finally, poorly crystalline iron oxides (Feo) were extracted with ammonium oxalic acid and quantified according to McKeagne and Day (1966). Particle size distribution was determined by using a 0.1 M NaOH solution under slow stirring as a dispersant, and the clay fraction was quantified with the pipette method (Donagema et al., 2011).

1.3.3.2 Mineralogical analysis

1.3.3.2.1 X-ray diffraction

Clay fraction of the 300 samples was used to quantify Hematite (Hm), goethite (Gt) and maghemite (Mh) by powder X-ray diffraction (XRD). The concentrated Fe-oxides fraction were obtained by boiling the clay in 5 mol L^{-1} NaOH (Norrish and Taylor, 1961), whereas kaolinite (Kt), gibbsite (Gb) and the Gb/(Gb + Kt) ratio were estimated after removing iron oxides from the clay fraction (Mehra and Jackson, 1960). Samples were diffracted on a Bruker D8 Advance instrument using Cu Kα radiation. The proportions of Gt, Hm and Mh in the iron oxide concentrate were calculated from the areas of the (110), (012) and (220) peaks, respectively, as well as the difference Fed–Feo. The areas for the (012) and (220) peaks were multiplied by a factor of 3.5 because there was overlap by any other peak. The total area was taken to be the combination of (110), 3.5 times (012) and 3.5 times (220) (Equations 1–3). Finally, the Kt/(Kt + Gb) ratio was calculated from the areas of the reflection peaks (002) for gibbsite and (001) for kaolinite.

$$\mathrm{Gt}\% = \left(\frac{\text{area Gt}(110)}{\text{total area}}\right) \times 100 \quad (1)$$

$$\mathrm{Hm}\% = \left(\frac{\text{area Hm}(012)\times 3.5}{\text{total area}}\right) \times 100 \quad (2)$$

$$\mathrm{Mh}\% = \left(\frac{\text{area Mh}(220)\times 3.5}{\text{total area}}\right) \times 100 \quad (3)$$

The proportions of Gt, Hm and Mh were also determined by applying the Rietveld refinement as implemented in the software Powder Cell v. 2.4. The files with

the crystal structures of the oxides were obtained from the American Mineralogist Crystal Structure Database (Downs and Hall-Wallace, 2003). Spectra were adjusted by using a polynomial function for the baseline and reflections with the pseudo-Voigt model, and the width at half-height was calculated from the angular parameters *U*, *V* and *W*: $WHH = (U\tan^2\theta + V\tan\theta + W)^{1/2}$. The refinement quality was assessed in terms of R_{exp} and goodness of fit (GOF) (Young et al., 1995). Thus, R_{exp} values < 10 and GOF values < 2 were deemed good, whereas R_{exp} values > 10 but < 20 and GOF values > 2 but < 5 were judged acceptable.

1.3.3.2.2 Diffuse reflectance spectroscopy

Alternatively, samples were also analyzed by DRS. For this purpose, an amount of 1 g of air-dried fine earth (ADFE) was ground to constant color in a mortar and placed in a cylindrical holder of 16 mm in diameter. Reflectance measurements (*R*) were obtained with a Lambda 950 UV/Vis/NIR spectrometer coupled to an integrating sphere of 150 mm in diameter. Spectra were recorded at 0.5 nm intervals over the wavelength range of 250–2500 nm (Vis-NIR), using an integration time of 2.43 nm s^{-1} and Halon (PTFE) as a blank.

The spectral data were used to calculate the second derivative of the Kubelka-Munk function over the wavelength range of 380–710 nm (Kubelka and Munk, 1931). A spline procedure involving 30 data points was used to estimate the Hm/(Hm + Gt) ratio according to Scheinost et al. (1998). This procedure allowed comparing DRS potential in the estimation of Gt and Hm obtained by XRD. According to Torrent and Barrón (2002), this procedure allows Gt and Hm contents lower than 0.1% – which is one order of magnitude lower than the limit for the XRD technique – to be determined.

1.3.3.3 Selective dissolution in 1.8 mol L^{-1} H_2SO_4

Triplicate 0.1 g portions of clay previously treated with boiling 5M NaOH to concentrate the iron oxides were digested with 1.8 mol L^{-1} H_2SO_4 at 75 °C for 2 h (Schwertmann and Fetcher, 1984; modified by Costa et al., 1999). In order to selectively dissolve Fe from Mh (Mh-H_2SO_4), the extraction procedure was optimized

with the aid of low-frequency magnetic susceptibility (χ_{lf}) measurements (Costa et al., 1999); thus, digestion was finished when χ_{lf} decreased to 5% of its initial value. Iron thus extracted was quantified by atomic absorption spectroscopy and the results multiplied by a factor of 1.43 to calculate the amount of Mh-Fe_2O_3.

1.3.3.4 Magnetic susceptibility measurements

Magnetic susceptibility (χ) was measured at a low frequency (lf, 0.47 kHz) and a high frequency (hf, 4.7 kHz), using a Bartington MS2 instrument for measurements in (1) air-dried fine earth [χ_{lf}-ADFE], (2) the clay fraction and (3) the (silt + sand) fraction. Dual frequency measurements allowed us to calculate the frequency-dependent percent magnetic susceptibility ($\chi_{fd\%}$, Eq. 4) (Dearing, 1999), a proxy for the presence of single, multiple and superparamagnetic minerals of the magnetic domain. Samples with very high χ_{fd} values (≥ 14%) were reanalyzed for confirmation.

$$\chi\mathrm{fd}\% = \left(\frac{\chi\mathrm{lf} - \chi\mathrm{hf}}{\chi\mathrm{lf}}\right) \times 100 \quad (4)$$

Where, χ_{lf}, χ_{hf} and $\chi_{fd\%}$ are the low-frequency, high-frequency and percent frequency-dependent magnetic susceptibility, respectively.

Triplicate samples of ADFE were also extracted with DCB for 16 h (Mehra and Jackson, 1960). This was followed by centrifugation, removal of the supernatant and washing with deionized water, the process being repeated three times at 3000 rpm for 10 min. The centrifuged residue was used to measure χ_{lf} and the difference in χ_{lf} before and after extraction with DCB was assumed to correspond to maghemite (Mh-χ_{lf}-DCB). A conversion factor of 763 × 10^{-6} m^3 kg^{-1} was used in Equation 5 to estimate Mh in g kg^{-1} (Peters and Dekkers, 2003). An identical procedure was used to quantify magnetite (McKeague and Day, 1966), the content in which was estimated from the magnetic susceptibility remaining in the residual (sand + silt) fraction [χ_{lf}-rem], using a conversion factor of 1000 × 10^{-6} m^3 kg^{-1} in Equation 6.

$$\mathrm{Mh} = \left(\frac{\chi\mathrm{lf\ ADFE} - \chi\mathrm{lf\ rem}}{763 \times 10^{-6}}\right) \times 10 \quad (5)$$

$$\mathrm{Mt} = \left(\frac{\chi\mathrm{lf\ rem} \times 100}{1000 \times 10^{-6}}\right) \times 10 \quad (6)$$

Where, χ_{lf} and χ_{lf}-rem are the low-frequency magnetic susceptibility of the ADFE fraction before and after extraction, respectively.

Maghemite was also determined in the oxide-concentrated clay fraction obtained by boiling in 5 mol L^{-1} NaOH, the content thus obtained being designated Mh-χ_{lf}-NaOH:

$$\mathrm{Mh} = \left(\frac{\chi\mathrm{lf\ concentrated\ clay}}{763 \times 10^{-6}}\right) \times 10 \quad (7)$$

Where, χ_{lf} is the low-frequency magnetic susceptibility of the oxide-concentrated clay fraction.

1.3.4 Statistical and geostatistical analysis

The analytical results were initially used to calculate means, maximum and minimum values, medians, standard deviations, coefficients of variation, asymmetry, and kurtosis. The means for landscape dissection units were compared by the Tukey's test (5%), and Gt and Hm contents were estimated from XRD patterns, and the DRS alternative procedure was subjected to regression analysis. XRD and DRS results were compared in terms of the following parameters: coefficient of determination (R^2), mean error (ME, Eq. 8), standard deviation of the error (SDE, Eq. 9), residual prediction deviation (RPD, Eq. 10), and root mean square error (RMSE, Eq. 11). The RPD is the ratio of the standard deviation of the original data by the RMSE of cross validation predictions. RPD values were classified according to Chang et al. (2001) as excellent (RPD > 2), acceptable (1.4 < RPD < 2) or unreliable (RPD < 1.4). Usually, accurate

models have high R^2 and RPD values but low RMSE and SDE values. These parameters were calculated according to Viscarra Rossel et al. (2006).

$$ME = \frac{1}{N}\sum_{i=1}^{n}(\hat{y}_i - y_i) \quad (8)$$

$$SDE = \frac{\sum_{i=1}^{n}(\hat{y}_i - y_i)^2}{N-1} \quad (9)$$

$$RPD = {SD}/{RMSE} \quad (10)$$

$$RMSE = \sqrt{\frac{1}{N}\sum_{i=1}^{n}(\hat{y}_i - y_i)^2} \quad (11)$$

Where, N is the number of estimated values, $\hat{y}_i$ is the predicted value, and y_i is the observed value; ME < 0 indicates that observed values are underestimated by predicted values, and ME > 0 indicates overestimated values.

1.3.4.1 Spatial variability

Spatial variability of Hm and Gt values obtained with the two techniques was assessed geostatistically. The experimental semivariance was calculated according to Oliver and Webster (2014) criteria from the following equation:

$$\hat{\gamma}(h) = \frac{1}{2N(h)}\sum_{i=1}^{N(h)}[Z(x_i) - Z(x_i+h)]^2 \quad (12)$$

Where, $\hat{\gamma}(h)$ is the semivariance at distance h, $N(h)$ is the number of pairs used to calculate h, $Z(x_i)$ is the value of the attribute Z at position x_i, and $Z(x_i + h)$ is the value of the attribute Z at a distance h from x_i.

The spherical mathematical model used was fitted to the variograms in terms of the number of pairs used to estimate the semivariance, the sum of the square of residuals (SQR), the presence of a sill in the variograms (Oliver and Webster, 2014),

and the coefficient of determination (R^2). Once variograms were modeled by GS$^+$ software (Robertson, 1998), the values corresponding to the unknown points were estimated by ordinary kriging and the maps processed with Surfer (1999) software. The degree of spatial dependence (DSD) was estimated from the ratio of the nugget effect (C_0) to the sill ($C_0 + C_1$). An attribute was assumed to have high, moderate or low DSD if its $C_0/(C_0 + C_1)$ ratio was lower than 25%, 25–75% or higher than 75%, respectively (Cambardella et al., 1994).

1.3.4.2 Validation of spectral maps

The spatial patterns for Gt and Hm obtained from XRD and DRS results were compared through traits. The percent variability at a local scale was calculated from the following equation:

$$\Delta\,(\%) = \frac{\text{DRS-XRD}}{\text{XRD}} \times 100 \qquad (13)$$

A Δ value of up to 20% for XRD values was taken to be acceptable here. This criterion was assumed based on the degree of similarity between DRS and XRD maps and geology (Camargo et al., 2016; Silva et al., 2020). Positive and negative Δ values were assumed to represent over- and underestimation, respectively, in an attribute. This parameter allowed us to classify Hm and Gt estimates as acceptable or unacceptable.

1.3 References

Almeida JA, Torrent J, Barrón V (2003) Cor de solo, formas do fósforo e adsorção de fosfatos em Latossolos desenvolvidos de basalto do extremo-sul do Brasil. **Revista Brasileira de Ciência do Solo** 27:985-1002.

Anand RR, Gilkes RJ (1987) The association of maghemite and corundum in Darling Range laterites, Western Australia. **Australian Journal of Soil Research** 35:303–311.

Bahia ASRS, Marques Jr J, Siqueira DS (2015) Procedures using diffuse reflectance spectroscopy for estimating hematite and goethite in Oxisols of São Paulo, Brazil. **Geoderma** 5:150–156.

Balsam W, Ji J, Renock D, Deaton BC, Williams E (2014) Determining hematite content from NUV/Vis/NIR spectra: Limits of detection. **American Mineralogist** 99:2280–2291.

Barbieri DM, Marques Jr J, Pereira GT, La Scala Jr N, Siqueira DS, Panosso AR (2013) Comportamento dos óxidos de ferro da fração argila e do fósforo adsorvido, em diferentes sistemas de colheita de cana-de-açúcar. **Revista Brasileira de Ciência do Solo** 37:1557–1568.

Barbosa RS, Marques Jr J, Barrón V, Martins Filho MV, Siqueira DS, Peluco RG, Camargo LA, Silva LS (2019) Prediction and mapping of erodibility factors (USLE and WEPP) by magnetic susceptibility in basalt-derived soils in northeastern São Paulo state, Brazil. **Environmental Earth Sciences** 78:1-12.

Barrón V, Mello JWV, Torrent J (2000) Caracterização de óxidos de ferro em solos por Espectroscopia de Reflectância Difusa. In.: Novais RF, Alvarez VH, Schaefer CEGR (Eds.) **Tópicos em ciência do solo**. Viçosa: Sociedade Brasileira de Ciência do Solo, p. 139-162.

Barrón V, Torrent J (1986) Use of the Kubelka-Munk theory to study the influence of iron oxides on soil color. **Journal of Soil Science** 37:499-510.

Barrón V, Torrent J (2002) Evidence for a simple pathway to maghemite in earth and mars soils. **Geochimica et Cosmochimica Acta** 66:2801-2806.

Batista MA, Costa ACS, Bigham JM, Santana H, Zaia DAM, Souza Junior IG (2010). Mineralogical, Chemical, and Physical Characterization of Synthetic Al-substituted Maghemites (γ-$Fe_{2-x}Al_xO_3$). **Clays and Clay Minerals** 58:451–461.

Bazaglia Filho O (2012) **Comparação entre mapas de solos obtidos pelos métodos convencional e digital numa área complexa**. 190 f. Dissertation (MSc in Soils and Plant Nutrition) – Escola Superior de Agricultura Luiz de Queiroz/USP, Piracicaba.

Ben-Dor, E, Heller D, Chudnovsky A (2008) A novel method of classifying soil profiles

in the field using optical means. **Soil Science Society of American Journal** 72:1113−1123.

Bigham JM, Fitzpatrick RW, Schulze D (2002) Iron oxides In.: Dixon JB, Schulze DG. **Soil mineralogy with environmental applications**. Madison: Soil Science Society of America, p. 323-366. (Book Series, 7).

Budiman M, McBratney AB, Mendonça-Santos ML, Santos HG (2003) **Revisão sobre funções de pedotransferência (PTFs) e novos métodos de predição de classes e atributos do solo**. Rio de Janeiro: Embrapa Solos, 50 p. (Documento 45).

Camargo LA, Marques J Jr, Pereira GT (2013) Mineralogy of the clay fraction of Alfisols in two slope curvatures: III – Spatial variability. **Revista Brasileira de Ciência do Solo** 37:295–306.

Camargo LA, Marques Jr J, Barrón V, Alleoni LRF, Barbosa RS, Pereira GT (2015) Mapping of clay, iron oxide and adsorbed phosphate in Oxisols using diffuse reflectance spectroscopy. **Geoderma** 251–252:124–132.

Camargo LA, Marques Jr J, Pereira GT, Alleoni LRF, Bahia ASRS, Teixeira DDB (2016) Pedotransfer functions to assess adsorbed phosphate using iron oxide content and magnetic susceptibility in an Oxisol. **Soil Use and Management** 32:172–182.

Camargo LA, Marques Jr J, Pereira GT, Bahia ASRS (2014) Clay mineralogy and magnetic susceptibility of Oxisols in geomorphic surfaces. **Scientia Agricola** 71:244-256.

Camargo LA, Marques Jr J, Pereira GT, Horvat RA (2008a) Variabilidade espacial de atributos mineralógicos de um Latossolo sob diferentes formas do relevo: II - correlação espacial entre mineralogia e agregados. **Revista Brasileira de Ciência do Solo** 32:2279–2288.

Camargo LA, Marques Jr J, Pereira GT, Horvat RA (2008b) Variabilidade espacial de atributos mineralógicos de um Latossolo sob diferentes formas de relevo. I-Mineralogia da fração argila. **Revista Brasileira de Ciência do Solo** 32:2269–2277.

Cambardella CA, Moorman TB, Novak JM, Parkin TB, Karlen DL, Turco RF, Konopka AE (1994) Field-scale variability of soil properties in Central Iowa Soil. **Soil Science Society of America Journal** 58:1501-1508.

Camêlo DL, Ker JC, Fontes MPF, Corrêa MM, Costa ACS, Melo VF (2017) Pedogenic iron oxides in iron-rich Oxisols developed from mafic rocks. **Revista Brasileira de Ciência do Solo** 41:e0160379.

Campos MCC, Marques Jr J, Pereira GT, Montanari R, Camargo LA (2007) Relações solo-paisagem em uma litossequência arenito-basalto na região de Pereira Barreto, SP. **Revista Brasileira de Ciência do Solo** 31:519-529.

Cañasveras JC, Barrón V, Del Campillo MC, Torrent J, Gómez JA (2010) Estimation of aggregate stability indices in Mediterranean soils by diffuse reflectance spectroscopy. **Geoderma** 158:78–84.

Carioca AC, Costa GM, Barrón V, Ferreira CM, Torrent J (2011) Aplicação da espectroscopia de reflectância difusa na quantificação dos constituintes de bauxita e de minério de ferro. **Revista Escola de Minas** 64:199–204.

Carrer H, Barbosa AL, Ramiro DA (2010) Biotecnologia na agricultura. **Estudos Avançados** 24:149–164.

Carvalho CCN, Nunes FC, Antunes MAH (2013) Histórico do levantamento de solos no Brasil: da industrialização brasileira à era da informação. **Revista Brasileira de Cartografía** 65:681-694.

Carvalho Filho A, Inda AV, Fink JR, Curi N (2015) Iron oxides in soils of different lithological origins in Ferriferous Quadrilateral (Minas Gerais, Brazil). **Applied Clay Science** 118:1-7.

Chen J, Ji J, Balsam W, Chen Y, Liu ZA (2002) Characterization of the Chinese loess–paleosol stratigraphy by whiteness measurement. **Palaeogeography, Palaeoclimatology, Palaeoecology** 183:287–297.

Chinese Soil Taxonomy Research Group, Institute of Soil science, Chinese Academy Sciences, Cooperative Research Group on Chinese Soil Taxonomy (2001). **Keys to Chinese Soil Taxonomy**. 3rd ed. Hefei: Chinese Science and Technological University Press.

Coblinski JA, Giasson É, Demattê JAM, Dotto AC, Costa JJF, Vašát R (2020) Prediction of soil texture classes through different wavelength regions of reflectance spectroscopy at various soil depths. **Catena** 189:104485.

Cornell RM, Schwertmann U (2003) **The Iron Oxides:** Structure, Properties, Reactions, Occurrence, and Uses. Weinheim: Wiley VCH. 664 p.

Cornell RM, Schwertmann, U (1996) **The Iron Oxides:** Structure, Properties Reactions Occurrence and Uses. New York: Weinheim-VCH. 573 p.

Costa ACS, Bigham JM, Rhoton FE, Traina SJ (1999) Quantification and characterization of maghemite in soils derived from volcanic rocks in southern Brazil. **Clays and Clay Minerals** 47:466–473.

Coventry RJ, Taylor R, Fitzpatrick RW (1983) Pedological significance of the gravel in some red and grey earth of central North Queensland. **Australian Journal of Soil Research** v. 21:219–240.

Curi N, Franzmeier DP (1984) Toposequence of Oxisols from the central plateau of Brazil. **Soil Science Society of America Journal** 48:341-346.

Daniels RB, Gamble EF, Cady JG (1971) The relation between geomorphology and soil morphology and genesis. **Advances in Agronomy** 23:51-87.

Dantas JS, Marques Jr J, Martins Filho MV, Resende JMA, Camargo LA, Barbosa RS (2014) Gênese de solos coesos do Leste Maranhense: relação solo-paisagem. **Revista Brasileira de Ciência do Solo** 38:1039–1050.

Dearing, JA (1994) **Environmental magnetic susceptibility**: using the Bartington MS2 system. England: British Library. 104 p.

Dearing JA (1999) **Environmental magnetic susceptibility:** Using the Bartington MS2 system. 2nd ed. Keniloworth: Chi Publishing. 54 p.

Demattê JAM, Araújo SR, Fiorio PR, Fongaro CT, Nanni MR (2015) Espectroscopia VIS-NIR-SWIR na avaliação de solos ao longo de uma topossequência em Piracicaba (SP). **Revista Ciência Agronômica** 46:679– 688.

Demattê JAM, Galdos MV, Guimarães R, Genú AM, Nanni MR, Zullo Jr J (2007) Quantification of tropical soil attributes from ETM+/Landsat-7 data. **International Journal of Remote Sensing** 8:3813–3829.

Demattê JAM, Genú AM, Fiorio PR, Ortiz JL, Mazza JA, Leonardo HCL (2004) Comparação entre mapas de solos obtidos por sensoriamento remoto espectral e pelo método convencional. **Pesquisa Agropecuária Brasileira** 39:1219–1229.

Demattê JAM, Terra F, Quartaroli CF (2012) Spectral behavior of some modal soil profiles from São Paulo State, Brazil. **Bragantia** 71:413-423.

Donagema GK, Campos DVB, Calderano SB, Teixeira WG, Viana JHM (2011). **Manual de métodos de análise do solo**. 2nd ed. Rev. Rio de Janeiro: Embrapa Solos.

Dotto AC, Dalmolin RSD, Araújo Pedron F, Caten A, Ruiz LFC (2014) Mapeamento digital de atributos: granulometria e matéria orgânica do solo utilizando espectroscopia de reflectância difusa. Revista Brasileira de Ciência Do Solo, 38:1663–1671.

Downs, RT and Hall-Wallace, M (2003) The American Mineralogist Crystal Structure Database. **American Mineralogist** 88, 247-250. Available on: <http://rruff.geo.arizona.edu/AMS/amcsd.php> (accessed on: Feb. 10, 2020).

Fabris JD, Viana JHM, Schaefer CEGR, Wypych F, Stucki JW (2009) Métodos físicos de análises em mineralogia do solo. In.: Alleoni LRF, Melo VF (Eds.) **Química e mineralogia dos solos**. Viçosa: Sociedade Brasileira de Ciência do Solo, p. 611–694.

Fernandes LA, Castro AB, Basilici G (2007) Seismites in continental sand sea deposits of the Late Cretaceous Caiuá Desert, Bauru Basin, Brazil. **Sedimentary Geology** 199:51–64.

Fernandes RBA, Barrón V, Torrent J, Fontes MPF (2004) Quantificação de óxidos de ferro de Latossolos brasileiros por espectroscopia de refletância difusa. **Revista Brasileira de Ciência do Solo** 28:245–257.

Ferreira SAD, Santana DP, Fabris JD, Curi N, Nunes Filho E, Coey JMD (1994) Relações entre magnetização, elementos traços e litologia de duas seqüências de solos do estado de Minas Gerais. **Revista Brasileira de Ciência do Solo** 18:167-174.

Fidêncio PH, Ruisánchez I, Poppi RJ (2001) Application of artificial neural networks to the classification of soils from São Paulo state using near-infrared spectroscopy. **Analyst** 126:2194–2200.

Fitzpatrick RW, Schwertmann U (1982) Al-substituted goethite – an indicator of pedogenic and other weathering environments in South Africa. **Geoderma** 27:335-347.

Fontes MPF, Oliveira TS, Costa LM, Campos AAG (2000) Magnetic separation and evaluation of magnetization of Brazilian soils from different parent materials. **Geoderma** 96:81-99.

Fontes MPF, Weed SB (1991) Iron oxides in selected Brazilian Oxisols: I. Mineralogy. **Soil Science Society of America Journal** 55:1143-1149.

Geladi P, Kowalski BR (1986) Partial least-squares regression: a tutorial. **Analytica Chimica Acta** 185:1–17.

Ghidin AA, Melo VF, Lima VC, Lima JMJC (2006) Topossequências de Latossolos originados de rochas balsáticas no Paraná. I - Mineralogia da fração argila. **Revista Brasileira de Ciência do Solo** 30:293–306.

Gillot B, Rousset A (1990) On the limit of aluminum substitution in Fe3O4 and g-Fe_2O_3. **Physica Status Solidi (a) - Applied Research** 118: K5-K8.

Gmur S, Vogt D, Zabowski D, Moskal LM (2012) Hyperspectral Analysis of Soil Nitrogen, Carbon, Carbonate, and Organic Matter Using Regression Trees. **Sensors** 12:10639–10658.

Gomes, RP (2017) **Gênese, mineralogia e dinâmica do fósforo nos solos do Planalto Ocidental Paulista**. 76 f. Dissertação (Mestrado em Ciência do Solo) – Unesp, Jaboticabal.

Grimley DA, Arruda NK, Bramstedt MW (2004) Using magnetic susceptibility to facilitate more rapid, reproducible, and precise delineation of hydric soils in the midwestern USA. **Catena** 58:83–213.

Grimley DA, Vepraskas MJ (2000) Magnetic Susceptibility for Use in Delineating Hydric Soils. **Soil Science Society American Journal** 64:2174–2180.

Hanesch M, Scholger R (2005) The influence of soil type on the magnetic susceptibility measured throughout soil profiles. **Geophysical Journal International**, 161:50–56.

Hanesch M, Scholger R, Dekkers MJ (2001) The application of fuzzy c-means cluster analysis and non-linear mapping to a soil data set for the detection of polluted sites, **Physics and Chemistry of the Earth** 26:885–891.

Hu P, Liu Q, Torrent J, Barrón V, Jin C (2013) Characterizing and quantifying iron oxides in Chinese loess/paleosols: Implications for pedogenesis. **Earth and Planetary Science Letters** 369-370:271–283.

Hunt GR, Salisbury JW, Lenhoff CJ (1971) Visible and near-infrared spectra of minerals and rocks: III. Oxides and hydroxides. **Modern Geology** 2:195-205.

Inda Júnior AV, Kämpf N (2005) Variabilidade de goethita e hematita via dissolução redutiva em solos de região tropical e subtropical. **Revista Brasileira de Ciência do Solo** 29:851–866.

Janik LJ, Keeling JL (1996) **Quantitative determination of halloysite using FT-IR PLS analysis and itsapplicaton to the characterisation of kaolins from north-western Eyre Peninsula, South Australia**. Divisional Report 129. Adelaide: CSIRO Division of Soils, 59 p.

Jenkins R, Snyder RL (1996) **Introduction to X-ray Powder Diffractometry**. New York: John Wiley & Sons. 403 p.

Jordanova D, Hoffmann V, Thomas Fehr K (2004) Mineral magnetic characterization of anthropogenic magnetic phases in the Danube river sediments (Bulgarian part), **Earth and Planetary Science Letters** 221:71–89.

Kämpf N, Curi N (2000) Óxidos de Ferro: indicadores de ambientes pedogênicos. In.: Novais RF, Alvarez VH, Schaefer CEGR (Eds.) **Tópicos em Ciência do Solo**. Viçosa: Sociedade Brasileira de Ciência do Solo, p. 107-138.

Kämpf N, Schwertmann U (1982) The 5 M NaOH concentration treatment for iron oxides in solis. **Clays and Clay Minerals** 30:401–408.

Ker JC (1997) Latossolos do Brasil: uma revisão. **Geonomos** 5:17–40.

Kodaira M, Shibusawa S (2013) Using a mobile real-time soil visible–near infrared sensor for high resolution soil property mapping. **Geoderma** 199:64–79.

Kubelka P, Munk F (1931) Ein beitrag zur optic der farbanstriche. **Zhurnal tekhnicheskoi fiziki** 12:593-620.

Lagacherie P, McBratney AB (2007) Spatial soil information systems and spatial soil inference systems: perspectives for digital soil mapping. In.: Lagacherie P, McBratney AB, Voltz M (Eds.) **Digital soil mapping:** an introductory perspective. Amsterdam: Elsevier, p. 3–24.

Legros JP (2006) **Mapping of the soil**. Translated from french by Sarma, V. A. K. Enfield: Science Publishers p. 411.

Long X, Ji J, Balsam W (2011) Rainfall-dependent transformations of iron oxides in a tropical saprolite transect of Hainan Island, South China: spectral and magnetic measurements. **Journal of Geophysical Research** 116:F03015.

Maher BA, Alekseev A, Alekseeva T (2003) Magnetic mineralogy of soils across the Russian Steppe: climatic dependence of pedogenic magnetite formation. **Palaeogeography, Palaeoclimatology, Palaeoecology** 201:321–341.

Marques Jr J, Alleoni LRF, Teixeira DDB, Siqueira DS, Pereira GT (2015) Sampling planning of micronutrients and aluminium of the soils of São Paulo, Brazil. **Geoderma Regional** 4: 91-99.

Marques Jr J, Lepsch IF (2000) Depósitos superficiais neocenozóicos, superfícies geomórficas e solos em Monte Alto, SP. **Geociências** 19:90-106.

Marques Jr J, Silva Jr JF, Pereira GT, Camargo LA, Teixeira DBB, Panosso AR (2012) Simulação geoestatística na caracterização espacial de óxidos de ferro em diferentes pedoformas. **Revista Brasileira de Ciência do Solo** 36:1690–1703.

Marques Jr J, Siqueira DS, Camargo LA, Teixeira DDB, Barrón V, Torrent (2014) Magnetic susceptibility and diffuse reflectance spectroscopy to characterize the spatial variability of soil properties in a Brazilian Haplustalf. **Geoderma** 219–220:63–71.

Martens H, Naes, T (1989) **Multivariate Calibration**. Chichester: John Wiley & Sons, 419 p.

McBratney AB, Minasny B, Cattle SR, Vervoort RW (2002) From pedotranfer functions

to soil inference systems. **Geoderma** 109:41–73.

McBratney AB, Minasny B, Viscarra Rossel RA (2006) Spectral soil analysis and inference systems: a powerful combination for solving the soil data crisis. **Geoderma** 136:272–278.

McBratney AB, Odeh IOA, Bishop TFA, Dunbar MS, Shatar TM (2000) An overview of pedometric techniques for use in soil survey. **Geoderma** 97:293–327.

Mckeague JA, Day JH (1966) Dithionite and oxalate-extractable Fe and Al as aids in differentiating various classes of soils. **Canadian Journal of Soil Science** 46:13–22.

Mehra OP, Jackson ML (1960) Iron oxide removal from soils and clays by a dithionite-citrate system buffered with sodium bicarbonate. In.: Swineford A (Eds.) **National conference on clays and clay mineral**. Washington: Pergamon Press, p. 317–342.

Melo VF, Alleoni LRF (2009) **Química e mineralogia do solo**. Viçosa: Sociedade Brasileira de Ciência do Solo. 2695 p.

Minasny B, McBratney AB (2008) Regression rules as a tool for predicting soil properties from infrared reflectance spectroscopy. **Chemometrics and Intelligent Laboratory Systems** 94:72–79.

Montanari R, Marques Jr J, Campos MCC, Souza ZM, Camargo LA (2010) Caracterização mineralógica de Latossolos em diferentes feições do relevo na região de Jaboticabal, SP. **Revista Ciência Agronômica** 41:191–199.

Mullins BA (1977) Magnetic susceptibility of the soil and its significance in soil science. **Journal of Soil Science** 28:223-246.

Munsell (1994) **Soil color charts**. Baltimore: Munsell Color Company, 28 p.

Murad E, Johnston JH (1987) In.: Long GJ (Eds.) **Mössbauer Spectroscopy Applied to Inorganic Chemistry**. Vol. 2. New York: Plenum Press, p. 507.

Nguyen TT, Janik LJ, Raupach M (1991). Diffuse reflectance infrared Fourier transform (DRIFT) spectroscopy in soil studies**. Australian Journal of Soil Research** 29: 49-67.

Norrish K, Taylor RM (1961) The isomorphous replacement of iron by aluminum in soil goethites. **Journal of Soil Science** 12:294-306.

O'Rourke SM, Minasny B, Holden NM, McBratney AB (2016) Synergistic Use of Vis-NIR, MIR, and XRF Spectroscopy for the Determination of Soil Geochemistry. **Soil Science Society of America Journal** 80:888.

Oliveira IA (2017) **Suscetibilidade magnética da terra preta arqueológica amazônica**. 85 f. Tese (Doutorado em Ciência do Solo) – Unesp, Jaboticabal.

Oliveira Júnior M (2011) **Marco regulatório das políticas de desenvolvimento regional no Brasil: fundos de desenvolvimento e fundos constitucionais de financiamento**. Núcleo de Estudos e Pesquisas do Senado Federal. Texto para Discussão n. 101. Available on: <https://www12.senado.leg.br/publicacoes/estudos-legislativos>. Accessed on: Feb. 10, 2020.

Oliver MA, Webster R (2014) A tutorial guide to geostatistics: computing and modelling variograms and kriging. **Catena** 113:56-69.

Peluco RG, Marques Jr J, Siqueira DS, Pereira GT, Barbosa RS, Teixeira DDB (2015) Mapeamento do fósforo adsorvido por meio da cor e da suscetibilidade magnética do solo. **Pesquisa Agropecuária Brasileira** 50:259-266.

Peters C, Dekkers MJ (2003) Selected room temperature magnetic parameters as a function of mineralogy, concentration and grain size. **Physics and Chemistry of the Earth** 28:659–667.

Poggere GC, Inda AV, Barrón V, Kämpf N, Brito ADB, Barbosa, JZ, Curi N (2018) Maghemite quantification and magnetic signature of Brazilian soils with contrasting parent materials. **Applied Clay Science** 161:385–394.

Polidoro et al. (2016) **Programa Nacional de Solos do Brasil (PronaSolos)**. Rio de Janeiro: Embrapa Solos, 53 p. – (Documentos / Embrapa Solos, 183).

Resende M, Santana DP, Franzmeier DP, Coey JMD (1988) Magnetic properties of Brazilian Oxisoils. In: INTERNATIONAL SOIL CLASSIFICATION WORKSHOP, **Proceedings…** Rio de Janeiro: Embrapa, p. 78–108.

Salvaggio C, Miller CJ (2001). Methodologies and protocols for the collection of midwave and longwave infrared emissivity spectra using a portable field spectrometer. In: **Proceedings** of the SPIE, SPIE AeroSense, Image Exploitation and Target Recognition, Algorithms and Technologies for Multispectral, Hyperspectral, and Ultraspectral Imagery VII, vol. 4381. Orlando, Florida, USA, 539-548.

Santos HG, Carvalho Júnior W, Dart RO, Áglio MLD, Souza JS, Pares JG, Fontana A, Martins ALS, Oliveira AP (2011) **O novo mapa de solos do Brasil:** legenda atualizada. 2nd ed. Rio de Janeiro: Embrapa Solos, 67 p. (Documentos/Embrapa Solos, 130).

Santos HG, Jacomine PKT, Anjos LHC, Oliveira VA, Lumbreras JF, Coelho MR, Almeida JA, Araujo Filho JC, Oliveira JB, Cunha TJF (2018) **Sistema brasileiro de classificação de solos**. 5 ed. Brasília: Embrapa Solos, 356 p.

Schaefer CEGR, Fabris JD, Ker JC (2008) Minerals in the clay fraction of brazilian latosols (oxisols): a review. **Clay Minerals** 43:137-154.

Scheinost A, Chavernas A, Barrón V, Torrent J (1998) Use and limitations of second-derivative diffuse reflectance spectroscopy in the visible to near-infrared range to identify and quantify Fe oxide minerals in soils. **Clays and Clay Minerals** 46:528–536.

Schoorl JM, Sonneveld MPW, Veldkamp A (2000) Three-dimensional landscape process modeling: The effect of DEM resolution. **Earth Surface Processes and Landforms** 25:1025–1034.

Schulze DG (1989) An introduction to soil mineralogy. In.: Dixon JB, Weed SB (Eds.) **Minerals in soil environments**. 2nd ed. Madison: Soil Science Society of America, p. 11–34.

Schwertmann U (1964) The differentiation of iron oxide in soil by a photochemical extraction with acid ammoniun oxalate. **Zeitschrift fuer Pflanzenernaehrung und Bodenkunde** 105:104–201.

Schwertmann U (1985) The effect of environments on iron oxide minerals. **Advances in Soil Science** 1:172–200.

Schwertmann U (1993) Relations between iron oxides, soil color, and soil formation. In.: Bigham JM, Ciolkosz EJ (Eds.) **Soil color**. Madison: Soil Science Society of America, p. 51-69. (Special publication, 31).

Schwertmann U, Carlson L (1994) Aluminum influence on iron oxides: XVII. Unit-cell parameters and aluminum substitution of natural goethites. **Soil Science Society of America Journal** 58:256-261.

Schwertmann U, Cornell RM (1991) **Iron oxides in laboratory**. New York: Cambridge –VCH, 137 p.

Schwertmann U, Fechter H (1984) The influence of aluminium on iron oxides: XI. Aluminium–substituted maghemite in soils and its formation. **Soil Science Society of America Journal** 48:1462–1463.

Schwertmann U, Taylor RM. Iron oxides (1989) In.: Dixon, J. B.; Weed, S. B (Eds.) **Minerals in soil environments.** 2nd ed. Madison: Soil Science Society of America, p. 379–438.

Sellitto VM, Fernandes RBA, Barrón V, Colombo C (2009) Comparing two different spectroscopic techniques for the characterization of soil iron oxides: Diffuse versus bi-directional reflectance. **Geoderma** 149:2-9.

Silva AR, Souza Junior IG, Costa ACS (2010) Magnetic susceptibility of B horizon of soils in the state of Paraná. **Revista Brasileira de Ciência do Solo** 34:329-337.

Silva LS, Marques Jr J, Barrón V, Gomes RP, Teixeira DDB, Siqueira DS, Vasconcelos V (2020) Spatial variability of iron oxides in soils from Brazilian sandstone and basalt. **Catena**, 185:104258.

Siqueira DS, Marques Jr J, Matias SSR, Barrón V, Torrent J, Baffa O, Oliveira LC (2010) Correlation of properties of Brazilian Haplustalfs with magnetic susceptibility measurements. **Soil Use and Management** 26:425–431.

Smith B, Sandwell D (2003) Accuracy and resolution of Shuttle Radar Topography Mission data. **Geophysical Research Letters** 30:20-24.

Soil Survey Staff (2010) **Keys to Soil Taxonomy**. 11th ed. Washington: USDA-Natural Resources Conservation Service, 338 p.

Sposito G (1989) **The surface chemistry of soils**. New York: Oxford University Press. 234 p.

Stenberg B (2010) Effects of soil sample pretreatments and standardised rewetting as interacted with sand classes on Vis-NIR predictions of clay and soil organic carbon. **Geoderma** 158:15-22.

Teixeira DDB, Marques Jr J, Siqueira DS, Vasconcelos V, Carvalho OA, Martins E, Pereira GT (2018) Mapping units based on spatial uncertainty of magnetic susceptibility and clay content. **Catena** 164:79–87.

Teixeira DDB, Marques Jr J, Siqueira DS, Vasconcelos V, Carvalho OA, Martins ES, Pereira GT (2017) Sample planning for quantifying and mapping magnetic susceptibility, clay content, and base saturation using auxiliary information. **Geoderma** 305:208–218.

Thompson R, Oldfield F (1986) **Environmental Magnetism**. London: Allen and Unwin, 227 p.

Thornthwaite CW (1948) An approach towards a rational classification of climate. **Geographical Review**, 38:55-94.

Torrent J, Barrón V (1993) Laboratory measurement of soil color: theory and practice. In: Bigham JM, Ciolkosz EJ (Eds.) **Soil color**. Madison: Soil Science Society of America, p. 21-33. (Special publication, 31).

Torrent J, Barrón V (2002) Diffuse reflectance spectroscopy of iron oxides. **Encyclopedia of Surface and Colloid Science** 1:1438-1446.

Torrent J, Barrón V (2008) Diffuse Reflectance Spectroscopy. In.: Ulery AL, Drees LR (Eds.) **Methods of Soil Analysis**. Part 5. Mineralogical Methods. Madison: Soil Science Society of America Journal, p. 367–385.

Torrent J, Liu QS, Barrón V (2010) Magnetic minerals in Calcic Luvisols (chromic) developed in a warm Mediterranean region of Spain: origin and paleoenvironmental significance. **Geoderma** 154:465–472.

Trasferetti BC, Davanzo CU (2001) Introdução às técnicas de reflexão especular e reflexão-absorção no infravermelho: (1) reflexão especular. **Quimica Nova** 24:94-98.

Troeh FR (1965) Landform equations fitted to contour maps. **Soil Science Society of**

America Journal 263:616-627.

Vasconcelos V, Carvalho Júnior OA, Martins ES, Couto Júnior AF, Guimaraes RF, Gomes RAT (2012) Sistema de classificação geomorfométrica baseada em uma arquitetura sequencial em duas etapas: árvore de decisão e classificador espectral, no Parque Nacional da Serra da Canastra. **Revista Brasileira de Geomorfologia** 13:171-186.

Viscarra Rossel A, Bui EN (2015) A new detailed map of total phosphorus stocks in Australian soil. **Science of the total Environment** 542:1040–1049.

Viscarra Rossel RA (2008) **ParLeS:** Software for chemometric analysis of spectroscopic data. **Chemometrics and Intelligent Laboratory Systems** 90:72-83.

Viscarra Rossel RA, Bui EN, Caritat P, McKenzie NJ (2010) Mapping iron oxides and the color of Australian soil using visible–near-infrared reflectance spectra. **Journal of Geophysical Research** 115:1-13.

Viscarra Rossel RA, Cattle S, Ortega A, Fouad Y (2009) In situ measurements of soil colour, mineral composition and clay content by vis–NIR spectroscopy. **Geoderma** 150:253–266.

Viscarra Rossel RA, McBratney AB (1998) Soil chemical analytical accuracy and costs: implications from precision agriculture. **Australian Journal of Experimental Agriculture** 38:765–775.

Viscarra Rossel RA, McGlynn RN, McBratney AB (2006) Determining the composition of mineral-organic mixes using UV-vis-NIR diffuse reflectance spectroscopy. **Geoderma** 137:70–82.

Wang X, Lu H, Zhang W, Hu P, Zhang H, Han Z, Wang S, Li B (2016) Rock magnetic investigation of loess deposits in the Eastern Qingling Mountains (central China) and its implications for the environment of early humans. **Geophysical Journal International** 207:889–900.

Whitting LD, Allardice WRX (1986) ray diffraction techniques. In.: Klute A (Eds.) **Methods of soil analysis**. Part 1. Madison: American Society of Agronomy, p. 331-362. (Agronomy Series, 9).
Williams J, Coventry RJ (1979) The contrasting hydrology of red and yellow earths in

a landscape of low relief. In.: SYMPOSIUM INTERNATIONAL HYDROLOGY OF AREAS OF LOW PRECIPITATION, **Proceedings...** Canberra: International Association of Hydrological Science, p. 385–395.

Wolska E, Schwertmann U (1989) The vacancy ordering and distribution of aluminum ions in g-(Fe, $Al)_2O_3$. **Solid State Ionics** 32/33:214-218.

Wyszecki G, Stiles WS (1982) Color Science: concepts and methods, **quantitative data and formulae**. (2nd ed.). New York: Wiley.

CHAPTER 2 - Spatial variability of iron oxides in soils from brazilian sandstone and basalt

ABSTRACT - Iron oxides as goethite (Gt) and hematite (Hm) are key minerals to better understand the soil–landscape relationships. Soil samples were collected at three stages of landscape dissection from the geological formations of Vale do Rio do Peixe (sandstone) and Serra Geral (basalt) in the Western Paulista Plateau (WPP), Brazil. Both iron oxides were quantified by X-ray diffraction (XRD) and diffuse reflectance spectroscopy (DRS), and the results were subjected to geostatistical analysis in order to assess the usefulness of DRS for characterizing the spatial variability in Gt and Hm. The prevalence and spatial variability of Hm and Gt in the soils were governed by the sandstone/basalt lithological contrast and landscape dissection. Iron oxides in the clay fraction exhibited high spatial variability over a large area and can be robust indicators of geological diversity and landscape dissection in pedoenvironments with low or high contents of iron oxides. Goethite had the highest spatial variability. Based on the spatial pattern of the differences between DRS and XRD estimates, the saturated red color in soil made DRS less useful for quantifying Hm in environments with high iron oxide contents. The maps indicate the sensitivity of XRD and DRS techniques to represent Hm and Gt spatial variability patterns. Gt was more sensitive to landscape dissection while Hm sensitive to lithology. Thus, the DRS technique is efficient in characterizing the spatial variability of these soil oxides in large areas, even considering the complex relations between soil and landscape.

Keywords: diffuse reflectance spectroscopy, goethite, hematite, pedometrics; mapping

2.1 Introduction

Outdated soil maps conceal important spatial information and are thus of limited use for agricultural and environmental purposes. Also, they can compromise the feasibility of public policies (Embrapa, 2016) and impair competitiveness in agricultural produce on foreign markets. Agricultural progress in this scenario requires developing effective technologies for determining soil attributes with a view to establishing specific management areas based on soil–landscape models at a detailed scale (Siqueira et al., 2015, Teixeira et al., 2018). The Brazilian National Soil Program “PronaSolos” has undertaken the enormous task of mapping the country’s territory at a large scale (1:25 000) over the next 30 years (Embrapa, 2016). One plausible alternative would be improving available knowledge about minerals such as iron oxides in soil, which accurately reflect their formation environment and whose spatial variability is governed by relief and parent material (Camargo et al., 2013).

Iron oxides are major diagnostic attributes in the Brazilian Soil Classification System (Santos et al., 2018), which defines and classifies soils at the family level. Goethite (Gt, α-FeOOH) and hematite (Hm, α-Fe_2O_3) are two major components of the clay fraction in tropical soils and used as pedoenvironmental indicators on the grounds of their resisting environmental changes altering soil color (Fitzpatrick, 1988; Cornell and Schwertmann, 2003). The fact that iron oxides strongly influence soil physical and chemical properties (Duiker et al., 2003; Cornell and Schwertmann, 2003; Camargo et al., 2013) makes their spatial characterization essential and raises the need for detailed scale maps to reflect covariate attributes accurately. In recent years many studies have also reported the importance of iron oxides in retaining the leaching of potential hazardous elements (Arenas-Lago et al., 2014; Saikia et al., 2014; Martinello et al., 2014). Therefore, to investigate the spatial variability of iron oxides will be of great importance for future environmental studies.

However, quantifying iron oxides is expensive and makes mapping large areas with conventional techniques such as X-ray diffraction (XRD) unfeasible. In fact, mapping large areas of widely ranging lithology, relief, and soil types requires using fast, accurate, environmentally friendly alternative techniques (Dalmora et al., 2016a; Dalmora et al., 2016b). Several agricultural sensors have been used in recent

decades for the rapid determination of soil attributes (Ferrari et al., 2019; Sánchez-Peña et al., 2018). In this respect, the diffuse reflectance spectroscopy (DRS) technique has been deemed as a promising choice for characterizing Fe oxides (Torrent and Barrón, 2002). In fact, DRS is fast, easy to use, inexpensive (especially with large numbers of measurements), and non-destructive; also, it uses minimal amounts of sample (Guerrero et al., 2010). These advantages have promoted its use in Soil Science. Thus, DRS has enabled the simultaneous determination of many organic and inorganic components (Guerrero et al., 2010), and hence the accurate characterization of soil mineralogy. For example, iron oxides can be identified from their absorption bands in the Vis-NIR spectral region (350–2550 nm), which are associated with specific minerals (Torrent and Barrón, 2008).

Soils in the Western Paulista Plateau (Brazil) are originated mainly from sandstone and, to a lesser extent, basalt. As a result, they span wide ranges of contents in iron oxides including Hm and Gt. However, the ability of DRS to detect small amounts of these two oxides in soils is less usual, and so is its accuracy and efficiency in areas of widely variable geology and geomorphology, which could be assessed by comparison with the traditional choice for this purpose, using XRD. However, assessing the usefulness of DRS in this context requires considering the pedoenvironmental specificities (e.g., lithology, relief, grain size distribution, and morphology) of the target area in order to expose any technical limitations and evaluate the potential indication of this technique.

In this study, we assessed the efficiency of DRS for estimating the spatial variability in Gt and Hm in the framework of soil–landscape relationships in the Western Paulista Plateau (Brazil) to facilitate the development of ancillary methods for mapping large areas.

2.2 Results and discussion

2.2.1 Physical and chemical properties (attrbutes) of soil profiles

The total contents in Fe as Fe_2O_3 extracted by sulfuric acid from ADFE ranged from 228 to 14 g kg^{-1} (Table 1). The highest contents (198–228 g kg^{-1}) were those of basaltic soils from SG and the lowest (14–57 g kg^{-1}) those of sandy soils from VRP.

Based on the results of sulfuric digestion tests, clayey and very clayey soils from SG were ferric ($18 \leq Fe_2O_3 < 36\%$), while sandy clay loam and sandy loam soils from VRP were hypoferric ($Fe_2O_3 < 8\%$) (Santos et al., 2018). These results are similar to those found by other authors who identified Fe_2O_3 variability as the main pedoindicator for soils from contrasting parent materials (Cunha et al., 2005; Carvalho Filho et al., 2015; Camargo et al., 2016). Relatively high sand and silt content in SG soils, especially in highly dissected landscapes, were found in the profiles (Table 1). This is possibly due to the mixture of basalt-sandstone, which actually occurs in the POP (Verdade, 1960; Fernandes et al., 2007).

As shown in Table 1, the weathering indices K_i and K_r calculated from the mole ratios of SiO_2, Al_2O_3, and Fe_2O_3 were influenced by differences in lithology and landscape dissection. Thus, K_i and K_r for basaltic Latosols (LVef_SG) were 0.48–1.69 and 0.35–1.13, respectively, and hence lower than those for sandy Latosols (LVd_VRP) and Argisols (PVA_VRP): 1.36–2.37 and 1.02–1.63, respectively. It was a result of the abundance of Fe_2O_3 in basaltic rocks and their easier weathering (Campos et al., 2007). The high degree of weathering was consistent with the loss of silica from soils, as implied by the negative correlations of Fe_2O_3 content with K_i ($r = -0.86$, $p < 0.05$) and K_r ($r = -0.92$, $p < 0.05$). These correlations indicate that both indices decreased with increasing Fe_2O_3 and Al_2O_3 contents but decreasing SiO_2 content (Santos et al., 2018). Also, the fact that K_r was lower than 0.7 allowed the soils from SG to be classified as oxidic and those from VRP as kaolinitic.

In morphogenetic and pedogenetic terms, the variability in Fe_2O_3 content, K_i, and K_r ware related to the degree of landscape dissection (Table 1). Thus, K_i and K_r were lower in soils from Hd landscape units, where concave and convex landforms prevailed (Chapter 1, Figure 6b), than they were in soils from Sd units at the top heights, with convex and linear landforms and less markedly weathered soil. Queiroz Neto and Pellerin (1994) found Hd units to be strongly weathered, less stable steep V-shaped valleys where morphogenesis prevailed over pedogenesis. For Tricart (1968), morphogenesis concerns the shape of the landscape, this predominate on steep slopes, while pedogenesis is expressive on soft slopes with a deeper pedological coverage. Gomes (2017) and Silva et al. (2020) suggested pedogeomorphological relationships is an excellent tool to understand the origin of

Table 1. Oxide contents as determined by sulfuric digestion, sand, silt, and clay contents, weathering indices, and soil color of six typical soils profiles in slightly, moderately, and highly dissected units of SG (basalt) and VRP (sandstone).

Horizon	Depth	SiO_2	Al_2O_3	Fe_2O_3	Sand	Silt	Clay	K_i[1]	K_r[2]	Munsell color
	(m)	(g kg^{-1})			(g kg^{-1})					
1- Rhodic Eutrudox (Eutroferric Red Latosol, RLef) from a slightly dissected unit in SG (Soil Survey Staff, 2010)										
Ap	0–0.2	130	360	211	120	240	650	0.61	0.45	2.5YR 3/3.5
Bw_1	0.2–0.5	111	390	227	110	260	630	0.48	0.35	2.5YR 3/4
Bw_2	0.5–0.9	196	380	228	100	260	640	0.88	0.64	2.5YR 3/4
Bwc	0.9–2.5	137	450	228	100	270	630	0.52	0.39	2.5YR 3/4
2 - Rhodic Eutrudox (Eutroferric Red Latosol, RLef) from a moderately dissected unit in SG (Soil Survey Staff, 2010)										
A	0–0.1	172	355	204	200	450	350	0.82	0.60	2.5YR 3/3
AB	0.1–0.3	149	358	206	130	370	500	0.71	0.52	2.5YR 3/3.5
Bw	1.6–2.0	163	375	217	160	370	410	0.74	0.54	2.5YR 3/4
Bwc	2–2.2	182	345	217	190	400	410	0.90	0.64	2.5YR 3/5
3 - Rhodic Eutrudox (Eutroferric Red Latosol, RLef) from a highly dissected unit in SG (Soil Survey Staff, 2010)										
Ap	0–0.2	242	278	196	440	100	460	1.48	1.02	2.5YR 3/4
Bw	0.2–0.5	260	286	200	400	80	520	1.55	1.07	2.5YR 3/4
B/C	0.5–1.2	257	260	198	410	70	520	1.68	1.13	5YR 4/4
4 - Rhodic Hapludox (dystroferric Red Latosol, RLd) from a slightly dissected unit in VRP (Soil Survey Staff, 2010)										
A	0–0.3	83	82	56	770	15	245	1.72	1.20	5YR 3/3
B	0.3–0.5	72	90	40	740	20	240	1.36	1.06	5YR 3/3.5
B/C	0.5–0.9	64	58	46	790	20	190	1.88	1.25	7.5YR 5/3
5 - Rhodic Hapludox (dystroferric Red Latosol, RLd) from a moderately dissected unit in VRP (Soil Survey Staff, 2010)										
A	0–0.3	46	33	36	870	10	120	2.37	1.40	7YR 4/5
B	0.3–0.5	71	64	56	740	20	240	1.89	1.08	7.5YR 4/5
B/C	0.3–0.9	74	72	54	760	10	230	1.75	1.19	7.5YR 4/5
6 - Typic Kandiudalf (Red–Yellow Argisol, RYA) from a highly dissected unit in VRP (Soil Survey Staff, 2010)										
Ap	0-0.2	35	31	14	900	60	40	1.92	1.5	10YR 4/6
B/C	0.2-0.7	100	87	27	740	240	20	1.95	1.63	8YR 3/6

[1,2]Weathering indices: $K_i = 1.7 \times \%SiO_2/\%Al_2O_3$; $K_r = 1.7 \times \%SiO_2/[\%Al_2O_3 + (0.6325 \times \%Fe_2O_3)]$.
Fe_2O_3 and K_i ($r = -0.86$, $p<0.05$).
Fe_2O_3 and K_r ($r = -0.92$, $p<0.05$).

soils. According to Cunha et al. (2005), top surfaces are more stable and have more developed and stable soils than more unstable surfaces. It was also the case here, where LVef_SG and PVA_VRP soils in the Hd units were younger (K_i and K_r were both greater than unity), shallow, and with lithic contact (C horizon) within the top 2 m.

Color hues ranged from 2.5 YR to 10 YR, and no soil was purely red or yellow (Table 1). Color parameters clearly reflect the almost exclusive legacy of the parent material to soil color. Thus, soil color is an accurate indicator of the presence of iron oxides (Torrent, 2005; Viscarra Rossel et al., 2010) and also of components of the parent material. The high variability of Fe_2O_3 contents requires identifying the iron oxides present in the soil, particularly hematite and goethite, not only because they give soils their color but also because their presence is related to soil formation environment (Schwertmann, 1993).

2.2.2 Identification of iron oxides

2.2.2.1 X-ray diffraction

The XRD patterns for iron oxides in the clay fraction treated with boiling 5M NaOH revealed the presence of antiferromagnetic minerals such as Hm and Gt, and ferrimagnetic minerals such as Mh. The latter, however, was only found in some soils from SG (Figure 1; Table 2). The wide range of Hm and Gt contents (1–120 and 1–97 g kg^{-1}, respectively) reflects the diversity of parent materials; also, the prevalence of these oxides was a result of the intrinsic nature of rocks. This assumption is supported by the significant differences in Hm and Gt contents between soils in the lithological sections. The average contents and their ranges are consistent with previous results of Camargo et al. (2016) and Barbieri et al. (2013), in similar experiments conducted at a smaller scale in the same region.

Despite their concomitance, Hm and Gt were significantly related ($p < 0.05$) to the nature of the parent material (Table 2). The abundance of Hm and Gt, which jointly accounted for 89% of the overall iron oxide content, led to the Fe_2O_3 content of the basaltic soils (>180 g kg^{-1}) being 54% higher than that of sandy soils. According

to Schwertmann and Taylor (1989), the increased Fe content of basalt, in combination with free drainage, favors Hm formation. It was indeed the case here judging by strong XRD peaks for Hm and only moderate peaks for Gt in soils from SG (Figure 1).

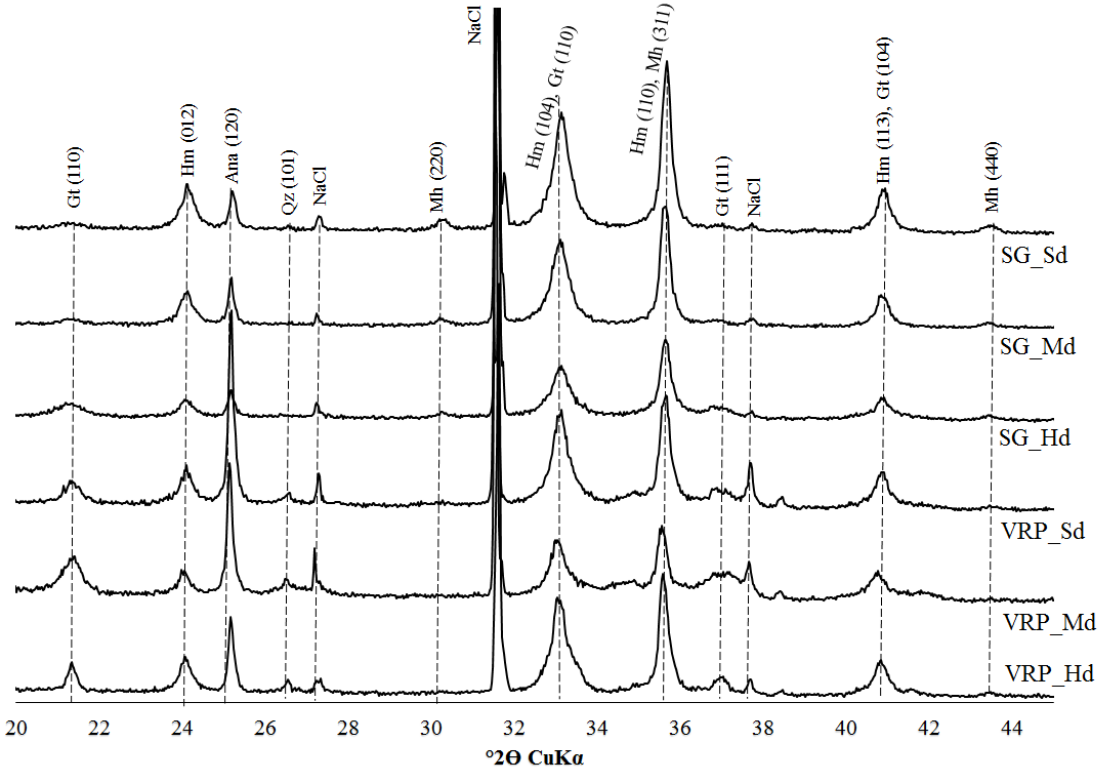

Figure 1. XRD patterns of the clay fraction (0 – 0.20 m) for six profiles after concentration of iron oxides (5M NaOH) representing the basaltic soils in the Serra Geral formation (SG) and sandstone soils in the Vale do Rio do Peixe formation (VRP). Sd, Md, and Hd denote slightly, moderately, and highly dissected units, respectively. Gt, goethite. Hm, hematite. Qz, quartz. Ana, anatase. Mh, maghemite. NaCl, sodium chloride.

The degree of landscape dissection significantly influenced ($p < 0.05$) Hm content, concentrating on Sd units (Table 2; Figure 1), where soils are more developed and have good internal drainage. Gt did not respond to the degree of dissection, but the increase in Gt concentration towards Hd units indicates a better environmental condition to its growth. Aspects of the Hd units, such as low Fe content and a more humid pedoenvironment (mainly in VRP soils), due to the proximity to the material concretions, justified the persistence of goethite in highly dissected units. A fact also observed by Coventry and Williams (1984) in a highly dissected landscape with poor drainage. Motta et al. (2002) stated that in the occurrence of highly dissected units in

the most depressed landscape regions, soils undergo a reduction process (mainly goethitization) in humid pedoenvironments favorable to Gt stability and preferential to Hm dissolution (Macedo and Bryant, 1987).

Table 2. Descriptive statistics for goethite (Gt) and hematite (Hm) as determined by XRD in 200 (0 – 0.20 m) soils samples in slightly (Sd), moderately (Md), and highly dissected (Hd) units of the Serra Geral (SG) and Vale do Rio Peixe (VRP) formations.

Mineral[1]	Soil dissection	Mean	Overall mean	Min	Median	Max	Skew.	Kurt.	SD	CV (%)
Basalt –SG										
Hm	RLef_Sd	59ab	48A	16	47	120	0.68	–0.7	33	56
	RLef_Md	41b		6	41	70	–0.2	–0.77	18	44
	RLef_Hd	44a		11	40	84	0.76	1.24	30	68
Gt	RLef_Sd	44a	41A	10	34	87	0.37	–1.36	27	61
	RLef_Md	40a		8	37	97	0.66	0.19	22	55
	RLef_Hd	34a		21	28	60	1.54	2.12	18	53
Sandstone –VRP										
Hm	RLd_Sd	16a	16B	2	19	33	–0.01	–1.55	11	69
	RLd_Md	17a		1	14	88	2.57	9.6	16	94
	RLd_Hd	14a		2	12	30	0.27	–1.08	8	57
Gt	RLd_Sd	17a	19B	5	15	34	0.45	–0.68	9	53
	RLd_Md	18a		3	18	37	0.39	–0.61	9	50
	RYA_Hd	20a		1	18	55	1.24	2.51	10	50

[1] Content in g kg^{-1}. LVef, Eutroferric Red Latosol. LVd, Dystrophic Red Latosol. PVA, Red–Yellow Argisol. SD, standard deviation. CV, coefficient of variation. Min, minimum value. Max, maximum value. Skew, skewness. Kurt., kurtosis. Means followed by the same uppercase letter in the column or lowercase letter in the row were not significantly different by the Tukey's test at 5% probability level.

2.2.2.2 Diffuse reflectance spectroscopy

The use of DRS in ADFE also indicated the coexistence of Hm and Gt in soils, and their persistence is determined by lithology and landscape dissection units (Figure 2). It occurs because Fe oxides are the main inorganic constituents to determine soil color (Resende, 1976; Schwertmann, 1993; Viscarra Rossel et al., 2010) and their occurrence and persistence depend on the parent material and environmental

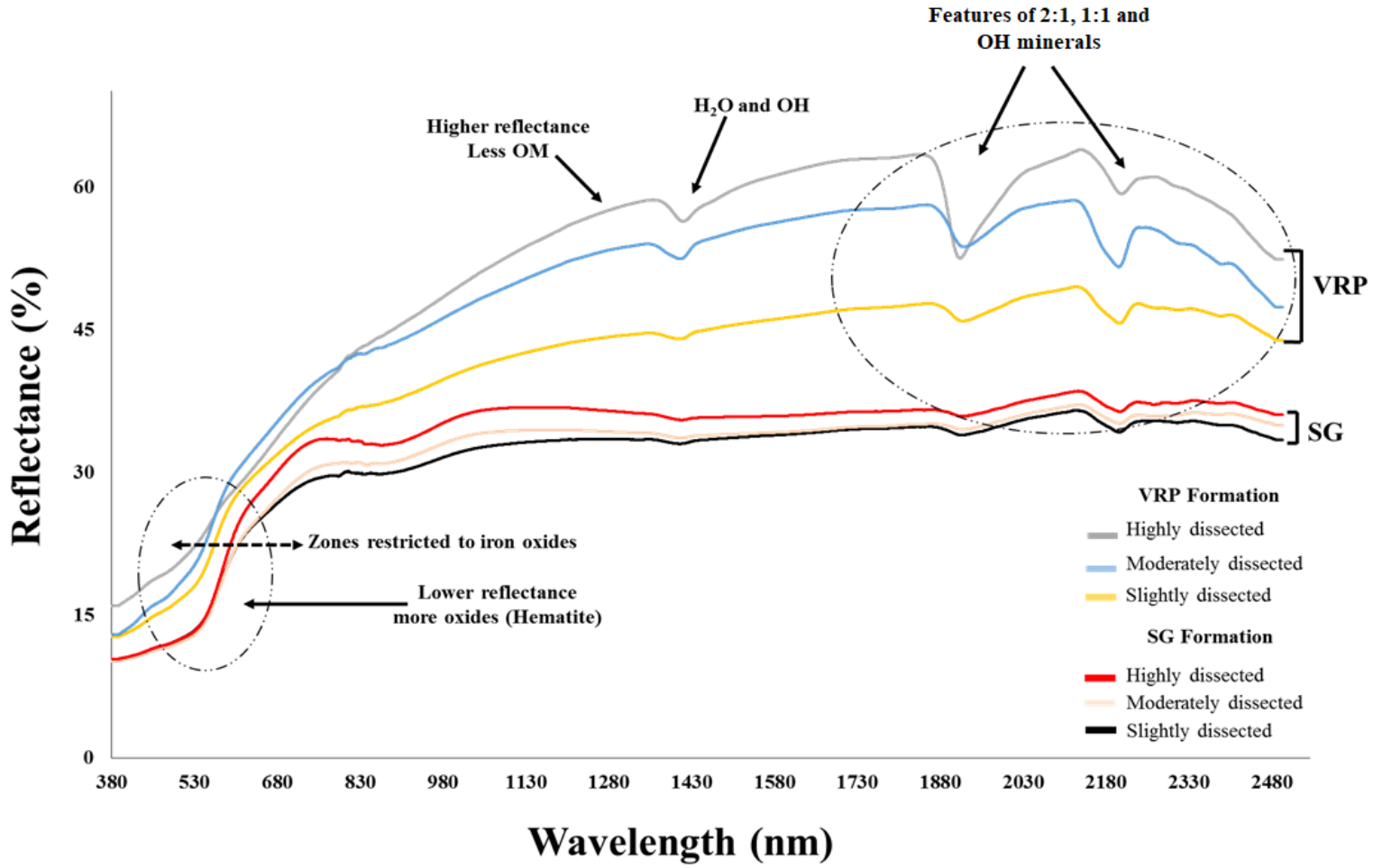

Figure 2. Diffuse reflectance spectra in the ADFE (0 – 0.20 m) for six soil profiles typical of three different dissection levels in Serra Geral (SG) and Vale do Rio Peixe (VRP) formations, Western Paulista Plateau.

conditions. In the visible region (400–780 nm), a typical zone of Fe oxides (Sherman and Waite, 1985), reflectance intensities and spectral curve features indicated a wide variation in Hm and Gt content, indicating a distinct preference for their formation, subordinated to lithologic and landscape characteristics.

The reflectances separated the lighter and yellowish (7YR, 7.5YR, 8YR, and 10YR, Table 1) LVd and PVA of VRP from the redder LVef and more intense red (2.5YR and 5YR, Table 1) of SG (Figure 2), as a consequence of opposite characteristics of basalt and sandstone rock and landscape. The low Fe_2O_3 contents and better performance of Gt affected the increase of reflectivity in soils from VRP because yellow soils have a lower light absorption potential when compared to red soils typical of Hm (Fernandes et al., 2004). On the other hand, the sharp decay of the spectral curve defined SG soils, where a more pronounced concavity of around 530 nm indicates a predominance of Hm, justifying the lower reflectance, considering its higher light absorption capacity.

The DRS technique separated soils by dissection units whose reflectance decreased in the visible range in the following sequence: Hd > Md > Sd. It can be attributed to the fact that landscape dissection (Coventry et al., 1983) and relief (Curi and Franzmeier, 1984; Camargo et al., 2013; Dotto et al., 2014) is the main factor of soil formation at the local scale to determine the type of Fe oxides present. Thus, less differentiated curves and more pronounced concavities represented the most stable relief of SG, while contrary reasons pointed out the rugged landscape of VRP. Thus, the spectral behavior indicated that soils in the same lithological section might present different reflectance intensities subordinated to landscape dissections. In a cause-and-effect relationship, changes in mineralogy, variations in the flow of water and sediments brought about by landscape and climate evolution resulted in different environments (Vidal-Torrado and Lepsch, 1993), consequently, different spectral curves (Demattê et al., 2015b).

The results of sulfuric extracts (Table 1) and XRD patterns (Table 2; Figure 1) in combination exposed a relationship of the spectral data (Figure 2) with soil weathering, parent material, and landscape dissection. Thus, the decreased reflectance of basaltic soils in Sd units, which is consistent with K_i and K_r values, and with the increased Fe_2O_3 contents, is also apparent from DRS results. Therefore, both

techniques led to identical interpretations. Also, the results suggest that soil color is an effective pedoenvironmental indicator strengthening the potential of DRS for environmental characterization.

2.2.2.3 XRD versus DRS for characterizing iron oxides in surface soils

In the 200 surface samples, Hm and Gt contents spanned the ranges of 1–120 and 1–97 g kg^{-1}, respectively, according to XRD, and 4–109 and 1–90 g kg^{-1}, respectively, according to DRS (Table 3). Based on Student's *t*-test, the contents were not significantly different ($p > 0.05$) among landscape dissection levels regardless of the used technique, and only those in Gt differed significantly with DRS. Probably, in those situations where the proportions of the two oxides are much higher and the prevalence of Hm is favored as a result, DRS may be unable to detect Gt – hence the differences between both techniques.

Table 3. Descriptive statistics for Hm and Gt contents as determined by XRD and estimated by DRS in 200 soil samples from the Western Paulista Plateau.

Technique	Unit	Overall mean	Mean	Min	Median	Max	Skewness	Kurtosis	SD	CV
	Sd		30.6 a	2	23	120	1.74	2.70	30	98
Hm_XRD[1]	Md	26.3 A	27.1 a	1	18	121	1.60	2.75	25	92
	Hd		14.9 a	2	9	84	2.75	9.09	17	114
	Sd		33.9 a	4	26	111	1.44	1.24	28	82
Hm_DRS[1]	Md	31.8 A	33.8 a	5	22	101	0.98	–0.15	26	77
	Hd		21.7 a	6	15	94	2.47	5.28	22	101
	Sd		29.5 a	5	20	87	1.34	0.71	23	78
Gt_XRD[1]	Md	26.7 A	26.2 a	1	21	97	1.93	4.66	18	69
	Hd		22.6 a	3	21	75	2.29	8.64	13	57
	Sd		24.0 a	1	16	78	1.50	1.73	18	75
Gt_DRS[1]	Md	22.3 B	22.8 a	1	17	75	1.33	0.97	17	74
	Hd		17.1 a	2	16	44	1.05	3.42	8	47

[1] g kg^{-1}. Means followed by the same uppercase letter in the column or lowercase letter in the row were not significantly different by the Tukey's test at 5% probability level. Min, minimum value. Max, maximum value. SD, standard deviation. CV, coefficient of variation (%).

The intercepts the linear regression equations (8.04 for Hm_XRD and 4.22 for Gt_XRD) were very high (Figures 3a and 3b), corroborating other studies (Bahia et al., 2015, Camargo et al., 2016). This result supports the idea that under defauld conditions XRD is less efficient to detect small amounts of Hm and Gt oxides in the soil (Kämpf and Curi, 2000; Schaefer et al., 2008). This phenomenon was observed in Gt content (Figure 1), which was almost imperceptible in the slightly dissected units of basaltic soils, while DRS efficiency has been registered even in soils with low Fe contents (<0.05%), which is the minimum detection limit of conventional XRD (Barrón et al., 2000; Balsam et al., 2014).

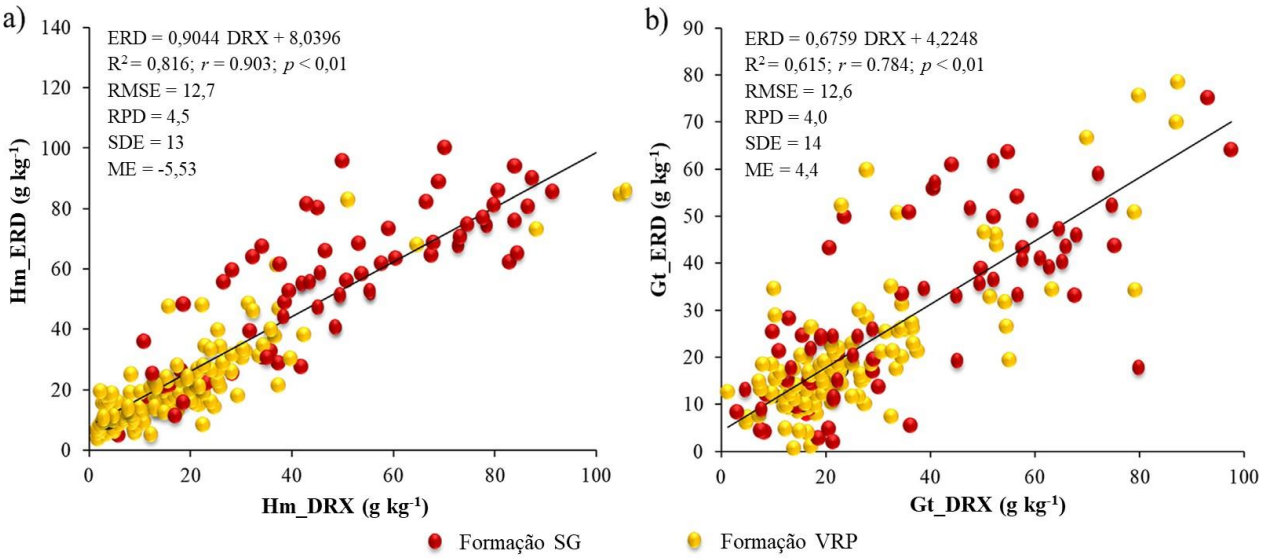

Figure 3. Regression models for (*a*) hematite as determined by X-ray diffraction (XRD) and estimated by diffuse reflectance spectroscopy (DRS); and (*b*) goethite as determined by XRD and estimated by DRS.

The prediction accuracy of regression models (Figures 3a and 3b), assuming high values of R^2 and RPD and low of RMSE and SDE, classified the models as excellent (Chang et al., 2001). Negative and positive ME values showed that DRS underestimates Hm and overestimates Gt content. However, it is not a limiting factor of DRS in estimating Fe oxides, as confirmed by a strong significant correlation between XRD and DRS found for Hm ($R^2 = 0.82$; $p < 0.01$) and Gt ($R^2 = 0.61$; $p < 0.01$). This result is consistent of those reported by Bahia et al. (2015) for Hm ($R^2 = 0.99$; $p < 0.01$) and Gt ($R^2 = 0.79$; $p < 0.01$), Camargo et al. (2016) for Hm

(R^2 = 0.70; p < 0.01) and Gt (R^2 = 0.71; p < 0.01), and Cezar et al. (2013) for the correlation between the synthetic Hm content and its reflectance factor (R^2 = 0.99).

2.2.3 Geostatistical analysis and mapping of iron oxides

According to Warrick and Nielsen (1980) criteria for coefficients of variation, those for Hm and Gt (48–117%) exceed 24% and, therefore, the variability in XRD (Table 2) and DRS values (Table 3) for the two oxides was high. However, this descriptive statistics may not accurately reflect the facts, as it refers to the overall mean of a dataset (Siqueira et al., 2015). Consequently, it is preferable to use geostatistical kriging tools instead as they operate on local means (Siqueira et al., 2015; Teixeira et al., 2018).

In both techniques, Hm and Gt presented spatial dependence described by the spherical model (Figure 4). This model is common in the investigation of soil phenomena (Vieira, 2000) with more abrupt variations (Isaaks and Srivastava, 1989), confirming the influence of geology and the degree of landscape dissection. In fact, the degree of spatial dependence (DSD) classified the spatialization of oxides as moderate (25 < DSD > 75%), revealing that the spherical model explains most of the variance of the experimental data, with R^2 > 0.6%. As assigned herein, Zheng et al. (2009) cited that moderate and high special dependences are associated with soil variables controlled by the parent material, such as mineralogy.

Hm presented a lower spatial variability when compared to Gt, expressed by the range (a) values (Figure 4), which is an indicative parameter of the spatial distance that the variables are correlated (Tabi and Ogunkunle, 2007). Ranges of 72 and 42 km (XRD) for Hm and 81 and 29 km (DRS) for Gt suggest that the variability occurred at different spatial scales, coordinated by lithological contrast and landscape dissections. Ranges from 20 to 1.400 km found by Viscarra Rossel et al. (2010) and 24 m by Camargo et al. (2008a) indicate a higher spatial variability for Gt. The ubiquitous nature of this mineral formed in the soil solution from several Fe sources through a solution-nucleation crystallization process (Cornell and Schwertmann, 2003) justifies its sensitivity to environmental changes in relation to Hm, which is formed in the solid

phase from ferrihydrite (Inda and Kämpf, 2005) or inherited from the parent rock (Santana et al., 2001).

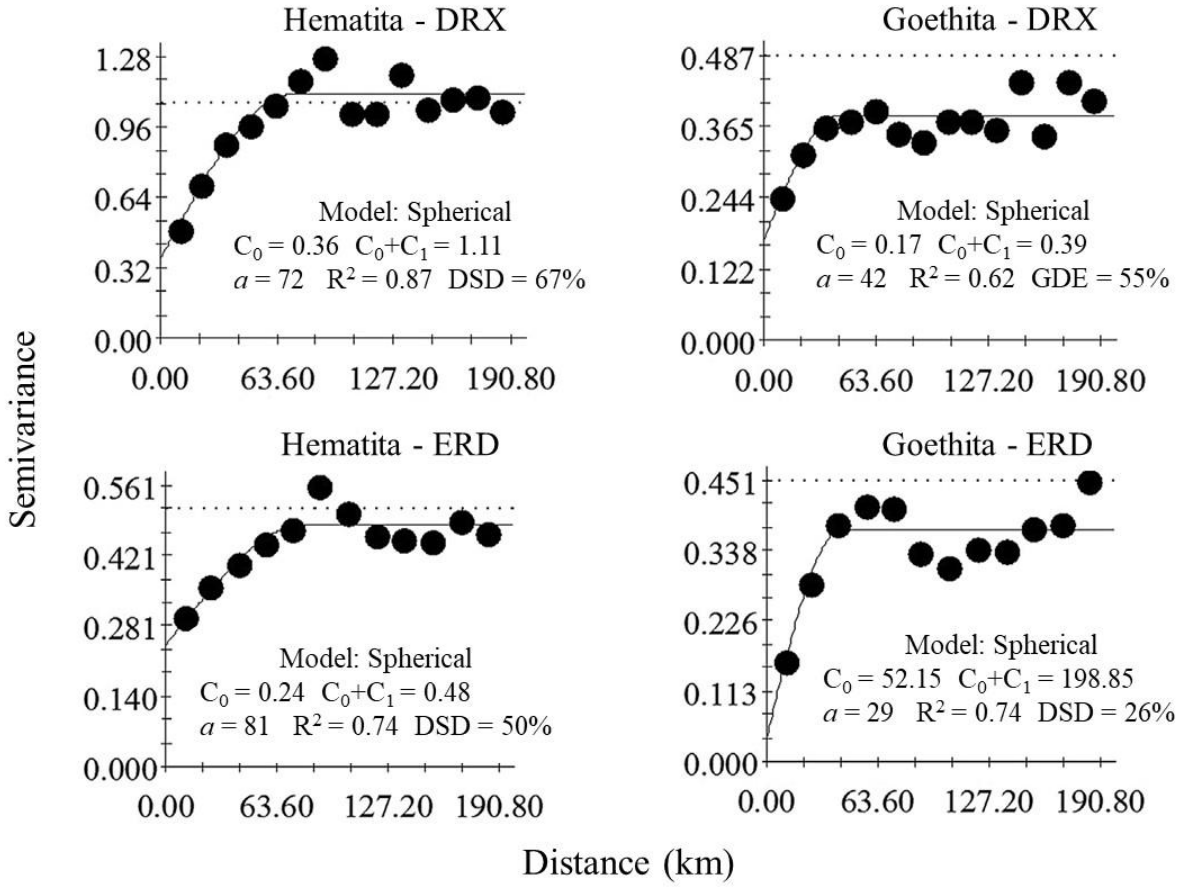

Figure 4. Variograms for hematite and goethite as obtained from XRD and DRS data for soils from the lithostratigraphic units of the Western Paulista Plateau. Co = Nugget effect; C_0 + C_1 = sill, *a* = range; DSD = Degree of spatial dependence (moderate with 25–75%, weak with > 75%, strong with ≤ 25%).

The spatial patterns of Hm and Gt by XRD and DRS are shown in Figures 5a-5f. The XRD maps presented more definite delimitations for Hm (Figure 5a), while the larger indentations and less defined limits of isolines confirm a higher spatial variability for Gt, attesting the lower ranges found in Figure 5. The spatial pattern illustrated the lithological contrast (Figure 5a–g), which is consistent with the geological map of Fernandes et al. (2007) (Figure 5g), where basaltic soils were concentrated in the peripheries of SG, and the large central spot referred to sandstones of VRP. Thus, the XRD and DRS maps indicated the spatialization of Hm and Gt, indicators of soils from parent materials with low and high Fe contents, and dissected units landscape.

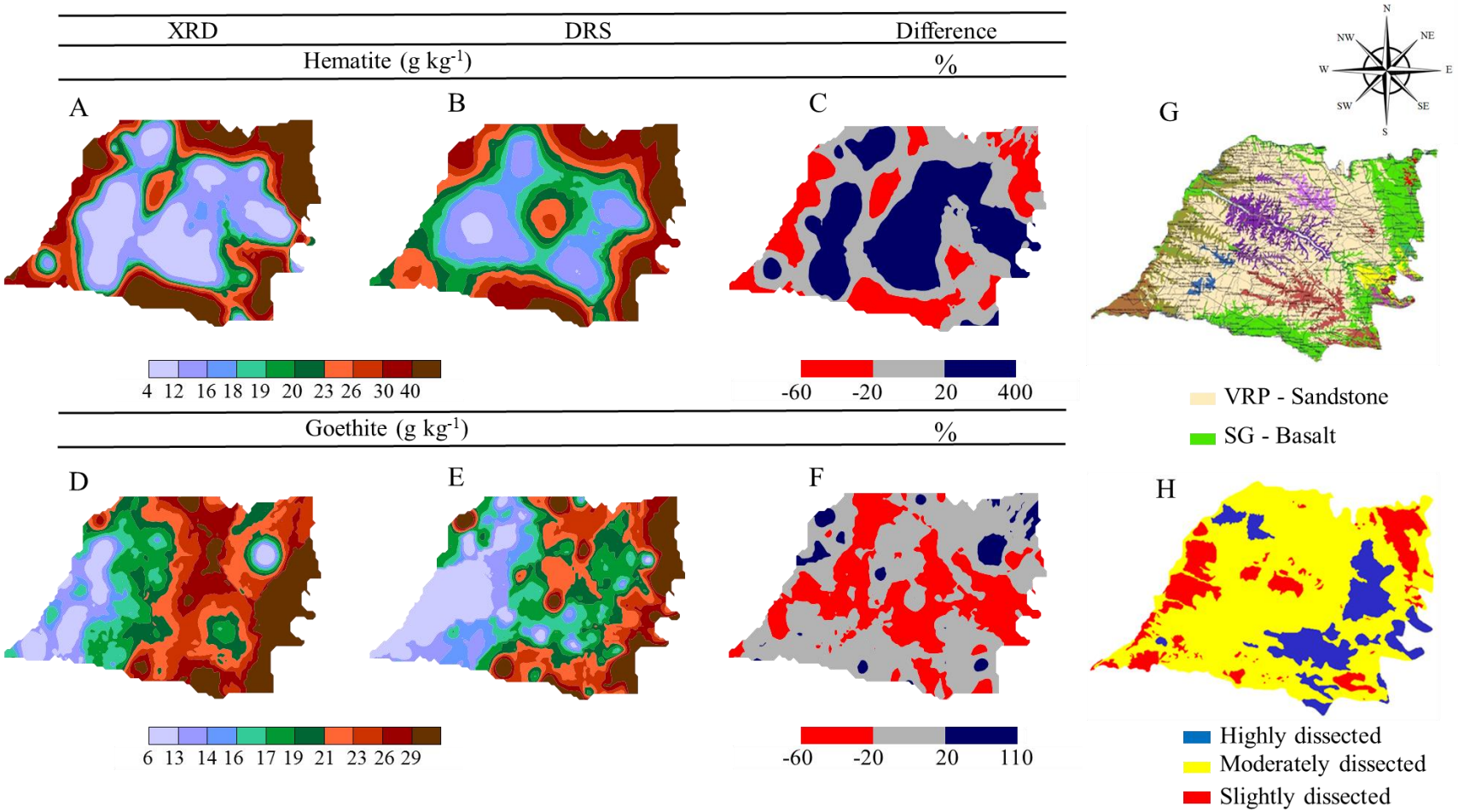

Figure 5. Spatial patterns for hematite as estimated by XRD (*a*) and DRS (*b*), and validation between the two techniques (*c*). Spatial patterns for goethite as estimated by XRD (*d*) and DRS (*e*), and validation between the two techniques (*f*). Geological maps (*g*) and landscape dissection units (*h*).

In the estimates of Hm, the lowest contents, between 4 and 16 g kg^{-1} (Figures 5a and 5b), occurred in the central region under the domain of sedimentary rocks and the highest contents at the edges of WPP. A similar observation was carried out by Camargo et al., 2008a and Camargo et al., 2008b in a basalt/sandstone transect, where Hm was the main pedoindicator of the basaltic soils and Gt of sandstone soils, with a lower total Fe content. Therefore, both XRD and DRS discriminated sandstone (center) and basaltic (edges) soils by the amplitude of Fe oxides, clearly showing a low Fe concentration in the center of the map, in the essentiality of sandstones of VRP.

The DRS technique underestimated the contents of 23 to 40 g kg^{-1} for 19 to 23 g kg^{-1} of Hm in the west and southeast direction, especially in the edges under the domain of basaltic soils. This region corresponds in large part to Sd pedoenvironments, in which the enriched Fe_2O_3 (>210 g kg^{-1} Fe_2O_3, Table 1) of soils saturated the red color (hue 2.5 YR, Table 1) by the almost absolute presence of Hm, which constituted up to 33% of Fe_2O_3 of soils from SG. According to Fernandes et al. (2004), it would be a limitation of DRS in soil samples with Hm content around 15% of total Fe oxides. Bahia et al. (2015) also addressed this problem in soils with>18% Fe_2O_3, in which Hm was the predominant Fe oxide.

Map validations (Figures 5g–5h) showed that the spatial pattern of Hm, although similar, had higher overestimated errors (>20% of XRD values) in the range from 4 to 12 g kg^{-1} (Figures 5a and 5b). From 21 to 29 g kg^{-1}, Gt contents were underestimated at 16 to 19 g kg^{-1} by DRS, mainly in the central region (Figure 5e). Basaltic flows among sandstones (Fernandes et al., 2007) overestimated Hm in sandstone environments due to the mixture of soils. Water table fluctuation, given the drainage networks that cut VRP, favors redox cycles, precipitating Fe in the wet season and its conversion into Hm in the dry season (Coventry et al., 1983), underestimating Gt by DRS. Macedo and Bryant (1987) recorded in dissected environments a change from dark red to yellow in Oxisols of the Brazilian Central Plateau due to water table fluctuation.

The DRS technique was more assertive in the spatial pattern of Gt (Figure 5h). Assuming a 20% error, it can be used in 89 and 53% of the WPP area to estimate Gt and Hm, respectively, under study conditions (Figure 5g). Fe oxides obtained by DRS were underestimated by 37% and overestimated by 23% of the total WPP area in

relation to XRD. For Hm, the over- and underestimated values of DRS were 3.4 and 23%, respectively. The results confirm the acceptable accuracy of DRS in the estimation of Hm and Gt in large areas with geomorphological complexity, large variation of total Fe, and type of predominant Fe oxides.

From the pedometrics point of view, there is a need for new methods that make more efficient the mapping of soil attributes (Viscarra Rossel et al., 2010; Marques Jr et al., 2014; Siqueira et al., 2015; Teixeira et al., 2018). The good correlations obtained for Hm and Gt, determined by XRD and estimated by DRS, indicate the potential and viability of this method in characterizing these Fe oxides in a large number of ADFE samples, quickly, with a low cost, and in large areas. This technique can assist the conventional methods of mapping, detailed survey of soils, and covariate attributes of the oxidic mineralogy of tropical environments since the estimated results and spatial pattern were very close to those observed.

2.3 Conclusions

The sandstone/basalt lithological contrast and the degree of landscape dissection are the main factors governing the prevalence and spatial variability of Hm and Gt in soils from the Western Paulista Platform. Iron oxides in the clay fraction exhibit spatial variability over large areas and are robust indicators of geological diversity and landscape dissection in environments with soils containing large amounts of iron oxides. Goethite is the most spatially variable oxide in the Plateau. Based on the spatial pattern of differences between DRS and XRD measurements, red color saturation makes the DRS technique less useful for quantifying Hm in soils with high Fe oxide contents. The maps indicate the sensitivity of XRD and DRS techniques to represent Hm and Gt spatial variability patterns. Gt was more sensitive to landscape dissection while Hm sensitive to lithology. Thus, the DRS technique is efficient in characterizing the spatial variability of these soil oxides in large areas, even considering the complex relations between soil and landscape.

2.4 References

Arenas-Lago D, Vega FA, Silva LF, Andrade ML (2014) Copper distribution in surface

and subsurface soil horizons. **Environmental Science and Pollution Research International** 21:10997-11008.

Bahia ASRS, Marques Jr J, Siqueira DS (2015) Procedures using diffuse reflectance spectroscopy for estimating hematite and goethite in Oxisols of São Paulo, Brazil. **Geoderma** 5:150-156.

Balsam W, Ji J, Renock D, Deaton BC, Williams E (2014) Determining hematite content from NUV/Vis/NIR spectra: limits of detection. **American Mineralogist** 99:2280-2291.

Barbieri DM, Marques Jr J, Pereira GT, La Scala N, Siqueira DS, Panosso AR (2013) Comportamento dos óxidos de ferro da fração argila e do fósforo adsorvido, em diferentes sistemas de colheita de cana-de-açúcar. **Revista Brasileira de Ciência do Solo** 37:1557-1568.

Barrón V, Mello JWV, Torrent J (2000) Caracterização de óxidos de ferro em solos por Espectroscopia de Reflectância Difusa. In.: Novais RF, Alvarez VH, Schaefer CEGR (Eds.) **Tópicos em ciência do solo**. Viçosa: Sociedade Brasileira de Ciência do Solo, p. 139-162.

Camargo LA, Marques Jr J, Pereira GT, Alleoni LRF, Bahia ASRS, Teixeira DDB (2016) Pedotransfer functions to assess adsorbed phosphate using iron oxide content and magnetic susceptibility in an Oxisol. **Soil Use and Management**. 32:172–182.

Camargo LA, Marques Jr J, Pereira GT (2013) Mineralogy of the clay fraction of Alfisols in two slope curvatures: III – Spatial variability. **Revista Brasileira de Ciência do Solo** 37: 295-306.

Camargo LA, Marques Jr J, Pereira GT, Horvat RA (2008a) Spatial variability mineralogical of an Oxisol under different landforms. I. Mineralogy of the clay fraction. **Revista Brasileira de Ciência do Solo** 32:2269-2277.

Camargo LA, Marques Jr J, Pereira GT, Horvat RA (2008b) Spatial variability mineralogical of an Oxisol under different landforms. II. Spatial correlation between mineralogy and aggregates. **Revista Brasileira de Ciência do Solo** 32:2279-2288.

Campos MCC, Marques Jr J, Pereira GT, Montanari R, Camargo LA (2007) Relações solo-paisagem em uma litossequência arenito-basalto na região de Pereira Barreto, SP. **Revista Brasileira de Ciência do Solo** 31:519-529.

Carvalho Filho A, Inda AV, Fink JR, Curi N (2015) Iron oxides in soils of different lithological origins in Ferriferous Quadrilateral (Minas Gerais, Brazil). **Applied Clay Science** 118:1–7.

Chang CW, Laird DA, Mausbach MJ, Hurburgh CR (2001) Near-infrared reflectance spectroscopy-principal components regression analyses of soil properties. **Soil Science Society of America Journal** 65:480-490.

Cezar E, Nanni MR, Chicati ML, Souza Júnior IG, Costa ACS (2013) Uso de dados espectrais para estimar a relação entre óxidos de ferro e minerais 2:1 com suas respectivas reflectâncias. **Semina: Ciências Agrárias** 34:1479-1492.

Cornell RM, Schwertmann U (2003) **The iron oxides:** structure, properties, reactions, occurrences and uses. 2nd ed. Weinheim: Wiley-VCH Verlag GmbH and Co., 664 p.

Coventry RJ, Taylor RM, Fitzpatrick RW (1983) Pedological significance of the gravels in some red and grey earths of central north Queensland. **Australian Journal of Soil Research** 21:219-240.

Coventry RJ, Williams J (1984) Quantitative relationships between morphology and the current soil hydrology, in some Alfisols in semi-arid tropical Australia. **Geoderma** 33:191-218.

Cunha P, Marques Jr J, Curi N, Pereira GT, Lepsch IF (2005) Superfícies geomórficas e atributos de Latossolos em uma sequência arenítico-basáltica da região de Jaboticabal (SP). **Revista Brasileira de Ciência do Solo** 29:81-90.

Curi N, Franzmeier DP (1984) Toposequence of Oxisols from the central plateau of Brazil. **Soil Science Society of America Journal** 48:341-346.

Dalmora AC, Ramos CG, Querol X, Kautzmann RM, Oliveira MLS, Taffarel SR, Moreno T, Silva LF (2016a) Nanoparticulate mineral matter from basalt dust wastes. **Chemosphere** 144:2013-2017.

Dalmora AC, Ramos C, Oliveira M, Teixeira E, Kautzmann R, Taffarel S, De Brum I, Silva L.F (2016b) Chemical characterization, nano-particle mineralogy and particle size distribution of basalt dust wastes. **Science of the Total Environment** 539:560-565.

Demattê JAM, Araújo SR, Fiorio PR, Fongaro CT, Nanni MR (2015b) Espectroscopia

VIS-NIR-SWIR na avaliação de solos ao longo de uma topossequência em Piracicaba (SP). **Revista Ciencia Agronomica**. 46:679–688.

Dotto AC, Dalmolin RSD, Pedron FA, Caten A, Ruiz LFC (2014) Mapeamento digital de atributos: granulometria e matéria orgânica do solo utilizando espectroscopia de reflectância difusa. **Revista Brasileira de Ciência do Solo** 38:1663-1671.

Duiker SW, Rhoton FE, Torrent J, Smeck NE, Lal R (2003) Iron (Hydr)Oxide Crystallinity Effects on Soil Aggregation. **Soil Science Society of America Journal** 67:606-611.

Embrapa – Empresa Brasileira de Pesquisa Agropecuária (2016) **Programa Nacional de Solos do Brasil – PronaSolos**. Available on: <https://www.embrapa.br/busca-de-publicacoes/-/publicacao/1054924/programa-nacional-de-solos-do-brasil-pronasolos> (accessed on: Jan. 26, 2019).

Ferrari V, Taffarel SR, Espinosa-Fuentes E, Oliveira MLS, Saikia BK, Oliveira LFS (2019) Chemical evaluation of by-products of the grape industry as potential agricultural fertilizers. **Journal of Cleaner Production** 208:297-306.

Fernandes LA, Castro AB, Basilici G (2007) Seismites in continental sand sea deposits of the Late Cretaceous Caiuá Desert, Bauru Basin, Brazil. **Sedimentary Geology** 199:51-64.

Fernandes RBA, Barrón V, Torrent J, Fontes MPF (2004) Quantification of iron oxides in Brazilian latosols by diffuse reflectance spectroscopy. **Revista Brasileira de Ciência do Solo** 28:245-257.

Fitzpatrick RW (1988) Iron compounds as indicators of pedogenic processes: examples from the Southern Hemisphere. In.: Stucki JW, Goodman JM, Schwertmann U. (Eds.) **Iron in Soils and Clay Minerals**. Dordrecht: Springer, p. 351-396.

Guerrero C, Viscarra Rossel RA, Mouazen AM (2010) Special issue 'Diffuse reflectance spectroscopy in soil science and land resource assessment' preface. **Geoderma** 158:1-2.

Inda Júnior AV, Kämpf N (2005) Variabilidade de goethita e hematita via dissolução redutiva em solos de região tropical e subtropical. **Revista Brasileira de Ciência do Solo** 29:851-866.

Isaaks EH, Srivastava RM (1989) **An introduction to applied geostatistics**. New York: Oxford University Press, 561 p.

Kämpf N, Curi N (2000) Óxidos de Ferro: indicadores de ambientes pedogênicos. In.: Novais RF, Alvarez VH, Schaefer CEGR (Eds.) **Tópicos em Ciência do Solo**. Viçosa: Sociedade Brasileira de Ciência do Solo, p. 107-138.

Kubelka P, Munk F (1931) Ein beitrag zur optic der farbanstriche. **Zhurnal tekhnicheskoi fiziki** 12:593-620.

Macedo J, Bryant RB (1987) Morphology, Mineralogy, and Genesis of a Hydrosequence of Oxisols in Brazil. **Soil Science Society of America Journal** 51:690-698.

Marques Jr J, Siqueira DS, Camargo LA, Teixeira DDB, Barrón V, Torrent, J (2014) Magnetic susceptibility and diffuse reflectance spectroscopy to characterize the spatial variability of soil properties in a Brazilian Haplustalf. **Geoderma** 219-220:63-71.

Martinello K, Oliveira M, Molossi F, Ramos C, Teixeira E, Kautzmann R, Silva LF (2014) Direct identification of hazardous elements in ultra-fine and nanominerals from coal fly ash produced during diesel co-firing. **Science of the Total Environment** 470-471:444-452.

Motta PEF, Carvalho Filho A, Ker JC, Pereira NR (2002) Relações solo-superfície geomórfica e evolução da paisagem em uma área do Planalto Central Brasileiro. **Pesquisa Agropecuária Brasileira** 37:869-878.

Poggere GC, Inda AV, Barrón V, Kämpf N, De Brito ADB, Barbosa JZ, Curi N (2018) Maghemite quantification and magnetic signature of Brazilian soils with contrasting parent materials. **Applied Clay Science** 161:385–394.

Queiroz Neto JP, Pellerin J (1994) Solos e relevo no alto vale do Rio do Peixe – Oscar Bressane (São Paulo – Brasil). **Revista do Departamento de Geografia** 777:25-34.

Resende M (1976) **Mineralogy, chemistry, morphology and geomorphology of some soils of Central Plateau of Brazil**. 237 f. Thesis (PhD in Soil Science) – Purdue University, Lafayette.

Robertson GP (1998) **GS+ geostatistics for the environmental sciences:** GS+

user's guide. Plainwell: Gamma Design Software.

Saikia BK, Ward CR, Oliveira MLS, Hower JC, Braga M, Silva LF (2014) Geochemistry and nano-mineralogy of two medium-sulfur northeast Indian coals. **International Journal of Coal Geology.** 121:26-34.

Santana GP, Fabris JD, Goulart AT, Santana DP (2001). Magnetite and its transformation to hematite in a soil derived from steatite. **Revista Brasileira de Ciência do Solo**. 25:33-42.

Santos HG, Jacomine PKT, Anjos LHC, Oliveira VA, Lumbreras JF, Coelho MR, Almeida JA, Araujo Filho JC, Oliveira JB, Cunha TJF (2018) **Sistema brasileiro de classificação de solos**. 5 ed. Brasília: Embrapa Solos, 356 p.

Schaefer CEGR, Fabris JD, Ker JC (2008) Minerals in the clay fraction of brazilian latosols (oxisols): a review. **Clay Minerals** 43:137-154.

Sánchez-Peña NE et al. (2018) Chemical and nano-mineralogical study for determining potential uses of legal Colombian gold mine sludge: experimental evidence. **Chemosphere** 191:1048-1055.

Schwertmann U (1993) Relations between iron oxides, soil color, and soil formation. In.: Bigham JM, Ciolkosz EJ (Eds.) **Soil color**. Madison: Soil Science Society of America, p. 51-69. (Special publication, 31).

Schwertmann U, Taylor RM (1989) Iron oxides. In.: Dixon JB, Weed SB (Eds.) **Minerals in soil environments**. 2nd ed. Madison: Soil Science Society of America, p. 379-438.

Sherman DM, Waite TD (1985) Electronic spectra of Fe^{3+} oxides and oxyhydroxides in the near infrared to ultraviolet. **American Mineralogist** 70:1262-1269.

Siqueira DS, Marques Jr J, Pereira GT, Teixeira DDB, Vasconcelos V, Carvalho Júnior O.A., Martins E.S (2015) Detailed mapping unit design based on soil–landscape relation and spatial variability of magnetic susceptibility and soil color. **Catena** 135:149-162.

Soil Survey Staff (2010) **Keys to Soil Taxonomy**. 11th ed. Washington: USDA-Natural Resources Conservation Service, 338 p.

Surfer (1999) Surfer for Windows 7.0. **Contouring and 3D surface mapping for scientist's engineers**. User's Guide. New York: Golden software Inc., 619 p.

Tabi FO, Ogunkunle AO (2007) Spatial variation of some soil physico-chemical properties of an alfisol in Southwestern Nigeria. **Nigerian Journal of Soil and Environmental Research** 7:82-91.

Teixeira DDB, Marques Jr J, Siqueira DS, Vasconcelos V, Carvalho OA, Martins ES, Pereira GT (2018) Mapping units based on spatial uncertainty of magnetic susceptibility and clay content. **Catena** 164:79-87.

Torrent J, Barrón V (2002) Diffuse reflectance spectroscopy of iron oxides. **Encyclopedia of Surface and Colloid Science** 1:1438-1446.

Torrent J (2005) Mediterranean soils. In.: Hillel D (Eds.) **Encyclopedia of Soils in the Environment**. London: Academic Press, p. 418-427.

Torrent J, Barrón V (2008) Diffuse Reflectance Spectroscopy. In.: Ulery AL, Drees LR, (Eds.) **Methods of soil analysis – Part 5**. Mineralogical methods. Madison: Soil Science Society of America Journal, p. 367-385.

Tricart, J (1968). As relações entre a morfogênese e a pedogênese. **Notícia Geomorfológica**, 8: p. 5-18.

Verdade, F. C. **Composição química de alguns solos do Estado de São Paulo**. II. Fósforo e manganês. v.19, p.547-565, 1960.

Vieira SR (2000) Geoestatística em estudos de variabilidade espacial do solo. In.: Novais RF, Alvarez VH, Schaefer GR (Eds.) **Tópicos em ciência do solo**. Viçosa: Sociedade Brasileira de Ciência do Solo, p. 1-54.

Viscarra Rossel RA, Bui EN, Caritat P, McKenzie NJ (2010) Mapping iron oxides and the color of Australian soil using visible-near-infrared reflectance spectra. **Journal of Geophysical Research** 115:1-13.

Warrick AW, Nielsen DR (1980) Spatial variability of soil physical properties in the field. In.: Hillel D. (Eds.) **Applications of soil physics**. New York: Academic Press, p. 319-344

Zheng H, Wu J, Zhang S (2009) Study on the spatial variability of farmland soil nutrient based on the kriging interpolation. **2019 International conference on artificial intelligence and computational intelligence**, Shanghai: AICI, p. 550-555.

CHAPTER 3 - Estimation and mapping of magnetic minerals of lithopedogenic origin in Brazilian soils

ABSTRACT - In this work, we assessed the potential of magnetic susceptibility (χ) measurements for predicting spatial variability of ferrimagnetic minerals in lithological contrasting soils and compared it with others alternative methods for this purpose. The contents in ferrimagnetic minerals were determined by using various methods including sulfuric extraction (H_2SO_4), X-ray diffraction (XRD) with and without Rietveld refinement, and low-frequency magnetic susceptibility (χ_{lf}) measurements, the results being subjected to geostatistical analysis. The wide range of χ_{lf} values (0.2 – 76.6 × 10^{-6} m^3 kg^{-1}) was strongly influenced by the sandstone–basalt lithological contrast in the study area; also, the frequency-dependent magnetic susceptibility ($\chi_{fd\%}$) revealed the dominance of superparamagnetic minerals in the soils. The correlation found between magnetic susceptibility in the air-dried fine earth fraction (χlf-ADFE) and magnetite (r = 0.92) suggest that magnetic properties were largely inherited from the parent materials even in well weathered soils. χ_{lf}-ADFE was highly correlated with maghemite quantified in ADFE [*(a)* treated with sulfuric acid (r = 0.62), *(b)* sodium citrate-bicarbonate dithionite (r = 0.85)] and clay [*(c)* concentrated-Fe oxides clay with sodium hydroxide (r = 0.88), *(d)* area of the reflections obtained by XRD (r = 0.76) and *(e)* Rietveld refinement (r = 0.85)]; these results suggests that magnetic susceptibility provides a sensitive pedoenvironmental marker for ferrimagnetic minerals in soil. In fact, χ_{lf}-ADFE measurements made before and after extraction with DCB treatment allowed magnetite and maghemite to be discriminated and quantified in soils with high and low contents of iron oxides. Finally, the similar spatial dependence of ferrimagnetic minerals as determined the other alternative techniques and from magnetic measurements suggests magnetometry is an inexpensive indirect method for the accurate mapping of magnetite and maghemite in soil over large, lithologically complex areas.

Keywords: maghemite, magnetite, magnetic susceptibility, pedometrics, mapping

3.1 Introduction

Lithogenic minerals such as magnetite (Mt, Fe_3O_4), pedogenic minerals such as maghemite (Mh, γ-Fe_2O_3) and even mixed (lithopedogenic) minerals can be easily characterized from magnetic susceptibility (χ) measurements (Jordanova, 2017). In fact, χ is a sensitive indicator for soil formation factors and processes (Torrent et al., 2010); also, it has been used as a low-level taxonomic classification criterion in Oxisols (Resende, 1976). Conventional mapping methods for soil attributes require a detailed description of soil properties in the field and their subsequent laboratory validation, which often makes the process labor-intensive, time-consuming and expensive (CST, 2001; Soil Survey Staff, 2003; Santos et al., 2018). Magnetic susceptibility measurements can therefore provide an effective inexpensive alternative method for soil mapping and surveying (Marques Jr et al., 2014).

Iron oxides (magnetic phases included) are usually characterized by chemical extraction with a dithionite–citrate–bicarbonate (DCB) mixture (Mehra and Jackson, 1960) or ammonium oxalic acid (AOA) (Tamm, 1922; 1932), or by sulfuric dissolution (Schwertmann and Fechter, 1984). These well-established methods, however, fall short for the selective simultaneous characterization of all Fe oxide forms (Van Oorschot and Dekkers, 2001; Poggere et al., 2019). Because its results are influenced by the sample preparation method used, particle crystallinity and peak overlap between mineral phases, X-ray diffraction (XRD) spectroscopy is also largely ineffective for characterizing magnetic minerals (Cornell and Schwertmann, 2003).

Technological progress has promoted the agricultural use of pedometrics (McBratney et al., 2000) and numerical modeling techniques such as geostatistics (Oliver and Webster, 2014) to map soil attributes in an indirect manner (Marques Jr et al., 2014). Camargo et al. (2013) elucidated the spatial dependence of minerals in soil to delineate specific land management areas. Also, based on their pioneering studies, Marques Jr et al. (2014), Siqueira et al. (2015), and Teixeira et al. (2018) subsequently described for the first time spatial variability in soil attributes by using χ measurements as an alternative mapping method. In this way, they confirmed that, as hypothesized in the 1980s and 1990s (Resende, 1976; Resende and Santana, 1985), χ could be useful for soil classification at a low taxonomic level.

Methodological limitations and the need for detailed descriptions of soil attributes have hampered the development of alternative nondestructive, expeditious, inexpensive methods for soil mapping (Silva et al., 2020). The Brazilian National Soil Program “Pronasolos” (Embrapa, 2016) was recently launched to map the national territory and generate variably detailed information to support public policing, assist territorial management and promote precision agriculture. In this scenario, magnetic susceptibility may provide a promising method for assisting conventional mapping techniques; however, the usefulness of χ for characterizing the spatial pattern of soil magnetic minerals in large, geomorphologically and pedologically complex lithological areas remains unproven. In this work, we assessed the potential of χ measurements for predicting spatial variability in magnetic minerals in lithological contrasting soils and compared it with that of major conventional methods for this purpose.

3.2 Results and discussion

3.2.1 Soil attributes

The sand, silt and clay contents of the basalt soils in Serra Geral (SG) ranged from 102 to 643, 78 to 472 and 204 to 644 g kg^{-1}, respectively; and those of the sandstone soils in Vale do Rio do Peixe (VRP) from 103 to 920, 20 to 744 and 49 to 562 g kg^{-1}, respectively (Table 1). The ferric soils (180 ≤ Fe_2O_3 < 360 g kg^{-1}) separated basaltic environments from essentially low-iron sandstones (Fe_2O_3 ≤ 80 g kg^{-1}). The average Fe_d content (73 to 24 g kg^{-1}) and the Hm/(Hm + Gt) ratio (0.75–0.63) obtained illustrate the wide variability in soil formation conditions (especially in the parent rocks). The intrinsic properties of the parent rock prevailed even under conditions of advanced pedogenesis (mean Ki values from 0.9 to 1.8) and lithological complexity, which confirms previous results of Silva et al. (2020) in the same study area and of other experiments conducted under similar conditions (Camargo et al., 2013; Barbosa et al., 2019).

The contrasting composition of the sandstone–basalt sequence and geological deposits of basalt spills under and between cracks in the sandstones at different times in the Cretaceous (Fernandes et al., 2000; 2007) resulted in a high variability in soil

attributes that reflected in an also high coefficient of variation (CV > 24%; Warrick and Nielsen, 1980). However, Silva et al. (2020) examined Fe oxides in the same area and found variability in soil properties to depend not only on lithological diversity but also on landscape characteristics, climate and vegetation. Because Fe oxides are soil markers for their parent rocks (Shenggao, 2000; Carvalho Filho et al., 2015; Silva et al., 2020), magnetic measurements can be useful to investigate soil characteristics influenced by lithological complexity (Resende and Santana, 1985; Qin et al. 2012).

Table 1**.** Descriptive statistics for various attributes of soils from WPP classified according to parent material.

Variable	**Mean**	**Median**	**Min–Max**	**SD**	**CV**
Basalt – Serra Geral					
Sand (g kg^{-1})	343	308	102–643	172	50
Silt (g kg^{-1})	208	188	78–472	114	55
Clay (g kg^{-1})	448	484	204–644	135	30
Fe_2O_3 (g kg^{-1})	212	211	196–228	12	6
Ki	0.9	0.8	0.5–1.7	0.4	44
Fe_d (g kg^{-1})	73	72	19–157	37	51
Fe_o (g kg^{-1})	2	2	0–6	1	50
Fe_o/Fe_d	0.03	0.03	0.02–0.05	0.01	33
Hm/(Hm + Gt)	0.75	0.77	0.6–0.9	0.12	16
Kt/(Kt + Gb)	0.6	0.5	0.2–1.0	0.2	33
Sandstone – Vale do Rio do Peixe					
Sand (g kg^{-1})	748	776	103–920	132	18
Silt (g kg^{-1})	124	105	20–744	96	77
Clay (g kg^{-1})	129	114	49–562	76	59
Fe_2O_3 (g kg^{-1})	41	43	14–56	15	37
Ki	1.8	1.8	1.3–2.4	0.2	11
Fe_d (g kg^{-1})	24	22	10–104	13	54
Fe_o (g kg^{-1})	1	0	0–24	0.4	40
Fe_o/Fe_d	0.03	0.03	0.02–0.04	0.01	33
Hm/(Hm + Gt)	0.63	0.65	0.4–0.8	0.15	24
Kt/(Kt + Gb)	0.8	0.9	0.6–1.0	0.2	25

n = 291. Ki, soil weathering index (Ki = 1.7 × % SiO_2/% Al_2O_3). Hm, hematite. Gt, goethite. Kt, kaolinite. Gb, gibbsite. Min-Max, minimum and maximum values. SD, standard deviation. CV, coefficient of variation (%). Fe_d, crystalline iron as extracted with sodium dithionite–citrate–bicarbonate. Fe_o iron in poorly crystalline iron oxides as extracted with ammonium oxalic acid.

3.2.2 Magnetic susceptibility

The ranges spanned by the χ_{lf}, χ_{hf} and $\chi_{fd\%}$ (viz., 0.6–76.6 × 10^{-6}, 0.2–68.6 × 10^{-6} and 2.0–14%, respectively; (Table 2) were similar to those reported by Preetz et al. (2008) and Teixeira et al. (2018) for basic rock soils, and also to those of Barbosa et al. (2019) for basalt–sandstone transition soils. Thus, χ_{lf} for deferrified soil samples (*average value*: 7.9 × 10^{-6} m^3 kg^{-1}) was suggestive of removal of magnetic minerals from the clay fraction and, together with the value for the natural samples (*average value*: 20.8 × 10^{-6} m^3 kg^{-1}), indicated presence of lithogenic magnetic minerals in the sand and silt fractions (particularly in the basaltic soils; Camêlo et al., 2018; Silva Filho et al., 2019). The magnetic susceptibility values echoed the contents in Fe_2O_3 of the main parent materials (Table 2) and highlighted the contribution of the parent rocks to the magnetic properties of the soils; therefore, χ makes a useful pedoenvironmental marker (Torrent et al., 2010). Similar results were previously obtained by other authors in the same region (Siqueira et al., 2015; Camargo et al., 2016; Teixeira et al., 2018) which further testifies to the importance of χ as a major pedoindicator for magnetic minerals even in soils with a high parental complexity.

Table 2. Descriptive statistics for soil magnetic susceptibility in WPP basalt–sandstone lithological contrasts.

Variable	Mean	Median	Mix–Max	SD	CV
Basalt – Serra Geral					
χ_{lf} (10^{-6} m^3 kg^{-1})	23.1	13.7	0.6 – 76.6	22.6	97.8
χ_{hf} (10^{-6} m^3 kg^{-1})	20.8	12.7	0.5 – 68.6	20.5	98.6
χ_{lf} (deferrified) (10^{-6} m^3 kg^{-1})	7.9	4.1	0.0 – 47.1	9.4	119.0
$\chi_{fd\%}$	9.5	9.4	2.0 –14.0	2.5	26.3
Sandstone – Vale do Rio do Peixe					
χ_{lf} (10^{-6} m^3 kg^{-1})	2.4	1.3	0.2 – 47.2	5.4	225.0
χ_{hf} (10^{-6} m^3 kg^{-1})	2.2	1.1	0.2 – 43.4	5.0	227.3
χ_{lf} (deferrified) (10^{-6} m^3 kg^{-1})	0.6	0.0	0.0 – 11.3	2.0	333.3
$\chi_{fd\%}$	8.8	8.7	2.4 – 14.0	2.9	33.0

n = 291. Min-Max, minimum and maximum values. SD, standard deviation. CV, coefficient of variation. χ_{lf}, low-frequency magnetic susceptibility. χ_{hf}, high-frequency magnetic susceptibility. $\chi_{fd\%}$, percent frequency-dependent magnetic susceptibility.

χ_{fd} values were used to classify magnetic signals into medium (2–10%) and high (10–14%) according to Dearing (1999) (Table 2). The mean χ_{fd} values were consistent with the presence of mixtures of fine and extremely fine particles (ca. 0.03–0.05 μm) of superparamagnetic (SP) minerals in contents below 75%, which is a common occurrence in soils with χ_{fd} < 10% containing Mt and/or Mh (Dearing, 1999). As previously observed by Camargo et al. (2016), and Anand and Gilkes (1987), the high content in SP maghemite (> 75%) was associated to very high χ_{fd} values. According to these authors, χ_{fd} values equal 14% may result from burning in the pedoenvironment. In fact, the ancient practice of burning sugarcane in the region, which is the world's leading sugarcane producer (Barbieri et al., 2013), may have led to the formation of superparamagnetic Mh in the soil by oxidation of Mt and other Fe oxides such as Gt and Hm in the presence of a reductant such as organic matter.

χ_{lf} was significantly correlated with Fe_2O_3 (r = 0.82), Fe_d (r = 0.78) and the Fe_d/Fe_2O_3 ratio (r = –0.86) (see Table S1 in Supplementary Information and Figure 1). Lu et al. (2008) in Chinese basaltic soils, and Camêlo et al. (2018) in Brazilian soils of variable lithology, found a positive correlation between χ_{fd} and the Fe_d/Fe_2O_3 ratio which they ascribed to enrichment of the soil with SP Fe oxides. This result was supported by a negative correlation of χ_{fd} with the weathering-related parameters *K*i (r = –0.68) and *K*r (r = –0.93) found here (Table S1 and Figure 1), which is consistent with the dominance of pedogenic magnetic minerals in weathered soils (Liu et al., 2010). Poggere et al. (2018) found Mh contents to be negatively correlated with Ki (r = –0.54) and Kr (r = –0.67) and ascribed it to accumulation of the mineral in strongly weathered soils. However, χ only increases as pedogenesis develops in pedosystems with similar parent materials and degree of weathering (Sarmast et al., 2017).

The negative correlation of χ_{LF} with the Kt/(Kt + Gb) ratio found here (r = –0.78*;* Table S1) is consistent with the diamagnetic character of kaolinite and gibbsite (Dearing et al., 1999), two abundant minerals in sandstone soils. As can be inferred from the positive correlation between χ_{lf} and Fe_o (r = 0.67; Table S1 and Figure 1), strong weathering of basaltic soils favored physical fragmentation of Mt in the sand and silt fractions —Fe_o is known to account for a fraction of Mt present in the coarser soil particles of these soils (Van Oorschot and Dukkers, 2001). In absolute terms,

however, the insignificant correlation between χ_{lf} and sand does not exclude the presence of magnetite; rather, the dominance of nonmagnetic sand may have concealed the presence of Mt owing to its scarce presence in highly weathered soils and its absence from sandstone soils.

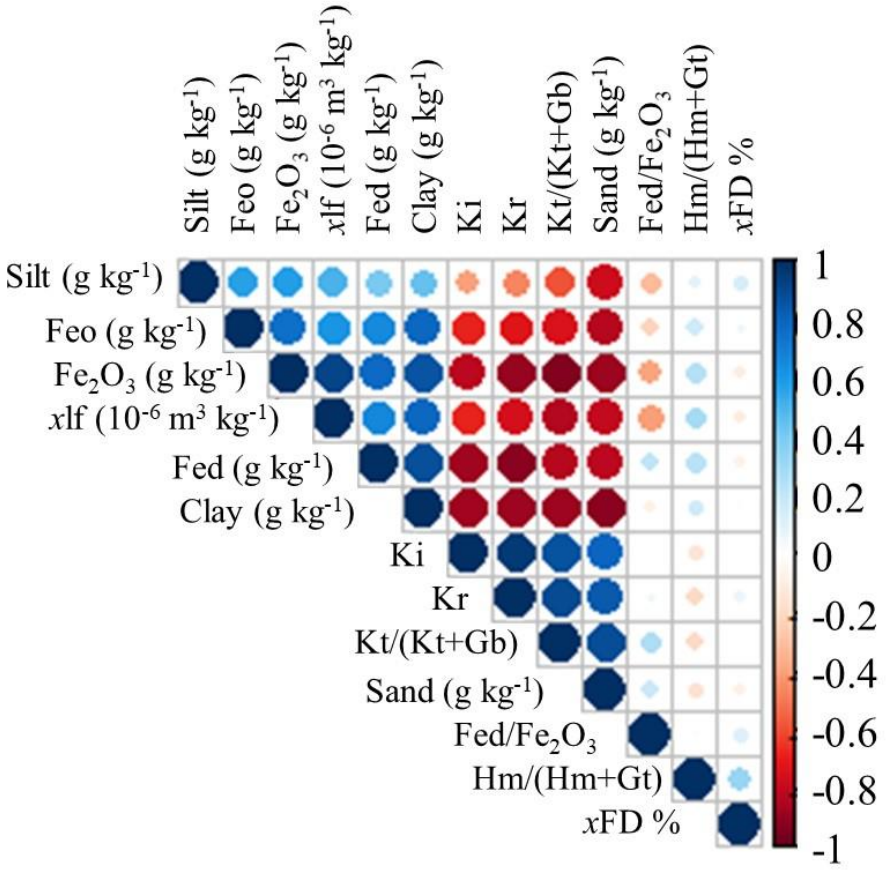

Figure 1**.** Correlations of low-frequency magnetic susceptibility (χ_{lf}), percent frequency-dependent susceptibility (χ_{fd}) in the air-dried fine earth (ADFE) fraction and various soil properties. Fe_d, iron in crystalline iron oxides as extracted with sodium dithionite–citrate–bicarbonate. Fe_o, iron in poorly crystalline iron oxides as extracted with ammonium oxalic acid.

The significant positive correlations of χ_{lf} with clay (r = 0.80) and silt (r = 0.53) in the grain size fractions was consistent with the presence of Mt and/or Mh in the soil (Table S1 and Figure 1). Under similar conditions, Peluco et al. (2013) found a positive correlation between χ_{lf} and clay in sandstone–basalt soils, and so did Fontes et al. (2000) in the sand, silt and clay fractions of sandstone soils. For these authors,

substantial χ_{lf} values for the clay fraction result from direct oxidation of Mt to Mh; by contrast, oxidation of Mt to Mh and then to Hm in the sand fraction reduces χ_{lf}. We can assume strong weathering and the low Fe_2O_3 content of the soils from VRP to have favored the formation of Hm from a ferrimagnetic ferrihydrite precursor (Michel et al., 2010; Jiang et al., 2018) since the XRD patterns revealed the absence of Mh from the sandstone soils (Figures S1a and S1b). Although both are antiferromagnetic, Hm and Gt have typically low χ_{lf} values (3.83×10^{-6} and 5.92×10^{-6} $m^3 kg^{-1}$, respectively; Peters and Dekkers, 2003). Consequently, the magnetic susceptibility of the sandstone soils was partly an expression of the previous oxides.

The magnetic signals for the sand, silt and clay fractions facilitate discrimination of soil magnetic sources (Alekseev et al., 2002; Suchodoletz et al., 2009; Quijano et al., 2014). The negative correlation of χ_{lf}-ADFE with the sand content suggests the presence of diamagnetic minerals (especially in the sandstone soils, where the high content in sand resulted in dilution of χ_{lf}). Thompson and Morton (1979) found low and high χ_{lf} values in soils to be associated to high contents in coarse and fine particles, respectively. In fact, our χ_{lf} values were highly correlated with clay ($R^2 = 0.8$; Table S1 and Figure 1), so the magnetic susceptibility of the clay fraction was due mainly to Mh. Souza Jr et al. (2010) previously found 98% of soil χ_{lf} to be explained by the clay fraction and susceptibility to vary linearly in basic rocky soils.

3.2.3 Estimating the contents in magnetic minerals with different methods

Overall, the highest and lowest values of χ_{lf}, and their coefficient of variation (CV > 25%), reflected a high variability in Mt and Mh with all methods tested as a result of the broad range of Fe_2O_3 contents of the soils and differences between the operational principles of the methods (Table 3). A quantitative comparison of the results obtained with them revealed the dominance of Mh, which is consistent with advanced pedogenesis (Cornell and Schwertmann 2003). The average Mh-XRD content of the concentrated clay fraction was not significantly different ($p < 0.01$) from that estimated from χ_{lf}-DCB in air-dried fine earth (ADFE). In contrast, the Mh contents determined by sulfuric and NaOH extraction differed mutually and with those provided by the other

methods.

Table 3. Descriptive statistics for maghemite (Mh) and magnetite (Mt) as determined with different methods in basalt–sandstone soils from WPP.

Method	Fraction	Mean	Min–Max	Skewness	Kurtosis	SD	CV
		g kg^{-1}		ad			%
Mh-H_2SO_4	Concentr.[1]	83a	17–603	5.5	37.4	65	78
Mh-χ_{lf}-NaOH		32b	0–182	2.3	4.9	40	125
Mh-R-XRD		17bc	1–64	1.2	1.0	15	88
Mh-XRD	ADFE[2]	14c	1–59	1.4	0.8	16	114
Mh-χ_{lf}-DCB		13c	0–82	1.9	2.8	20	154
Mt-χ_{lf}-rem		1.6	0–17	2.5	5.5	3	187

n = 291. [1] Oxide-concentrated clay. [2] Air-dried fine earth. Mh-H_2SO_4, maghemite determined by selective dissolution (1.8 M H_2SO_4). χ_{lf}, low-frequency magnetic susceptibility. Mh-χ_{lf}-NaOH, maghemite as determined from χ_{lf} after NaOH extraction. Mh-R-XRD and Mh-XRD, maghemite as determined by XRD with and without Rietveld refinement, respectively. Mh-χ_{lf}-DCB, maghemite as determined from χ_{lf} after DCB extraction. Mt-χ_{lf}-rem, magnetite as determined from remaining low-frequency magnetic susceptibility. Min-Max, minimum and maximum values. SD, standard deviation. CV, Coefficient of variation. ad, dimensionless quantities. Means followed by the same letters in each column did not differ significantly as per Tukey's test at $p < 0.01$.

χ_{lf}-ADFE values were invariably correlated at the $p < 0.01$ level with the quantitative measurements of Mh and Mt provided by the different methods (Figures 2a–2f). Similarity between methods increased as the linear coefficient "b" approached 0, the angular coefficient "a" approached 1, the mean square error (RMSE) and mean error (ME) decreased, and the coefficient of determination (R^2) increased. Based on these results, χ_{lf}-ADFE accounted for 85% of the magnetic signal for Mh-χ_{lf}-DCB (Figure 2a), 76% of that for Mh-DRX (Figure 2e) and 85% of that for Mh-R-XRD (Figure 2f). In addition, the RMSE and lowest ME values for Mh-χ_{lf}-DCB (7.5 and 0.16, respectively), Mh-XRD (10.5 and 4.5) and Mh-R-XRD (11.2 and –0.5) suggest that the Mh contents estimated with these methods were better correlated with χ_{lf}-ADFE (Figures 2a and 2f).

As suggested by the negative ME values (Figures 2d and 2e) and the presence of points near the y-axis, the χ_{lf}-ADFE values for a number of samples were underestimated or poorly correlated with Mh-χ_{lf}-DCB and Mh-H_2SO_4 in the oxide-concentrated clay fraction. This was a result of Mh, the magnetic susceptibility of which is lower than that of Mt (Peters and Dekkers, 2003), being the sole magnetic mineral present in the oxide-concentrated clay fraction. The low correlation of χ_{lf}-ADFE with

Mh-H_2SO_4 suggests that, as previously found by Poggere et al. (2018), part of Fe represented as Mh came from nonmagnetic iron oxides. In fact, there was drastic a reduction in contents but especially in Hm relative to Gt —the latter was much less affected (Figure S2). A similar result was previously obtained by Inda and Kampf (2005) in the selective dissolution of pedogenic hematite and goethite. In part, extensive replacement of Fe^{3+} with Al^{3+} in Gt, which is quite common in tropical soils (Kämpf and Curi, 2000), may have favored abrasive reactions.

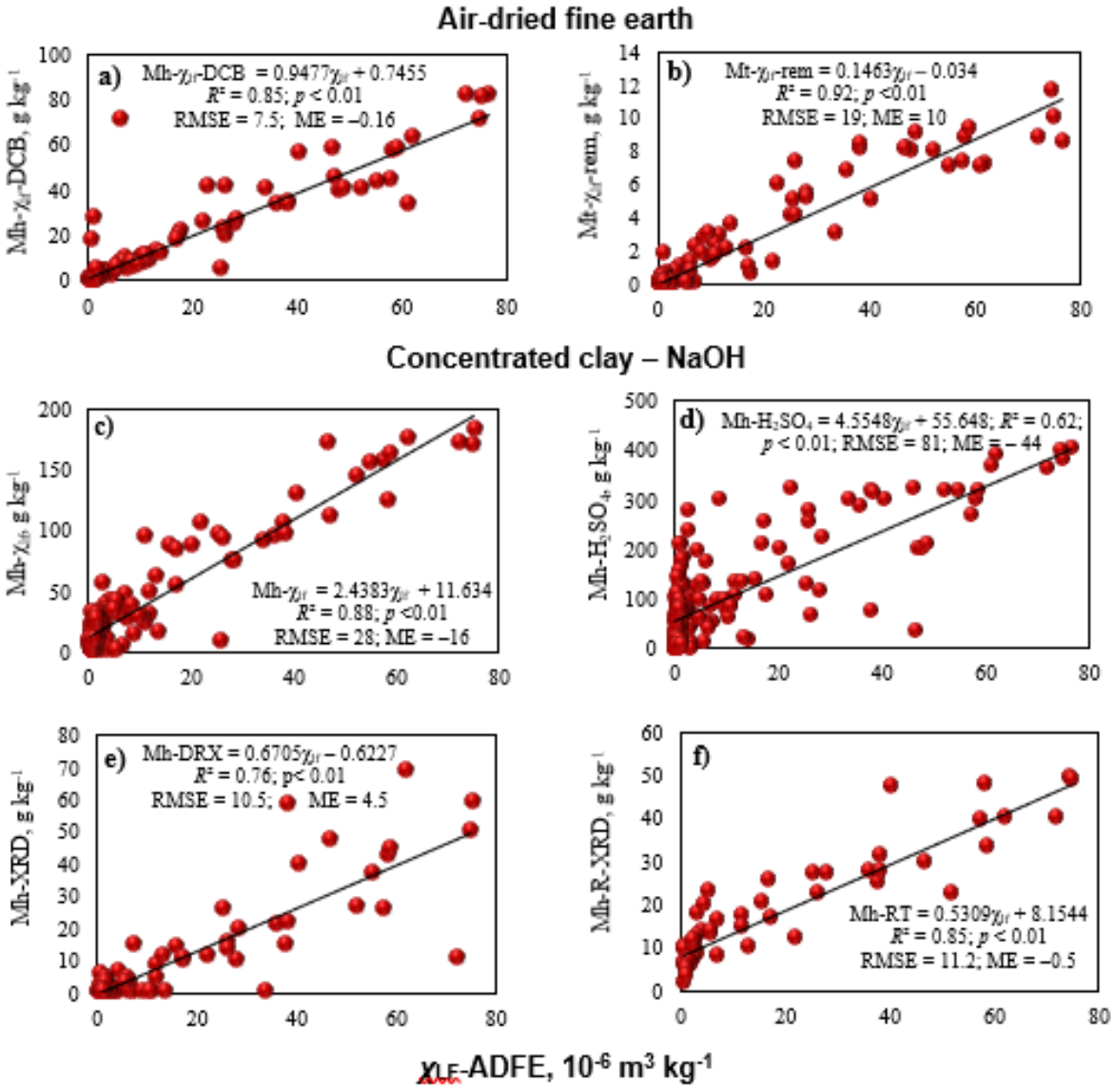

Figure 2. Regression between low-frequency magnetic susceptibility (χ_{lf}) and the contents in magnetic minerals as determined with various methods. (*a*) Maghemite from χ_{lf} after extraction with DBC. (*b*) Magnetite from remaining χ_{lf}. (*c*) Maghemite from χ_{lf} in oxide-concentrated clay fraction after extraction with 5M NaOH. (*d*)

Maghemite by 1.8M H_2SO_4. (*e*) and (*f*) Maghemite by X-ray diffraction without and with Rietveld refinement, respectively.

The magnetic susceptibility remaining in ADFE after treatment was due to Mt present in the sand + silt fraction (Figure 2b). Color conversion from reddish to gray attested to the complete removal of maghemite, hematite and goethite. χ_{lf}-ADFE was strongly associated (R^2 = 0.92) to Mt-χ_{lf}-rem, which was present in the sand + silt fraction (Figure 2b). Considering by the lithogenic origin of Mt, the strong correlation between χ_{lf}-ADFE and Mt-χ_{lf}-rem suggests that, even in highly weathered soils, 92% of the soil magnetic signal was inherited from the parent material (basalt in SG). This allowed lithopedogenic magnetic minerals to be discriminated.

As can be seen from Figure 2f, Rietveld refinement improved the identification and quantification of Mh, which was strongly correlated with χ_{lf}-ADFE (R^2 = 85%, Figure 2f) —even in relation to Mh-XRD (R^2 = 76%, Figure 2e). The low values of the noise parameters (R_{exp} < 10, GOF < 3) and a smooth baseline (Figures S2a–S2b) testified to the good, reliable fit obtained (Young, 1995) in quantifying Mh. By contrast, the sandstone soils exhibited a Mh-R-XRD value of 3% even though no peak for this mineral was found in the Mh-XRD patterns (Figure S1a). This led to a negative mean error (ME) (Figure 2f) suggesting the absence of correlation with χ_{lf}-ADFE when Mh was present in small amounts only. The Rietveld method compares XRD patterns with a theoretical spectrum for the crystal phases involved; because the concentrations and crystallinity of the mineral phases were too low to give any XRD peaks, however, Mh-R-XRD was ultimately overestimated. Alves et al. (2008) found the contents in all crystal soil phases present in the XRD spectra for samples containing substantial concentrations of poorly crystalline minerals to be overestimated by the Rietveld method.

The χ_{lf} values for the magnetic minerals exhibited high coefficients of variation CV ≥ 24), which, according to Warrick and Nielsen (1980), corresponds to a high variability irrespective of the particular quantification method used (Table 3). This in turn suggests that, whichever their nature, all estimation methods are subject to the high variability of magnetic minerals in soil. That of Mt and Mh in the study area can be ascribed to factors such as the broad range of Fe oxide contents, differences in

magnetic particle size, isomorphous substitutions, and the characteristics of the parent material and pedogenic processes. Because they are based on data averages, descriptive statistics may not accurately represent the facts (Siqueira et al., 2015; Silva et al., 2020) and an alternative method such as geostatistically based kriging may be more effective given the local averages.

3.2.4 Magnetic signature in the spatial distribution of magnetic oxides

The semivariograms adjusted for χ_{lf}, Mt and Mh as determined with the different methods in the ADFE and oxide-concentrated clay fractions revealed spatial variability in these parameters that conformed to a spherical model (Table 4). Spherical modeling is widely used to describe the variability on large scale of especially abruptly variable soil attributes (Isaaks and Srivastava, 1989; Silva et al., 2020). This confirms that the spatial dependence of Mh, Mt —and hence χ_{lf} — is influenced by the nature of the source materials. In some previous studies, spherical models also described the spatial variation pattern of soil χ_{lf} in geomorphologically complex environments (Siqueira et al., 2015; Camargo et al., 2016; Teixeira et al., 2018) and proved the most accurate for elucidating the influence of the parent materials on soil ferrimagnetic mineralogy and covariate attributes.

Table 4. Models adapted to the experimental semivariograms.

Method	Fraction	Model	C_0[a]	C_0+C_1[b]	$C_0/(C_0+C_1)\times 100$[c]	Range (km)	R^2[d]
χ_{lf}		Spherical	60	160.8	37	74	0.733
Mt-χ_{lf}-rem	ADFE[1]	Spherical	5.3	14.26	37	99	0.882
Mh-χ_{lf}-DCB		Spherical	69.3	151.1	46	76	0.681
Mh-χ_{lf}-NaOH	Concent.[2]	Spherical	3.28	10.06	33	83	0.843
Mh-H_2SO_4		Exponential	0.22	0.49	44	74	0.961
Mh-XRD		Spherical	68.3	248.4	27	93	0.704
Mh-R-XRD		Spherical	32.7	105.8	31	51	0.627

n = 291. [1]Air-dried fine earth. [2] Oxide-concentrated clay. [a] Nugget effect. [b] Sill. [c] Degree of spatial dependence (moderate with 25–75%, weak with > 75%, strong with ≤ 25%). [d] Coefficient of determination. Mh, Maghemite. Mt, magnetite. χ_{lf}, low-frequency magnetic susceptibility. Mt-χ_{lf}-rem, magnetite as determined from remaining magnetic susceptibility. Mh-χ_{lf}-DCB and Mh-χ_{lf}-NaOH, maghemite as determined from χ_{lf} after extraction with DCB and NaOH, respectively. Mh-H_2SO_4,

maghemite as determined after sulfuric digestion. Mh-XRD and Mh-R-XRD, maghemite as determined by X-ray diffraction spectroscopy without and with Rietveld refinement, respectively.

With all methods tested, the degree of spatial dependence of the soil attributes, $[C_0/(C_0 + C_1)] \times 100$, was greater than 25% but less than 75%, and hence moderate (Cambardella et al., 1994). Also, the coefficient of determination, R^2, as obtained by fitting models and validating semivariograms exceeded 60%; therefore, the models explained the variability in experimental semivariates (spatial variability in soil magnetic minerals included) quite well. This is confirmed by the good, significant correlations ($R^2 > 0.6$; $p < 0.005$) in the results of Figures 2a–2f. A moderate or strong spatial dependence is intrinsically due to the material, whereas a weak influence is more likely to be due to soil management practices (Isaaks and Srivastava, 1989).

The range values (*a*) for the magnetic minerals in the ADFE (99, 76 and 74 km) and oxide-concentrated clay fraction (93, 83, 74 and 51 km) were relatively similar irrespective of determination method (Table 4). This result testifies to the usefulness of soil χ_{lf} for the diagnosis and spatialization of magnetic minerals. Based on its short range of values, Mh was the least spatially variable magnetic mineral. This was a result of the formation and spatial occurrence of minerals in the clay fraction being strongly influenced by rock type, landscape variables, climate intensity and weathering as previously found in studies of the mineralogy–landscape relationship by Cunha et al. (2000) and Camargo et al. (2013). The exceptional presence of Mt detected from χ_{lf}-rem in SG soils led to the greatest range value (a = 99 km) and further confirmed their lithogenic origin and the joint presence of sandstone and basalt in SG (Chapter 1, Figure 6b).

Figures 3a–3e show the isoline maps obtained by using ordinary kriging to interpolate Mh, Mt and χ_{lf} estimates. Although the analytical results revealed overestimation of Mh-H_2SO_4 (Table 3), this was no hindrance to mapping as the ensuing spatial patterns for the ADFE and oxide-concentrated clay fractions were identical with those obtained with the other methods. Therefore, based on the size of the study area, the range values obtained suggest that, irrespective of the specific fraction used to evaluate magnetic Fe oxides, the conventional quantitative methods

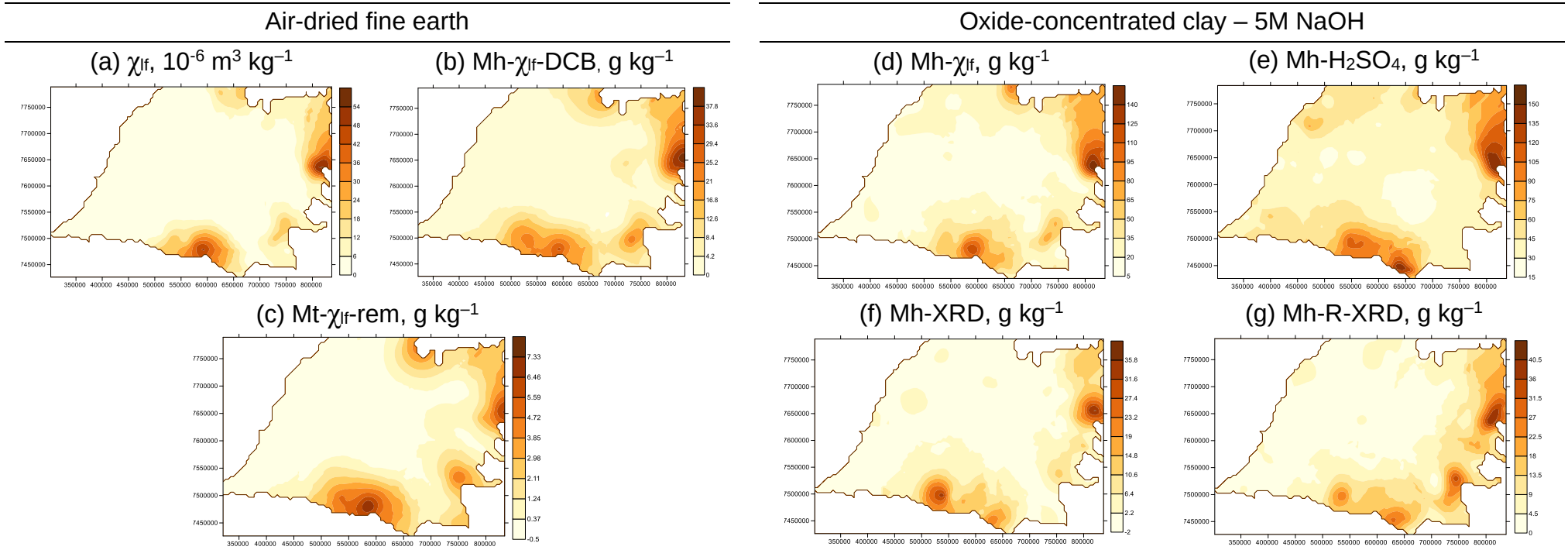

Figure 3. Spatial patterns of magnetic minerals in air-dried fine earth and oxide-concentrated clay. (*a*) Low-frequency magnetic susceptibility. (*b*) Maghemite as determined from χ_{lf} after extraction with DCB. (*c*) Magnetite as determined from remaining low-frequency susceptibility. (*d*) Maghemite as determined from χ_{lf}. (*e*) Maghemite as determined by sulfuric digestion. (*f*) and (*g*) Maghemite as determined by X-ray diffraction without and with Rietveld refinement, respectively.

of analysis and that based on magnetic susceptibility converged in estimating the spatial variability of iron oxides.

The spatial pattern of χ_{lf} showed a marked decrease in magnetic minerals from the edges to the center of the map (Figures 3a–3g), consistent with the depositional context for the Bauru basin reported by Fernandes and Coimbra (2000). The central area underwent strong particle-selective wind weathering and led to a VRP zone consisting of sand desert with calcium carbonate occasionally present in sandstones (Fernandes and Coimbra, 2000). The low Fe_2O_3 content and the presence of carbonate in the sandstone rocks in 70% of the WPP area led to reduced formation of ferrimagnetic minerals (Blundell et al., 2009). As confirmed by the results of Table 1, quartz and kaolinite were the dominant minerals in the B horizons of the VRP Latosol (Queiroz and Pellerin, 1994); therefore, the soils were essentially kaolinitic [Kt/(Kt + Gb) ≥ 0.8] and goethitic. This result is consistent with the large uniform zone in the center of the WPP as a result of the low magnetic susceptibility of the soil and the scarcity of magnetic minerals in it.

Based on the geological map (Chapter 1, Figure 6), the spatial variability of magnetic minerals and χ_{lf} in the ADFE fraction was governed by the parent material, which clearly delineated the zone of occurrence of basalt–sandstone lithological units (Figures 3a–3g). The spatial pattern of magnetic minerals estimated from χ_{lf} was very similar to that obtained with the XRD method, both revealing a marked influence of the parent material on the soil Mt and Mh contents. This interpretation is consistent with the similarity of the spatial patterns for magnetic oxides provided by all methods irrespective of operational principle.

Based on the evidence obtained and on pedometric principles, the good correlations found among estimates of magnetic minerals (Figure 2) and the similarity of spatial patterns (Figures 3a–3e) with all methods attest to the usefulness of the magnetic signature of soil for mapping magnetite and maghemite in large areas. The similar spatial patterns obtained with all methods and soil fractions not only confirm the accuracy of the classical methods, but also suggests that magnetic susceptibility measurements of the ADFE soil fraction can be useful to supplement conventional methods for the identification and quantification of magnetic minerals with a view to reducing time and costs in the detailed mapping of even lithologically complex areas.

3.3 Final considerations and applications

Magnetic minerals, which are very useful for elucidating the genesis and spatial variability of soil minerals, are usually discriminated by selective extraction, which makes their mapping in large geomorphologically and pedologically complex areas a time-consuming, labor-intensive task. In this context, the magnetic susceptibility of soil provides a sensitive, easily and nondestructively determined marker for quantifying lithopedogenic ferrimagnetic minerals and predicting covariate soil attributes of magnetic minerals. In combination with some properties of the parent material, mineral type, particle size and degree of soil weathering, the variability of magnetic susceptibility in soil can in fact be useful to define soil mapping units, optimize the management of areas differing in phosphorus and herbicide adsorption potential, and characterize production environments for crops.

3.4 Conclusions

The wide range of χ_{lf} values ($0.2 – 76.6 \times 10^{-6}$ m^3 kg^{-1}) was strongly influenced by the sandstone–basalt lithological contrast in the study area; also, the frequency-dependent magnetic susceptibility ($\chi_{fd\%}$) revealed the dominance of superparamagnetic minerals in the soils. The correlation found between magnetic susceptibility in the air-dried fine earth fraction (χ_{lf}-ADFE) and magnetite (r = 0.92) suggest that magnetic properties were largely inherited from the parent materials even in well weathered soils. χ_{lf}-ADFE was highly correlated with maghemite quantified in ADFE [*(a)* treated with sulfuric acid (r = 0.62), *(b)* sodium citrate-bicarbonate dithionite (r = 0.85)] and clay [*(c)* concentrated-Fe oxides clay with sodium hydroxide (r = 0.88), *(d)* area of the reflections obtained by XRD (r = 0.76) and *(e)* Rietveld refinement (r = 0.85)]; these results suggests that magnetic susceptibility provides a sensitive pedoenvironmental marker for ferrimagnetic minerals in soil. In fact, χ_{lf}-ADFE measurements made before and after extraction with DCB treatment allowed magnetite and maghemite to be discriminated and quantified in soils with high and low contents of iron oxides. Finally, the similar spatial dependence of ferrimagnetic

minerals as determined the other alternative techniques and from magnetic measurements suggests magnetometry is an inexpensive indirect method for the accurate mapping of magnetite and maghemite in soil over large, lithologically complex areas.

3.5 References

Alekseev A, Alekseeva T, Sokolowska Z, Hajnos M (2002) Magnetic and mineralogical properties of different granulometric fractions in the soils of the Lublin Upland Region, **International Agrophysics** 16:1–6.

Anand RR, Gilkes RJ (1987) The association of maghemite and corundum in Darling Range laterites, Western Australia. **Australian Journal of Soil Research** 35:303–311.

Barbosa RS, Marques Jr J, Barrón V, Martins Filho MV, Siqueira DS, Peluco RG, Camargo LA, Silva LS (2019) Prediction and mapping of erodibility factors (USLE and WEPP) by magnetic susceptibility in basalt-derived soils in northeastern São Paulo state, Brazil. **Environmental Earth Sciences** 78:12.

Blundell A, Dearing JA, Boyle JF, Hannam JA (2009) Controlling factors for the spatial variability of soil magnetic susceptibility across England and Wales. **Earth-Science Reviews** 95:158–188.

Camargo LA, Marques Jr J, Pereira GT, Alleoni LRF, Bahia ASRS, Teixeira DDB (2016) Pedotransfer functions to assess adsorbed phosphate using iron oxide content and magnetic susceptibility in an Oxisol. **Soil Use and Management** 32:172–182.

Camargo LA, Marques Jr J, Pereira GT (2013) Mineralogy of the clay fraction of Alfisols in two slope curvatures: III – Spatial variability. **Revista Brasileira de Ciência do Solo** 37:295–306.

Camêlo DL, Ker JC, Fontes MPF, Costa ACS, Corrêa MM, Leopold M (2018) Mineralogy, magnetic susceptibility and geochemistry of Fe-rich Oxisols developed from several parent materials. **Scientia Agricola** 75:410–419.

Cambardella CA, Moorman TB, Novak JM, Parkin TB, Karlen DL, Turco RF, Konopka AE (1994) Field-scale variability of soil properties in Central Iowa Soil. **Soil Science**

Society of America Journal 58:1501-1508.

Carvalho Filho A, Inda AV, Fink JR, Curi N (2015) Iron oxides in soils of different lithological origins in Ferriferous Quadrilateral (Minas Gerais, Brazil). **Applied Clay Science** 118:1–7.

Chinese Soil Taxonomy Research Group, Institute of Soil science, Chinese Academy Sciences, Cooperative Research Group on Chinese Soil Taxonomy (2001). **Keys to Chinese Soil Taxonomy**. 3rd ed. Hefei: Chinese Science and Technological University Press, p. 21-191.

Cornell RM, Schwertmann U (2003) **The Iron Oxides:** Structure, Properties, Reactions, Occurrence, and Uses. Weinheim: Wiley VCH. 664 p.

Dearing J (1999) **Environmental magnetic susceptibility:** Using the Bartington MS2 system. 2nd ed. Keniloworth: Chi Publishing. 54 p.

Santos HG, Jacomine PKT, Anjos LHC, Oliveira VA, Lumbreras JF, Coelho MR, Almeida JA, Araujo Filho JC, Oliveira JB, Cunha TJF (2018) **Sistema brasileiro de classificação de solos**. 5 ed. Brasília: Embrapa Solos, 356 p.

Fernandes LA, Castro AB, Basilici G (2007) Seismites in continental sand sea deposits of the Late Cretaceous Caiuá Desert, Bauru Basin, Brazil. **Sedimentary Geology** 199:51–64.

Fernandes LA, Coimbra AM (2000) Revisão estratigráfica da parte oriental da Bacia Bauru (Neocretáceo). **Revista Brasileira de Geociências** 30:717–728.

Fontes MPF, Oliveira TS, Costa LM, Campos AAG (2000) Magnetic separation and evaluation of magnetization of Brazilian soils from different parent materials. **Geoderma** 96: 81–99.

Inda Junior AV, Kämpf N (2005) Variabilidade de goethita e hematita via dissolução redutiva em solos de região tropical e subtropical. **Revista Brasileira de Ciência do Solo** 29:851–866.

Isaaks EH, Srivastava RM (1989) **An introduction to applied geostatistics**. New York: Oxford University Press, 561 p.

Jiang ZX, Liu QS, Roberts AP, Barrón V, Torrent J, Zhang Q (2018) A new model for transformation of ferrihydrite to hematite in soils and sediments: **Geology** 46:987–990.
Jordanova N (2017) **Soil magnetism:** Applications in pedology, environmental science and agriculture. 1st ed. Academic Press (Elsevier), 466 p.

Liu Q, Hu P, Torrent J, Barrón V, Zhao X, Jiang Z, Su Y (2010) Environmental magnetic study of a Xeralf chronosequence in northwestern Spain: Indications for pedogenesis. **Palaeogeography, Palaeoclimatology, Palaeoecology** 293:144–156.

Lu SG, Xue QF, Zhu L, Yu JY (2008) Mineral magnetic properties of weathering sequence of soils derived from basalt in eastern China. **Catena** 73:23–33.

Maher BA (2011) The magnetic properties of Quaternary aeolian dusts and sediments, and their palaeoclimatic significance. **Aeolian Research** 3:87–144.

Mehra OP, Jackson ML (1960) Iron oxide removal from soils and clays by a dithionite–citrate system buffered with sodium bicarbonate. In.: Swineford A (Eds.) **Seventh National Conference on Clays and Clay Minerals**. Washington: Pergamon Press, p. 317–342.

Mckeague JA, Day JH (1966) Dithionite and oxalate-extractable Fe and Al as aids in differentiating various classes of soils. **Canadian Journal of Soil Science** 46:13–22.

McBratney AB, Odeh IOA, Bishop TFA, Dunbar MS, Shatar TM (2000) An overview of pedometric techniques for use in soil survey. **Geoderma** 97:293–327.

Oliver MA, Webster AR (2014) A tutorial guide to geostatistics: computing and modelling variograms and kriging. **Catena** 113:56–69.

Peters C, Dekkers M (2003) Selected room temperature magnetic parameters as a function of mineralogy concentration and grain size. **Physics and Chemistry of the Earth** 28:659–667.

Poggere GC, Inda AV, Barrón V, Kämpf N, Brito ADB, Barbosa JZ, Curi N (2018) Maghemite quantification and magnetic signature of Brazilian soils with contrasting parent materials. **Applied Clay Science** 161:385–394.

Preetz H, Altfelder S, Igel J (2008) Tropical soils and landmine detection − An approach for a classification system. **Soil Science Society of America Journal** 72:151–159.

Peluco RG, Marques Jr J, Siqueira DS, Pereira GT, Barbosa RS, Teixeira DDB, Adame CR, Cortez LA (2013) Suscetibilidade magnética do solo na estimação da capacidade de suporte à aplicação de vinhaça. **Pesquisa Agropecuária Brasileira** 48:661–672.

Queiroz Neto JP, Pellerin J (1994) Solos e relevo no alto vale do Rio do Peixe – Oscar Bressane (São Paulo – Brasil). **Revista do Departamento de Geografia** 777:25-34.

Qin C-Z, Zhu A-X, Qiu W-L, Lu Y-J, Li B-L, Pei T (2012) Mapping soil organic matter in small low-relief catchments using fuzzy slope position information. **Geoderma** 171–172:64–74.

Quijano L, Chaparro MAE, Marie DC, Gaspar L, Navas A (2014) Relevant magnetic and soil parameters as potential indicators of soil conservation status of Mediterranean agroecosystems. **Geophysical Journal International** 198:1805–1817.

Resende M, Allan J, Coey JMD (1986) The magnetic soils of Brazil. **Earth and Planetary Science Letters** 78:322–326.

Rietveld HM (1969) A profile refinement method for nuclear and magnetic structures. **Journal of Applied Crystallography** 2:65–71.

Rossi, M (2017). **Mapa pedológico do Estado de São Paulo**: revisado e ampliado. Instituto Florestal, São Paulo.

Sarmast M, Farpoor MH, Esfandiarpour Boroujeni I (2017) Magnetic susceptibility of soils along a lithotoposequence in southeast Iran. **Catena** 156:252–262.

Schwertmann U, Fechter H (1984) The influence of aluminium on iron oxides: XI. Aluminium substituted maghemite in soils and its formation. **Soil Science Society of America Journal** 48:1462–1463.

Shenggao L (2000) Lithological factors affecting magnetic susceptibility of subtropical soils, Zhejiang Province, China. **Catena** 40:359–373.

Suchodoletz H, Kühn P, Hambach U, Dietze M, Zöller L, Faust D (2009) Loess-like and palaeosol sediments from Lanzarote (Canary Islands/Spain) – indicators of palaeoenvironmental change during the Late Quaternary. **Palaeogeography, Palaeoclimatology, Palaeoecology** 278:71–87.

Siqueira DS, Marques Jr J, Pereira GT, Teixeira DDB, Vasconcellos V, Carvalho Jr O, Martins E (2015) Detailed mapping unit design based on soil–landscape relation and spatial variability of magnetic susceptibility and soil color. **Catena** 135:149–162.

Silva LS, Marques Jr J, Barrón V, Gomes RP, Teixeira DDB, Siqueira DS, Vasconcelos V (2020) Spatial variability of iron oxides in soils from Brazilian sandstone and basalt. **Catena** 185:104258.

Soil Survey Staff (2010) **Keys to Soil Taxonomy**. 11th ed. Washington: USDA-Natural Resources Conservation Service, 338 p.

Souza Junior IG, Costa ACS, Vilar CC, Hoepers A (2010) Mineralogia e susceptibilidade magnética dos óxidos de ferro do horizonte B de solos do Estado do Paraná. **Ciência Rural** 40:513–519.

Tamm O (1932) Über die Oxalatmethode in der chemischen Bodenanalys, Medd. **Statens Skogsforsokanstalt** 27:1–20.

Teixeira DDB, Marques Jr J, Siqueira DS, Vasconcelos V, Carvalho OA, Martins ES, Pereira, GT (2018) Mapping units based on spatial uncertainty of magnetic susceptibility and clay content. **Catena** 164:79–87.

Torrent J, Liu QS, Barrón V (2010) Magnetic minerals in Calcic Luvisols (chromic) developed in a warm Mediterranean region of Spain: origin and paleoenvironmental significance. **Geoderma** 154:465–472.

Thornthwaite CW (1948) An approach towards a rational classification of climate. **Geographical Review** 38:55-94.

Thompson R, Morton DJ (1979) Magnetic susceptibility and particle-size distribution in recent sediments of the Loch Lomond drainage basin, Scotland. **Journal of Sedimentary Petrology** 49:801–812.

Van Oorschot IHM, Dekkers MJ (2001) Selective dissolution of magnetic iron oxides in the acid-ammonium oxalate/ferrous iron extraction method – I. **Synthetic samples.**

Geophysical Journal International 145:740–748.

Verosub KL, Fine P, Singer MJ, TenPas J (1993) Pedogenesis and paleoclimate: interpretation of the magnetic susceptibility record of Chinese loess-paleosol sequences. **Geology** 21:1011–1014.

Vieira SR, Millete J, Topp GC, Reynolds WD (2002) Handbook for geostatistical analysis of variability in soil and climate data. In.: Alvarezz VH, Schaefer CR, Barros NF, Mello JWV, Costa LM (Eds.) **Tópicos em Ciência do solo**. Viçosa: Sociedade Brasileira de Ciência do solo 2:1-45.

Young RA (1995) **The Rietveld Method**. I.U.C. New York: Oxford University Press, 298 p.

Warrick AW, Nielsen DR (1980) Spatial variability of soil physical properties in the field. In.: Hillel D. (Eds.) **Applications of soil physics**. New York: Academic Press, 350 p.

APPENDIX A. Supplementary information

Table S1. Correlation between low-frequency magnetic susceptibility (χ_{LF}), percent frequency-dependent susceptibility (χ_{FD}%) in air-dried fine earth (ADFE) and various soil properties.

	Fe_o	Fe_d	Fe_2O_3	$\frac{Fe_d}{Fe_2O_3}$	$\frac{Kt}{Kt+Gb}$	$\frac{Hm}{Hm+Gt}$	Ki	Kr	Sand	Silt	Clay
χ_{LF}	0.67**	0.78**	0.82**	–0.86**	–0.78**	0.50^{NS}	–0.68*	–0.93**	–0.78**	0.53**	0.80**
χ_{FD}%	0.02^{NS}	–0.03^{NS}	–0.11^{NS}	0.71*	0.52^{NS}	–0.59*	–0.45^{NS}	0.05^{NS}	–0.07^{NS}	0.14*	–0.001

n = 291. NS, not significant. * Significant at $p < 0.05$. ** Significant at $p < 0.01$.

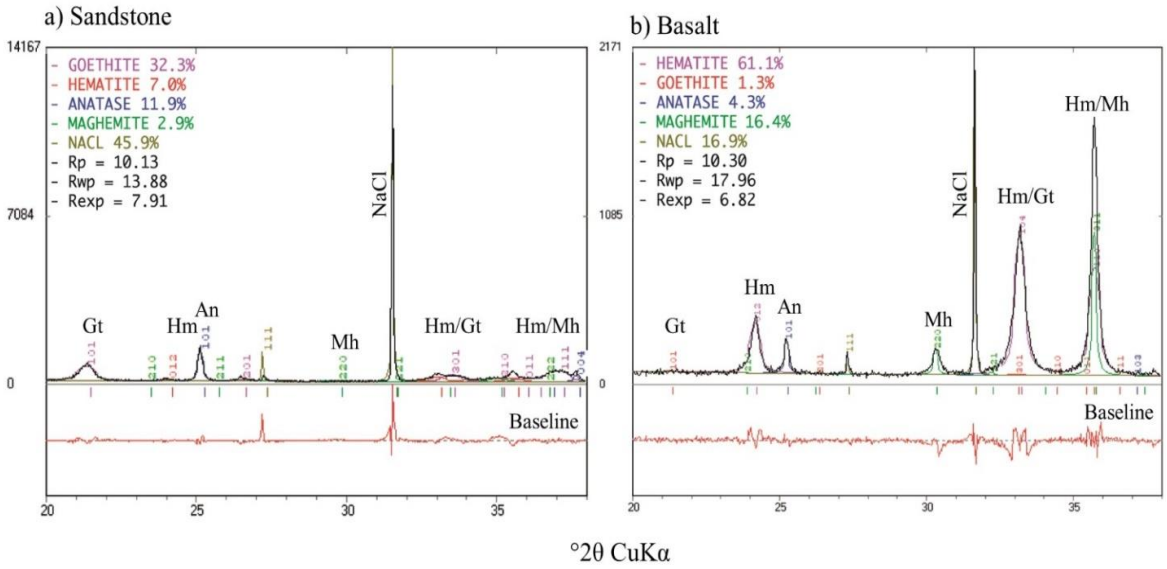

Figure S1. XRD diffraction patterns with Rietveld refinement for oxide-concentrated clay (5 mol L^{-1} NaOH). Mh, maghemite. Gt, goethite. Hm, hematite. An, anatase. NaCl, sodium chloride. Rp, Observed error/Calculated intensity (%) R_{wp}, weighted error (%).

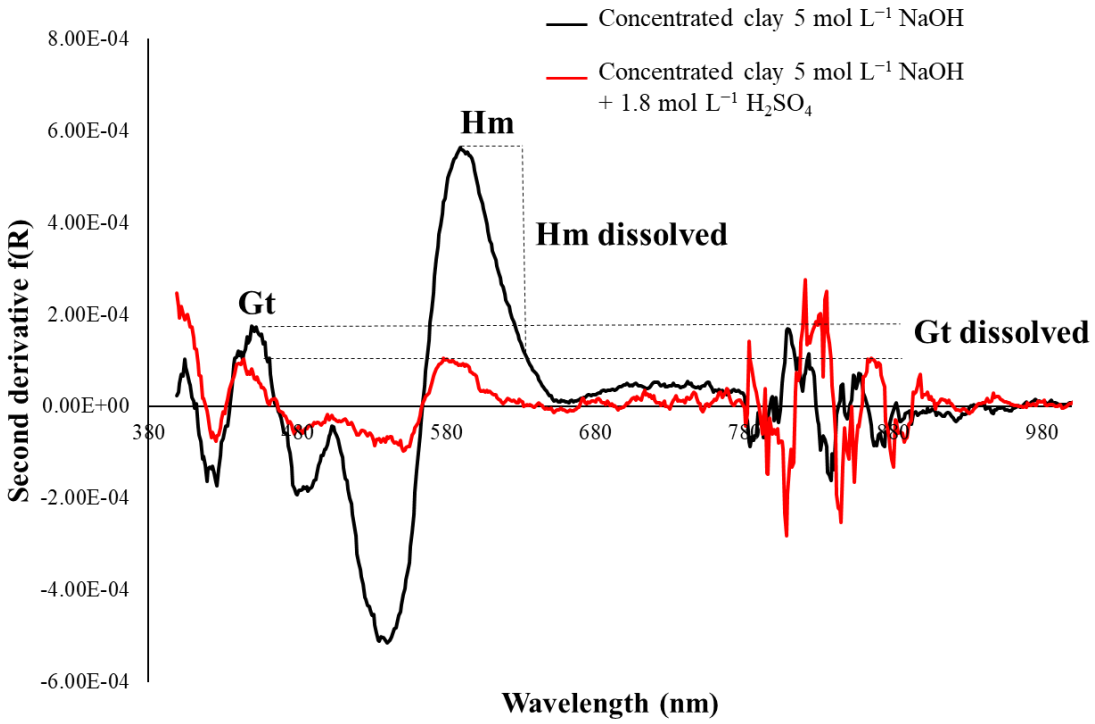

Figure S2. Vis–NIR spectra over the 400–2500 nm wavelength range for the iron oxides hematite (Hm) and goethite (Gt) before and after sulfuric digestion of the oxide-concentrated clay fraction.